INFLUENCE OF LOW TEMPERATURE EXPOSURE TIME ON THE MECHANICAL PROPERTIES OF A LEAD RUBBER BEARING

PhD Dissertation

Cansu YAŞAR

Eskişehir 2024

INFLUENCE OF LOW TEMPERATURE EXPOSURE TIME ON THE MECHANICAL PROPERTIES OF A LEAD RUBBER BEARING

Cansu YAŞAR

PhD Dissertation

Department of Civil Engineering

Programme in Mechanical

Supervisor: Prof. Dr. Gökhan ÖZDEMİR

Eskişehir

Eskişehir Technical University

Institute of Graduate Programs

August 2024

FINAL APPROVAL FOR THESIS

This thesis titled INFLUENCE OF LOW TEMPERATURE EXPOSURE TIME ON THE MECHANICAL PROPERTIES OF A LEAD RUBBER BEARING has been prepared and submitted by Cansu YAŞAR in partial fulfillment of the requirements in "Eskişehir Technical University Directive on Graduate Education and Examination" for the Degree of PhD in Civil Engineering Department has been examined and approved on 19/08/2024.

Committee Members		Title, Name and Surname	Signature
Member	:	Prof. Dr. Gökhan ÖZDEMİR	
Member	:	Prof. Dr. Uğurhan AKYÜZ	
Member	:	Prof. Dr. Beyhan BAYHAN	
Member	:	Doç. Dr. Hüseyin ÇİLSALAR	
Member	:	Dr. Öğrt. Üyesi Fatih SÜTCÜ	

Prof. Dr. Semra KURAMA
Director of the Institute of Graduate Programs

19/08/2024

SUPERVISOR APPROVAL

PhD student Cansu YAŞAR, whom I supervise, has completed this thesis titled INFLUENCE OF LOW TEMPERATURE EXPOSURE TIME ON THE MECHANICAL PROPERTIES OF A LEAD RUBBER BEARING. According to my inspections, the work is scientifically and ethically appropriate for the student to the thesis defense exam.

Supervisor
Prof. Dr. Gökhan ÖZDEMİR

ABSTRACT

INFLUENCE OF LOW TEMPERATURE EXPOSURE TIME ON THE MECHANICAL PROPERTIES OF A LEAD RUBBER BEARING

Cansu YAŞAR

Department of Civil Engineering

Programme in Mechanical

Eskişehir Technical University, Institute of Graduate Programs, August 2024

Supervisor: Prof. Dr. Gökhan ÖZDEMİR

This study investigates the change in hysteretic properties of lead rubber bearings (LRBs) exposed to low temperatures for several exposure times. For this purpose, a full-scale LRB was conditioned at temperatures of -20°C, -10°C and, 0°C for 3, 6 and, 24 hours and subjected to displacement-controlled cyclic motions at loading frequencies of 0.1 Hz and 0.5 Hz. During the cyclic tests, various levels of shear strain were applied to the isolator, including 50%, 100%, and 134%. Recorded force-displacement curves were analyzed to quantify the variations in hysteretic properties. Based on these findings, the accuracy of existing equations for estimating the amplification of mechanical properties was evaluated. It was found that the existing formulas do not account for the effect of exposure time on LRB characteristics at low temperatures. Consequently, new formulations were developed to provide more accurate predictions of these changes that account for both the effects of low temperatures and exposure time. Additionally, this study investigated the contribution of the lead core to modification in post-yield stiffness after low-temperature exposure for a different set of isolators. Four distinct LRBs were tested for this purpose, all different from the isolator examined in the tests involving varying exposure durations. Tests were performed on both large- and small-size LRBs, with and without lead cores, at a frequency of 0.1 Hz and a rubber shear strain of 100%, following conditioning at 0°C, -10°C, and -20°C for 24 hours. Force-displacement loops recorded during the tests were used to compute the hysteretic properties of bearings with and without a lead core.

Keywords: Lead rubber bearing, Seismic isolation, Low ambient temperature, Exposure time, Mechanical properties.

ÖZET

DÜŞÜK DIŞ ORTAM SICAKLIĞINA MARUZ KALMA SÜRESİNİN KURŞUN ÇEKİRDEKLİ KAUÇUK İZOLATÖR MEKANİK ÖZELLİKLERİNE ETKİSİ

Cansu YAŞAR

İnşaat Mühendisliği Anabilim Dalı

Mekanik Bilim Dalı

Eskişehir Teknik Üniversitesi, Lisansüstü Eğitim Enstitüsü, Ağustos 2024

Danışman: Prof. Dr. Gökhan ÖZDEMİR

Bu tez çalışmasında, düşük sıcaklıklara maruz kalan kurşun çekirdekli kauçuk izolatörlerin (KÇKİ) histeretik özelliklerindeki değişim incelenmiştir. Bu amaçla, büyük boyutlu bir KÇKİ, -20°C, -10°C ve 0°C sıcaklıklarda 3, 6 ve 24 saat süreyle bekletilmiş ve 0.1 Hz ile 0.5 Hz yükleme frekansları altında deplasman kontrollü dinamik testlere tabi tutulmuştur. Testler, %50, %100 ve %134 olmak üzere üç farklı kayma birim şekil değiştirmesi altında gerçekleştirilmiştir. Kaydedilen kuvvet-deplasman eğrileri, izolatörün histeretik özelliklerinde meydana gelen değişimleri analiz etmek için kullanılmıştır. Elde edilen bulgular kullanılarak, KÇKİ mekanik özelliklerinin düşük sıcaklık altında değişimini tahmin etmek için önerilen formüllerin doğruluğu değerlendirilmiştir. Mevcut formüllerin, düşük sıcaklıklara maruz kalan KÇKİ mekanik özelliklerini tahmin etmede yetersiz kaldığı ortaya konmuş ve hem düşük sıcaklığın mertebesini hem de bu sıcaklıklara maruz kalma süresinin etkisini dikkate alan yeni formülasyonlar geliştirilmiştir. Bu çalışmada ayrıca, düşük sıcaklığa maruz kalan KÇKİ'lerin mekanik özelliklerindeki değişime kauçuk ve kurşun çekirdeğinin katkısı da araştırılmıştır. Bu doğrultuda, biri kurşun çekirdekli diğeri çekirdeksiz olmak üzere bir çift büyük boyutlu ve bir çift küçük boyutlu kauçuk izolatör kullanılarak farklı düşük sıcaklıklar altında döngüsel testler gerçekleştirilmiştir. İzolatörler, 0°C, -10°C ve -20°C sıcaklıklarda 24 saat süreyle bekletildikten sonra %100 kayma birim şekil değiştirmesi altında 0.1 Hz yükleme frekansı ile test edilmiştir. Testler sırasında kurşun çekirdeği olan ve olmayan izolatörler için hesaplanan yatay rijitlik değerleri karşılaştırılarak kurşun çekirdeğinin izolatör rijitliğine katkısı, büyük ve küçük boyutlu izolatörler için incelenmiştir.

Anahtar Sözcükler: Kurşun çekirdekli kauçuk izolatör, Sismik izolasyon, Düşük dış ortam sıcaklığı, Etkime süresi, Mekanik özellikler.

ACKNOWLEDGEMENTS

This study was funded by the Turkish Scientific and Technical Research Council (TÜBİTAK) under grant numbers 119M573 and 122M762. Additionally, I received a scholarship from TÜBİTAK's 2211A program and the Council of Higher Education (YÖK) 100/2000 program during my studies. I gratefully acknowledge their support.

I would like to express my sincere appreciation to my supervisor, Prof. Dr. Gökhan ÖZDEMİR, for his invaluable guidance and support throughout the study.

I would also like to thank all the members of ESQUAKE: Osman Abi, Esengül, Volkan Hoca, Mustafa Bey, İbrahim Abi, and Erdinç Bey for their companionship throughout this study. I am grateful for their assistance and support whenever I needed it. Furthermore, I would like to thank Hakan Öztürk for his valuable suggestions during the time he spent at ESQUAKE.

I would further like to thank TİS and especially my managers for their understanding and patience throughout the final year of my thesis.

There is also a group of friends who made my life easier during this study and provided invaluable support while I was establishing a new life in Ankara. Their assistance was crucial and deeply appreciated. I would like to mention their names: Yılmaz, Gökçe, Gizem, Mustafa, and Cemile. I am deeply grateful for both their help and their friendship.

My special thanks go to my sister Yelis, who has accompanied me throughout my life and during this study. She is not just a sister to me but also my best friend, with her unconditional support. I feel very lucky to have her.

Finally, I wish to dedicate this dissertation to my mother and father. Their unwavering support, encouragement, and love have been my greatest source of strength throughout this journey. This work is a reflection of their belief in me.

Cansu YAŞAR

19/08/2024

STATEMENT OF COMPLIANCE WITH ETHICAL PRINCIPLES AND RULES

I hereby truthfully declare that this thesis is an original work prepared by me; that I have behaved in accordance with the scientific ethical principles and rules throughout the stages of preparation, data collection, analysis and presentation of my work; that I have cited the sources of all the data and information that could be obtained within the scope of this study, and included these sources in the references section; and that this study has been scanned for plagiarism with "scientific plagiarism detection program" used by Eskişehir Technical University, and that "it does not have any plagiarism" whatsoever. I also declare that, if a case contrary to my declaration is detected in my work at any time, I hereby express my consent to all the ethical and legal consequences that are involved.

Cansu YAŞAR

CONTENTS

Page

LIST OF TABLES

LIST OF FIGURES

Page

1. INTRODUCTION

1.1. General

Seismic isolation technique is proven to be a very effective way of protecting structures from the damaging effects of ground motions (Miyazaki, 2008; Sorrentino et al., 2023; Dilsiz et al., 2023; Hayır et al., 2023; Ozkula et al., 2023). It is based on shifting the fundamental periods of structures away from the dominant period range of strong ground motions. In order to do this, structural elements (called seismic isolator) that possess low horizontal stiffness are placed between the substructure and the superstructure. There are two main types of seismic isolators used to protect structures: elastomeric bearings and sliding bearings (Jangid & Datta, 1995; Kelly, 1986; Jangid, 2007). Among these seismic isolation systems, Lead Rubber Bearing (LRB) is one of the most extensively used seismic isolators in the world (Buckle et al., 2006). It consists of laminated layers of vulcanized rubber and steel that are placed on top of each other by bonding with each other via heat and pressure. In addition, there is a central core made of lead that passes through the height of the bearing. In this composition, rubber and steel layers are responsible for the horizontal and vertical stiffness of the bearing, respectively. On the other hand, the lead core provides an enhancement in terms of the energy dissipation capacity of the bearing (Skinner, 1992; Naeim & Kelly, 1999).

The mechanical properties of lead rubber bearings vary under different loading conditions (Robinson, 1982; Nakano, 1993). One of those conditions that has a significant effect on the behavior of an LRB is the low temperature. In order to estimate LRB's hysteretic behavior in a reliable manner, experiments need to be performed for different low temperatures.

In this thesis, an experimental research program to assess the effect of low temperature on the hysteretic properties of LRBs is presented. Thus, essential information is provided for the design of LRBs used in cold regions.

1.2. Lead Rubber Bearings

The lead rubber bearing was discovered in 1975 by W.H. Robinson in New Zealand (Kalpakidis, 2008). The basic components of the LRB system are rubber and steel layers and a central lead core, as shown in Figure 1.1. LRBs are typically constructed by bonding vulcanized rubber plates to steel shims via heat and pressure. Then, the lead core is placed into the preformed hole in the bearing (Buckle et al., 2006). In this system, steel plates reduce the lateral bulging of the rubber and increase the vertical stiffness of the isolator. Rubber layers are obtained from natural rubber or neoprene and are responsible for the low horizontal stiffness of the isolator unit. Lead core provides enhanced energy dissipation capacity. The top and bottom cover plates of the bearing are connected to the end shim through bolts, as depicted in Figure 1.1. Thus, the lead core, manufactured higher than the isolator height, is compressed and expands laterally into the rubber layers. This is called the confinement effect, and the lead core provides excellent energy dissipation capacity under this effect (Constantinou et al., 2007).

Figure 1.1. *Sectional view of an LRB (Constantinou et al.,2007).*

The behavior of lead rubber bearings is represented by a generic bi-linear force-displacement curve. Figure 1.2 illustrates the idealized force-deformation relation, in which Q is the characteristic strength, k_2 is the post-yield stiffness, and k_e is the initial elastic stiffness. In this representation, F_y and D_y are the yield force and yield displacement, respectively. The critical parameters dominate the LRB behavior are the characteristic strength, Q and post-yield stiffness, k_2. These parameters depend on both the geometric and material properties of LRBs as defined in Equations 1.1 and 1.2. In Equation 1.1, A_L is the area of the lead core while σ_L is the effective yield stress of lead. On the other hand, post-yield stiffness, k_2, is related to the shear modulus of rubber G_r, bonded rubber area A_r, and total rubber thickness T_r as seen in Equation 1.2. The parameter f_L of Equation 1.2 represents the effect of lead core on the post-yield stiffness and it is assumed to be close to unity, $f_L \approx 1$ (Kalpakidis, 2008). On the other hand, Energy

Dissipated per Cycle (EDC) is determined by computing the area enclosed by the hysteresis loop for each cycle.

$$Q=A_L\sigma_L \tag{1.1}$$

$$k_2=f_L\frac{G_rA_r}{T_r} \tag{1.2}$$

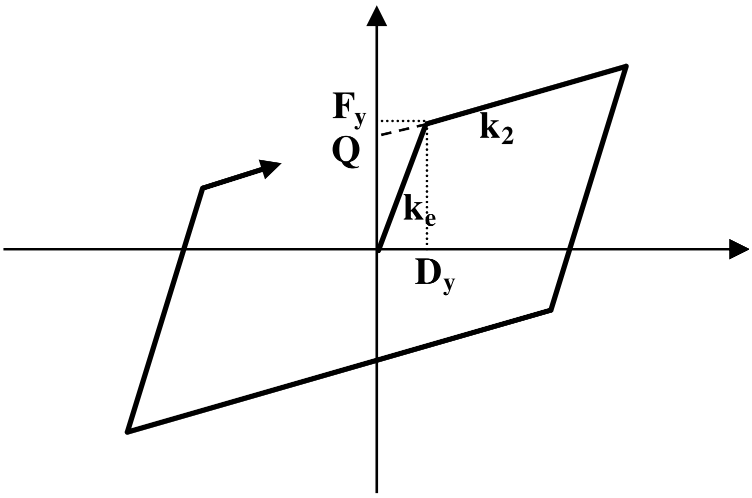

Figure 1.2. *Representative bi-linear force-displacement curve of LRBs.*

1.2.1. Mechanical characteristics of LRB components

The hysteretic behavior of LRBs depends on several parameters, such as temperature, rate of loading, level of stress, rate of shear strain, and bearing size. This chapter discusses in detail the mechanical characteristics of rubber, lead, and steel used in manufacturing LRBs to provide a better understanding of their characteristics.

1.2.1.1. Rubber

Rubber belongs to the elastomer family and is widely used in manufacturing seismic isolators due to its unique properties, such as high elasticity, durability, and abrasion resistance. The rubber used in elastomer-based seismic isolators can be obtained from natural or synthetic rubber (neoprene):

1) Natural rubber

Natural rubber is produced from latex, a milky fluid oozed from rubber trees, as seen in Figure 1.3. This latex is comprised of rubber particles suspended in water and a mixture of proteins, sugars, and other components. Then, agents like acid are applied to the latex, inducing the rubber particles to coagulate and separate from the aqueous latex. This process forms a solid mass of rubber referred to as raw rubber. The polymerization process begins by heating the raw rubber with additives such as curing agents, accelerators, and stabilizers. This heating process initiates chemical reactions that cause the rubber molecules to cross-link and form long chains. As a result, natural rubber, an elastomeric polymer, is manufactured (see Figure 1.4 for chemical structure).

Figure 1.3. *Oozing of the latex from the rubber tree (Semedi & Prasetya, 2014)*

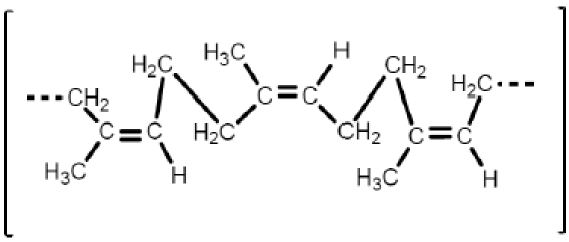

Figure 1.4. *Chemical formula of natural rubber.*

2) Neoprene

Neoprene is a synthetic rubber produced through a series of chemical reactions. The primary raw material for neoprene is chloroprene, a monomer derived from petroleum. It also contains various additives such as accelerators, activators, antioxidants, and fillers. Neoprene is valued for its resistance to oils, chemicals, ozone, and high temperatures. However, the stiffness of the neoprene increases at temperatures below 10ºC (Qayyum, 2016).

Rubber is a viscoelastic material that exhibits both viscous (fluid-like) and elastic (solid-like) properties when subjected to stress. It has extremely high deformation capacity under stress, like a viscous fluid, and the ability to return to its original shape, like elastic soil. At large strains, the behavior of rubber is described as nonlinear hysteretic (Mark et al., 2013)

Rubber is a nearly incompressible material with a Poisson's ratio (v) of approximately 0.5, which defines the ratio of transverse strain to axial strain in the material subjected to compressive stress. The bulk modulus, denoted as K, characterizes the resistance of rubber to hydrostatic pressure and is calculated as given in Equation 1.3 for the rubber, where E is the elastic modulus of the rubber. In elastomeric bearing analysis, a frequently utilized value for the bulk modulus of rubber, K, is 2000 MPa (Constantinou et al., 2007).

$$K=\frac{E}{3(1-2v)} \tag{1.3}$$

Rubber is commonly characterized by its shear modulus, G, which represents the resistance of the material to deformation under shear stress. The shear modulus of rubber, G, is determined according to the tests conducted following ASTM Standard D4014 (American Society for Testing and Materials, 1988). These procedures typically involve subjecting rubber specimens to controlled shear stress, τ and measuring the resulting shear strain, γ. The shear modulus can be calculated as follows:

$$G=\frac{\tau}{\gamma} \tag{1.4}$$

The shear modulus values for elastomers used in seismic isolation applications commonly range between 0.4 MPa and 0.8 MPa (Constantinou et al., 2007).

1.2.1.2. Lead

Lead is a scarce metal with a low yield strength, typically around 10 MPa. Due to its deformability under low levels of stress and ability to recover original mechanical properties, lead is used in elastomeric bearings to enhance their energy dissipation capacity.

It is well established that when an LRB is subjected to cyclic excitation, the hysteretic behavior of LRBs deteriorates (see Figure 1.5). Constantinou et al. (2007)

revealed that this reduction in isolator strength is due to the heating of the lead core. In lead rubber bearings, the energy dissipation process is initiated by the resistance of the lead core against motion. Thus, heat is produced within the lead core due to the resisting force exerted by the core. As the temperature of the lead core increases, its effective yield stress, σ_L, decreases. Accordingly, the characteristic strength, Q (see Equation 1.1), and energy dissipated per cycle (EDC) is reduced. As seen in Figure 1.6, while there is a significant reduction between the first and second cycles, the reduction tends to stabilize as the number of cycles increases. Furthermore, EDC recover almost entirely if the cyclic excitation is briefly interrupted and restarted.

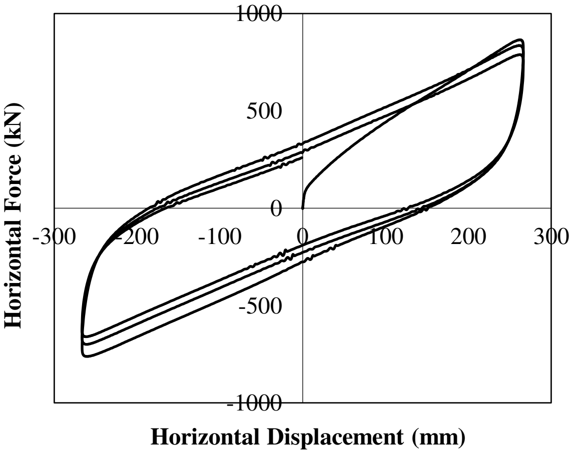

Figure 1.5. *Deteriorating hysteretic behavior of a typical LRB.*

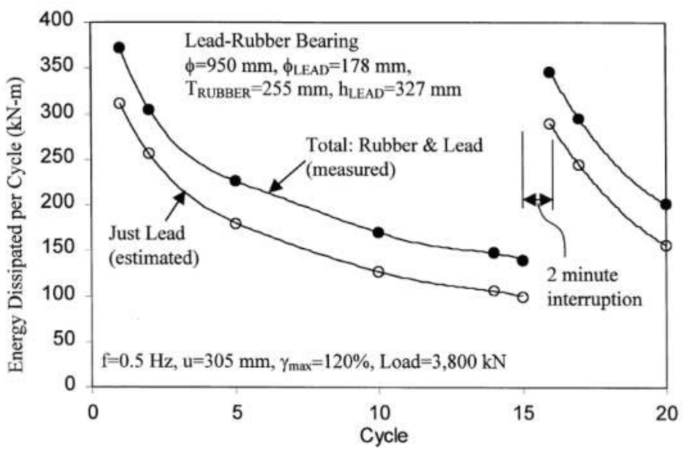

Figure 1.6. *Energy dissipated per cycle of a large size lead-rubber bearing (Constantinou et al., 2007).*

Table 1.1 presents the thermal conductivity of the materials used in manufacturing LRBs, namely lead, rubber, and steel. The lead used in LRBs is high purity, with values exceeding 99.9%, and the melting point of pure lead is approximately 327.5ºC. Accordingly, the value at 327°C represents the conductivity of lead just prior to melting. It is to be noted that the thermal conductivity of lead is nearly unaffected by temperature up to the melting point due to its unique electronic structure and lattice vibrations. On the other hand, the thermal conductivity of rubber is significantly lower than that of lead and steel due to its long molecular chains and weak intermolecular forces. As a result, the heat generated by the lead during cyclic motion is conducted entirely through the steel shim plates and end steel shims defined in Figure 1.1.

Table 1.1. *Thermal conductivity of lead, rubber, and steel (revised from Constantinou et al., 2007).*

Main features		Temperature					
		-25°C	**25°C**	**75°C**	**125°C**	**225°C**	**327°C**
Thermal Conductivity, *k* (W/(m°C))	**Lead**	36.0	35.3	34.7	34.0	32.8	31.4
	Rubber	-	0.16	-	-	-	-
	Carbon Steel	-	54.0	53.0	51.0	47.0	44.0

1.2.1.3. Steel

Steel is utilized to manufacture inner shims and end plates of lead rubber bearings, as seen in Figure 1.1. In accordance with (EN 1337-3, 2005), both the inner and outer reinforcing plates shall be of steel grade S235 or steel with a minimum equivalent elongation at break. The thickness of the inner plates should not be less than 2 mm. Outer plates must have a minimum thickness of 15 mm, with internal layers not exceeding 8 mm in thickness. However, if the internal layers surpass this thickness, the external plate thickness must be increased to 18 mm (EN 1337-3, 2005). Commonly, it comprises carbon steel, exhibiting a Young's modulus of 200.000 MPa, a density of 7900 kg/m³, and a Poisson's ratio of 0.33. Steel has a shear modulus several hundred times greater than rubber, ranging from 77 GPa to 82 GPa. As mentioned before, steel exhibits significantly higher thermal conductivity compared to rubber. Consequently, heat generated within the lead core during seismic excitations conducts through the inner steel shims and end plates.

1.2.2. Low temperature behavior of LRBs

Experimental research on the low-temperature behavior of LRBs is quite limited, primarily due to the scarcity of facilities capable of conducting dynamic tests with full-scale LRBs. In the experimental studies that focused on the variation of mechanical properties when the elastomer-based isolators were exposed to low ambient temperatures, test specimens were mostly comprised of rubber samples. These studies revealed that rubber properties are sensitive to temperature, and the stiffness of the rubber increases significantly when exposed to low temperatures (Murray & Detenber, 1961; Roeder et al., 1990; Constantinou et al., 2007; Cardone & Gesualdi, 2012). The increase in the stiffness of rubber depends on two phenomena: instantaneous thermal stiffening and crystallization stiffening (Roeder et al., 1990). Figure 1.7 describes the amplification in stiffness of rubber under low temperatures. In this figure, the stiffness of the rubber at ambient temperatures, T, is normalized by the stiffness at reference temperature, T_r, and presented as stiffness at T/stiffness at T_r. Accordingly, instantaneous thermal stiffening is observed when rubber is suddenly exposed to low temperature. It lasts during the time t_1 required for thermal equilibrium between the inside temperature of the bearing and the ambient temperature. Time t_1 depends on the order of temperature and size of the bearing. Roeder et al. (1990) stated that the value t_1 varies between 12 and 24 hours for large-size isolators used in seismic isolation applications. If the rubber is subjected to low temperatures for an extended period, a change in its stiffness is observed again at time t_2. This change is a result of the crystallites developed in the volume of the rubber and is called crystallization stiffening. Crystallization stiffening depends on the chemical composition of the elastomer and exposure time to low temperatures.

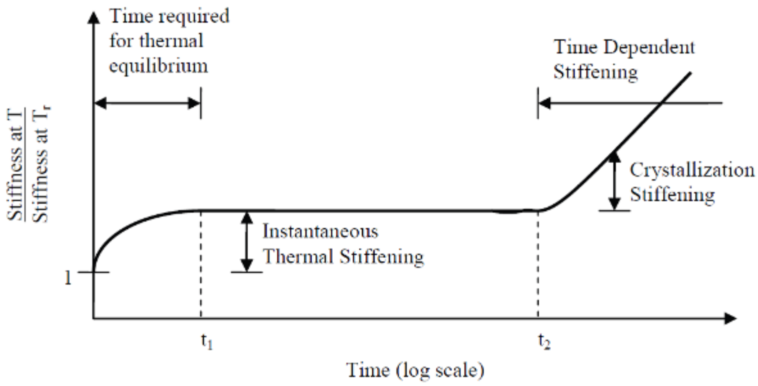

NOTE: T_r = reference temperature (typ. 20°C), $T<<T_r$

Figure 1.7. *Time-dependent stiffening behavior of rubber (Constantinou et al., 2007).*

In structures seismically isolated with elastomer-based isolators, the effectiveness of the isolation system in protecting the superstructure may be reduced due to the stiffening of rubber, and the forces transferred to the superstructure will increase. This phenomenon may considerably affect the design of structures with elastomeric bearings, particularly in near-fault regions. It is essential to emphasize that an accurately designed seismically isolated structure with elastomer-based bearings is necessary, and it can be achieved by considering the temperature dependence of the elastomer. Thus, the effect of low temperature on the hysteretic properties of elastomeric bearings is one of the most important topics addressed in previous studies, as provided in the next section.

1.3. Previous Research

1.3.1. Research with rubber specimens

In the literature, there are numerous research studies that focused on the variation in hysteretic behavior of LRBs under different temperatures. The stiffness of the rubber used in the composite form of an LRB has a key role in the cyclic response of LRBs. Thus, most of the previous studies solely investigated the response modification in rubber, as summarized below:

Murray and Detenber (1961)

Murray and Detenber (1961) performed tests with rubber specimens with dimensions of 89x89x6 mm to study the effects of crystallization. They focused on investigating the influence of curing, plasticizer type, vulcanization, and filler content on both the crystallization rate and brittleness temperature of rubber using several neoprene compounds. The rates of crystallization at 0, -5, -10, -15, and -20°C for two distinct neoprene compounds were determined by means of the durometer hardness method. Accordingly, the highest rate was observed for both neoprene vulcanizates at -12°C. The study revealed that the crystallization temperature of a compound dictates its minimum thawing temperature. At this temperature, the rubber compound reverts to a more flexible, non-crystalline state, with the thaw point typically occurring approximately 15°C above the crystallization temperature. Furthermore, the results of brittleness tests indicated that the crystallization process does not affect the brittleness temperature of neoprene.

<u>Stevenson (1983)</u>

In his research, Stevenson (1983) conducted experiments with rubber samples of 25x2x2 mm to investigate the changes in elastic modulus under different subzero temperatures and tensile strains. This phenomenon was studied at temperatures between 0 and -55°C for samples at tensile strains of up to 500%. Experiments were performed with samples obtained from natural rubber. The author reported that the elastic modulus of rubber increases with decreasing temperature due to the crystallization at low temperatures, especially at - 25°C. However, Stevenson also noted that no systematic dependence in the amplification of elastic modulus on tensile strain was observed.

<u>Fuller et al. (2004)</u>

Fuller et al. (2004) studied the effect of low temperature crystallization on the mechanical properties of natural rubber specimens 20x13x4 mm in size. The stiffness of the rubber was determined by subjecting it to a shear strain of approximately 35%, with experiments conducted at temperatures of 0°C, -10°C, and -25°C. As a result, stress-strain measurements have verified a substantial increase, sometimes up to 100-fold, in the initial stiffness induced by crystallization.

<u>Cardone and Gesualdi (2012)</u>

Cardone and Gesualdi (2012) examined the change in characteristics of 35x35x10 mm rubber samples when exposed to temperatures ranging from -20 to 40°C. Six different elastomers were used in the experiments with shear modulus ranging from 0.5 to 1.2 MPa. Experiments were repeated for shear strains varying between 25 and 125%. The testing procedure comprised of two phases: initially, the cyclic behavior of the two of the specimens (specimen A and B) was evaluated at temperatures ranging from 40°C to -20°C for specimen A and from -20°C to 40°C for specimen B. In the second phase, the impact of low temperatures on elastomers (represented by specimens C, D, E, and F) was scrutinized under long exposure times (ranging from 1 to 24 hours) at temperatures of 0°C, -10°C, and -20°C. At the end of the experiments, the authors underlined a significant increase in the stiffness of the rubber, especially when the air temperature drops below 0°C. Due to the instantaneous thermal stiffening, stiffness increases rapidly within 4 hours. Subsequently, a moderate increase in stiffness is observed after 4 hours, likely attributable to crystallization stiffening. On the contrary, the equivalent viscous damping remains consistent across the entire temperature range. The authors also stated that the cyclic mechanical behavior of elastomeric materials does not change significantly at high air temperatures.

1.3.2. Research with elastomeric bearings

There are also studies that investigate the modification in response of elastomeric bearings, composed of rubber and steel plates, subjected to low temperatures as given below:

Ritchie (1989)

Ritchie (1989) investigated the behavior of bridge bearings under cyclic movements at low temperatures. Two neoprene compounds were subjected to a 5% compression normal to the plane of shear and subsequently cooled to -25°C. The loading to which the bearings were subjected during the tests was applied very slowly. This corresponds to loading at a rate of one cycle per day for a period of 14 days with a shear strain of 25%. Ritchie (1989) stated that static (slow) loading under low ambient temperature is meaningless because it delays crystallization.

Roeder et al. (1990)

Roeder et al. (1990) investigated the change in mechanical properties of a 100x100 mm rubber bearing caused by instantaneous thermal stiffening and crystallization (as defined in Figure 1.7). They used elastomeric compounds made from natural rubber and neoprene. The authors followed a test program where the shear strain applied to the specimen was 25% and temperatures were ranging from -10 to -50°C. They underlined several significant conclusions from their research: instantaneous thermal stiffness occurred very quickly, and an increase in stiffness of more than 50 times that of room temperature was observed. On the other hand, the increase in stiffness caused by crystallization is often more than 15 times the room temperature stiffness. The most significant increase in stiffness was observed at temperatures ranging from -30°C to -

35°C. The stiffness due to crystallization is influenced by both the time of exposure of the elastomer to temperatures within the crystallization range and the current temperature of the elastomer. Furthermore, the room-temperature stiffness exhibited a recovery within a few hours subsequent to the sample being returned to room conditions.

Eyre and Stevenson (1991)

Eyre and Stevenson (1991) examined the increase in stiffness of rubber samples and elastomeric bridge bearings subjected to low temperatures. Experiments were performed at -25°C. For the small rubber samples, stiffness was measured at a shear strain of 3%, whereas for the full-scale bridge bearings, the stiffness values were determined at a shear strain of 7.5%. The comparison of the low temperature behavior between different-sized specimens revealed a lack of agreement in the results due to the varying levels of strains applied during the shear tests. Consequently, the authors emphasized that the level of shear strain applied to the specimen has a critical impact on the behavior of rubber.

Yakut and Yura (2002a, b)

Yakut and Yura (2002a, b) tested 44.5x229x356 mm elastomeric bearings at low temperatures of -10, -20, and -30°C for shear strains ranging from 12.5% to 30%. In their research, the exposure times were chosen as 1, 2, 4, 5, and 8 days to low temperatures. The authors performed cyclic loadings with a loading frequency of 0.01 Hz. The tested elastomeric bearings are made of natural rubber and neoprene. They emphasized that the increase in stiffness of rubber bearings is considerably sensitive to the exposure time of low temperatures. Furthermore, the crystallization stiffening is more pronounced in neoprene bearings than in natural bearings.

Pinarbasi et al. (2007)

Pinarbasi et al. (2007) investigated the effect of low temperature on elastomeric bearings having dimensions of 52x200x400 mm. The authors performed the tests once the bearings were conditioned at -29°C for 96 hours. Experiments were repeated for various levels of shear strain, ranging from 10% to 50%, to examine the shear behavior of the test bearings under different temperatures and strain levels. The results of the tests revealed that the shear stiffness of the test bearings at low temperatures was nearly double their stiffness at room temperature.

1.3.3. Research with LRBs

The primary reason for testing only rubber specimens rather than LRBs was generally the lack of ability to test full-scale LRBs. However, due to increasing number of test facilities capable of performing full-scale dynamic tests, the response modification in LRBs at low temperatures has been a research topic. The first low temperature tests of LRBs were carried out by Robinson (1982):

Robinson (1982)

In this research, a 356x356x140 mm square LRB was conditioned at temperatures of -15 and -35°C (exposure time is not reported) and then subjected to cyclic motions having loading frequencies of 0.5 and 0.9 Hz at 50% shear strain. The test results are presented comparatively using the force-displacement relationship recorded at a room temperature of 18°C as a reference. Accordingly, the ratios of the maximum forces of LRB, recorded at the first cycles of motions after exposed to -15 and -35°C, to the one recorded at 18°C are 1.2 and 1.4, respectively.

Hasegawa et al. (1997)

Another study that investigates the modification in hysteretic properties of LRBs at low temperatures was performed by Hasegawa et al. (1997). In their study, a 250 mm diameter LRB was dynamically tested under 100% rubber shear strain after being subjected to temperatures of 40, 20, 0, and -20°C. The authors recorded force-displacement curves for different temperatures and obtained mechanical properties using these curves. As a result, they proposed formulations to predict the change in mechanical properties, namely, post-yield stiffness and characteristic strength of LRBs at different temperatures. The proposed formulation includes an exponential expression that suggests a correlation between increasing characteristic strength and post-yield stiffness with decreasing temperature.

Constantinou et al. (2007)

Constantinou et al. (2007) tested a 381 mm diameter LRB with a lead core diameter of 70 mm. The amplitude of lateral sinusoidal motion corresponds to a shear strain of 58%, and tests were repeated for temperatures of 20 and -26°C. Based on the test results, the authors proposed some modification factors to estimate the mechanical properties at low temperatures. Accordingly, their proposals for the characteristic strength are 1.2, 1.4, and 1.8, while those for the post-yield stiffness are 1.1, 1.1, and 1.3 at 0, -10, and -30°C, respectively. Authors predicted more prominent increases in characteristic strength than post-yield stiffness when the temperature decreases.

Cho et al. (2008)

Another study examining the modifications in the mechanical properties of LRBs was undertaken by Cho et al. (2008). In contrast to prior investigations, the authors opted for a large-scale LRB featuring rubber and lead core diameters of 860 mm and 170 mm, respectively. Dynamic testing of the LRB was conducted at a shear strain of 15%, encompassing temperatures of -20°C, -10°C, 0°C, and 23°C. Subsequently, the shear properties derived from these tests were compared to the design values. The findings of the authors underscored significant disparities between the observed shear properties of the tested LRBs and their intended design specifications.

Park et al. (2012)

The variation in characteristics of an LRB exposed to low temperature was also assessed by Park et al. (2012). A large size LRB with a diameter of 800 mm was subjected to horizontal motion that corresponds to 100% rubber shear strain after being exposed to temperatures ranging from -10 to -40°C. The authors proposed equations to predict the amplification in mechanical properties of the tested LRB at low temperatures.

Chen et al. (2015)

Chen et al. (2015) conducted experimental investigations to determine the mechanical characteristics of 300x300 mm LRB under an ambient temperature of -10°C. They subsequently formulated equations to quantify this alteration. The experimental data revealed that the stiffness and damping ratio values of the LRB escalated by 22% and 15%, respectively, when exposed to -10°C temperature. The authors underscored that the formulated equations for predicting the rates of change in these parameters remained consistent with the experimental findings.

Mendez-Galindo et al. (2017)

Yet another set of experiments was performed by Mendez-Galindo et al. (2017) with a 550x550x236 mm square LRB. The LRB was conditioned at temperatures of -8 and -30°C for 72 hours and tested at shear strains ranging from 25% to 125% for -8°C, and 25% to 75% for -30°C. The authors underlined an increase in both characteristic strength and post-yield stiffness of the LRB. It is reported that both properties increased by a factor of 1.7 (corresponds to shear strain of 50% for characteristic strength, 75% for post-yield stiffness) at -30°C in comparison to the reference test conducted at 20°C.

Zhang and Li (2020)

Zhang and Li (2020) conducted experiments on circular rubber samples, with and without lead cores, measuring 220 mm in diameter. The experiments were performed at temperatures of -30°C, -20°C, -10°C, 0°C, and 20°C. In the study, the horizontal displacements applied to the isolators corresponded to 100, 200, and 300% shear strains. Experiments were conducted with a loading velocity of 1.5 mm/s. Utilizing the test results, the authors proposed various relationships to predict the characteristic strength and post-yield stiffness of the isolators exposed to low temperatures, aiming to facilitate their practical application.

Cavdar et al. (2022)

In one of the recent studies, Cavdar et al. (2022) focused on the variation in mechanical properties of an LRB with a dia meter of 1020 mm when exposed to a temperature of -30°C. The isolator was tested at a rubber shear strain of 100% with a loading frequency of 0.1 Hz. Consequently, the characteristic strength and post-yield stiffness of the LRB were observed to increase as the temperature decreased from 20°C to -30°C. Specifically, amplifications in strength and stiffness were noted to be approximately 50% and 10%, respectively.

1.3.3.1. Research addressed the individual contributions of rubber and lead core

The above cited studies that investigated the variation in mechanical properties of LRBs at low temperatures did not address the individual contributions of rubber and lead core to the amplification in mechanical properties of tested LRBs. In an attempt to quantify the contributions of rubber and lead to the stiffness of an LRB, as the inventor of LRB, Robinson (1982) conducted the first research:

Robinson (1982)

The author tested a bearing first without a lead core and then repeated the same loading after the lead core was inserted into the central hole of the bearing. The diameters of the bearing and the lead core were 650 mm and 170 mm, respectively. The amplitude of the motion applied to the bearing during the cyclic tests corresponds to 46% shear strain, while the loading frequency is 0.9 Hz. The author stated that the equivalent stiffness obtained for the bearing without a lead core is very close to the post-yield stiffness calculated for the bearing with a lead core.

Tyler and Robinson (1984)

A similar research was also performed by Tyler and Robinson (1984). The authors conducted tests with a 280x230x113 mm bearing with and without a lead core which has a diameter of 75 mm. Tests were conducted with a loading frequency of 1 Hz. Tyler and Robinson (1984) also reported that the equivalent stiffness calculated for the bearing without lead core is compatible with the post-yield stiffness of the lead rubber bearing after dynamic cyclic loadings conducted at 100% rubber shear strain.

It is to be noted that both Robinson (1982) and Tyler and Robinson (1984) did not consider the effect of low temperature on the contributions of rubber and lead core to the stiffness of the bearing.

Hasegawa et al. (1997)

Hasegawa et al. (1997) also considered the effect of low temperature and presented the post-yield stiffnesses of a bearing with and without lead core for different temperatures (20°C and -20°C), comparatively. In their study, a circular isolator with a diameter of 250 mm was tested first without a lead core, then with a lead core (38 mm in diameter) at a rubber shear strain of 100% with a loading frequency of 0.3 Hz. The authors showed that stiffness values were almost identical for the cases with and without lead core, while the stiffness increases with decreasing temperature.

The common point of the studies summarized above is that the same isolator was tested first without a lead core and tested again after the lead core was inserted. In such a testing campaign, it should be kept in mind that the characteristics of the rubber may be affected by previous loading cycles.

Constantinou et al. (2007)

To overcome the phenomenon mentioned above, Constantinou et al. (2007) performed cyclic tests on two identical bearings with a diameter of 185 mm, one with a lead core (38 mm in diameter) and one without a core. The authors showed that the contribution of lead to the isolator stiffness can reach up to 20% as a result of tests performed at room temperature for shear strains of 74% to 187%. However, Constantinou et al. (2007) stated that the effect of the lead core on the stiffness of LRB is a function of both the lead core and the bearing size. It should be noted that the LRB tested by Constantinou et al. (2007) was a small-size bearing, and the effect of low temperature was not considered.

Kalpakidis (2008)

In an attempt to investigate the low-temperature behavior of lead, Kalpakidis (2008) conducted experiments to examine the variation in the properties of lead over a temperature range of -30°C to 138°C. The study concluded that the stress-strain relationship of lead is significantly affected by temperature changes. This conclusion aligns with earlier findings by Hofmann (1970) and Guruswamy (2000) who similarly observed substantial variations in the stress-strain behavior of lead as a function of temperature.

The studies related to the thesis topic in the literature can be summarized as above. In order to make it easier to follow up, the studies cited above are presented in Table 1.2.

Table 1.2. *Summary of the literature review.*

Research Reference	Shear Strain (%)	Loading Frequency (Hz)	Testing Temperatures (°C)	Exposure Time	Test Specimen Type	Addressed rubber and lead contributions?
Murray and Detenber (1961)	Not specified	Not specified	-20, -15, -10, -5, 0	Not addressed	Rubber Specimen (89x89x6 mm)	No
Robinson (1982)	50%	~ 0.5, 0.9	-35, -15	Not addressed	Lead Rubber Bearing (356x356x140 mm)	No
Robinson (1982)	46%	0.9	20	Not addressed	Lead Rubber Bearing (Ø650 mm)	Yes
Stevenson (1983)	Focused on tensile strains of up to 500%		(-55) – (0)	Not addressed	Rubber Specimen (25x2x2 mm)	No
Tyler and Robinson (1984)	100	1.0	20	Not addressed	Lead Rubber Bearing (280x230x113 mm)	Yes
Ritchie (1989)	25	one cycle per day	-25	Not addressed	Rubber Bearing (sizes not specified)	No
Roeder et al. (1990)	25	0.01	(-50) – (-10)	1-24 days	Rubber Bearing (100x100 mm)	No
Eyre and Stevenson (1991)	3, 7.5	Not specified	-25	Not addressed	Specimen and Bearing (sizes not specified)	No
Nakano et al. (1993)	Not specified	Not specified	-18	A few minutes	Lead Rubber Bearing (sizes not specified)	No
Hasegawa et al. (1997)	100	0.3	-20, 0, 20, 40	Not addressed	Lead Rubber Bearing (Ø250 mm)	Yes
Yakut and Yura (2002a, b)	12.5 - 30	0.01	-30, -20, -10	1, 2, 4, 5, and 8 days	Rubber Bearing (229x356x45 mm)	No
Fuller et al. (2004)	35	Not specified	-25, -10, 0	Not addressed	Rubber Specimen (20x13x4 mm)	No
Pınarbasi et al. (2007)	10 - 50	0.01	-29	96 hours	Rubber Bearing (400x200x52 mm)	No
Constantinou et al. (2007)	58	0.035, 0.35	-26, 20	Not addressed	Lead Rubber Bearing (Ø381 mm)	No

Table 1.2 (Continued). *Summary of the literature review.*

Research Reference	Shear Strain (%)	Loading Frequency (Hz)	Testing Temperatures (°C)	Exposure Time	Test Specimen Type	Addressed rubber and lead contributions?
Cardone and Gesualdi (2012)	25 - 125	0.5	(-20) – (40)	1-24 hours	Rubber Specimen (35x35x10 mm)	No
Kalpakidis (2008)	Focused on tensile strain	0.0075, 0.25	(-30) – (138)	Not addressed	Lead Sample	No
Cho et al. (2008)	15	0.3	-20, -10, 0, 23	Not addressed	Lead Rubber Bearing (Ø860 mm)	No
Park et al. (2012)	100	0.02	(-10) – (40)	Not addressed	Lead Rubber Bearing (Ø800 mm)	No
Chen et al. (2015)	Not specified	Not specified	-10	Not addressed	Lead Rubber Bearing (300x300 mm)	No
Mendez-Galindo et al. (2017)	25-125	0.67 - 1.0	-30, -8, 20	72 hours	Lead Rubber Bearing (550x550x236 mm)	No
Zhang and Li (2020)	100, 200, 300	0.01	-30, -20, -10, 0, 20	Not addressed	Lead Rubber Bearing (Ø220 mm)	No
Cavdar et al. (2022)	100	0.1	-30	Not addressed	Lead Rubber Bearing (Ø1020 mm)	No

1.4. Research Motivation

The literature review related to modification in mechanical properties of LRBs subjected to low temperature revealed the following items: (i) the number of studies investigating the low-temperature response of rubber bearings is quite large. However, experimental data on the response of large-size LRBs exposed to low temperatures are scarce and need to be improved. (ii) There are only three studies performed with large-size LRBs, specifically with diameters larger than or equal to 800 mm. However, one of these studies was conducted at a very low shear strain (15%), while the other one has a loading frequency of 0.02 Hz. Moreover, in the third one conducted with a loading frequency of 0.1 Hz at a shear strain of %100, the exposure time to low temperatures was not considered as a parameter. (iii) The number of studies investigating the contribution of rubber and lead to modification in isolator properties is even less. There is only one study (Hasegawa et al., 1997) that investigated the contributions of lead and rubber to modification in LRB properties at low temperatures. In this study, the LRB under consideration was a small-size bearing and cannot be representative of large-size bearings used in highly seismic regions. In summary, the loading protocols followed in the tests were mainly not compatible with shear strains and loading frequencies experienced in regions with high seismicity. Additionally, the test programs utilized unrealistic definitions for the duration of exposure to low temperatures, with periods ranging from 1 day to 24 days. Thus, there is a need to conduct a systematic research program to assess the effect of low temperatures on the hysteretic properties of LRBs. This dissertation investigates the variation in hysteretic properties of full-scale LRBs under different low temperatures and exposure times. Dynamic tests performed during this study were conducted using earthquake-representative loading frequencies and shear strains. This thesis also includes a comprehensive investigation to quantify the contributions of lead and rubber to modifications in LRB properties at low temperatures for different size isolators.

1.5. Objective and Scope of the Research

In the design of seismic isolated structures, the "bounding analysis" method is used. The objective of this approach is not to determine the actual structural response but to identify the lower and upper bound values at which the real response varies in between. Hysteretic properties of LRBs used in bounding analysis are obtained by modifying the characteristic strength and post-yield stiffness of the isolator tested under laboratory conditions in order to mimic different loading combinations. One of the scenarios represented by these modifications is the behavior of seismic isolators under low temperature conditions. Specifications propose the lower and upper bound coefficients to account for the effect of low temperatures on the mechanical properties of isolators in design calculations. However, the coefficients recommended by the specifications are derived either by considering unrealistic climatic conditions (e.g., exposure to -30°C for 7 days) or from samples tested under shear deformations that are not representative of high seismicity. Therefore, there is a need to evaluate the effectiveness of the property modification factors suggested by specifications for low temperatures under reversed-cyclic motion, which results in a deteriorating force-displacement curve.

The first objective of this study is to determine the response modification of a large-size LRB due to the effect of low temperature and present the dependency of that modification to shear strain, loading velocity, level of temperature and the exposure time. For this purpose, a full-scale LRB was conditioned at temperatures of -20, -10, 0, and 20°C for 3,6 and 24 hours and then subjected to displacement-controlled cyclic motions that correspond to various levels of shear strains. Tests were conducted with loading frequencies of 0.1 Hz and 0.5 Hz. Characteristic strength and post-yield stiffness are the response parameters under investigation.

The second objective is to evaluate the effectiveness of existing empirical relations in estimating changes in the hysteretic properties of a full-scale lead rubber bearing (LRB) subjected to low temperatures. Force-displacement curves recorded during the experiments under the aforementioned loading conditions were used to compute the hysteretic properties, namely post-yield stiffness and characteristic strength, of the tested LRB. Subsequently, the efficiency of existing empirical formulations in estimating variations in these properties was presented in a comparative manner. Additionally, based on the test results, new formulations were proposed to predict the changes in the mechanical properties of lead rubber bearings (LRBs) at low ambient temperatures.

Finally, the third objective is to investigate the contribution of rubber and lead core to amplification in mechanical properties of lead rubber bearings (LRBs) when subjected to cyclic motion after low temperature exposure. In the experimental program, both large- and small-size LRBs were tested in order to observe the effect of bearing size on the results. For both sizes, tests were conducted with two identical bearings in terms of geometry and material properties. One of the bearings had a lead core, while the other had a hole in the center instead of a lead core. Displacement controlled cyclic tests were performed at a frequency of 0.1 Hz and a rubber shear strain of 100% after the bearings were conditioned at -20, -10, 0, and 20°C for a period of 24 hours. Force-displacement loops recorded during the tests were used to compute the hysteretic properties of bearings with and without a lead core. Comparison of hysteretic properties provides the contribution of the lead core to modification in post-yield stiffness of both large- and small-size LRBs.

1.6. Organization of the Dissertation

This dissertation comprises five primary chapters, with a summary of their contents provided as follows:

Chapter 1: A general overview of lead rubber bearings and their low temperature behaviors, along with a review of previous studies examining the response of elastomer-based bearings under low temperatures.

Chapter 2: An experimental program and corresponding test results aimed at investigating the modifications in mechanical properties of a large-size lead rubber bearing (LRB) at low temperatures.

Chapter 3: An assessment of the accuracy of the existing formulations to estimate the amplifications in LRB characteristics at low temperatures. Formulations that also consider the effects of exposure time to low temperatures and loading frequency are proposed to estimate these amplifications.

Chapter 4: An investigation on the contribution of lead rubber bearing (LRB) components, namely the rubber and lead core, to the amplification in mechanical properties of the isolator when subjected to low temperatures considering the size effect.

Chapter 5: A concise summary and conclusions are presented.

2. VARIATION IN MECHANICAL PROPERTIES OF AN LRB EXPOSED TO VARIOUS LOW TEMPERATURES

2.1. Introduction

This chapter presents the results of testing a large-size Lead Rubber Bearing (LRB). The primary objective of the experimental program was to analyze the impact of low temperature on the mechanical properties of the isolator, specifically focusing on post-yield stiffness and characteristic strength. The loading protocol followed in the experimental program represents all the conditions that an LRB may encounter during its service life.

Section 2.2 presents the geometric and material features of the tested LRB, whereas Section 2.3 describes the capabilities of the testing facility where experiments were conducted. The thermal analysis conducted to determine the appropriate low temperatures and exposure time for this study is detailed in Section 2.4. The test methodology followed during all loading conditions is explained in Section 2.5. Ultimately, the mechanical properties of the LRB are discussed in Section 2.6.

2.2. Test Specimen

The seismic isolator, tested in compliance with the objective of this study, is an LRB (low damping natural rubber + steel shims + lead core) with a rubber diameter of 850 mm (bonded rubber diameter is 838 mm). It has a lead core diameter of 220 mm. The height of the LRB is 339 mm, including the top and bottom plates and the end shim at the top. It consists of 18 layers of rubber plates, each 11 mm in thickness. There are 17 steel plates, and their individual thickness is 3 mm (see Figure 2.1). Detailed geometric properties of the LRB are provided in Table 2.1.

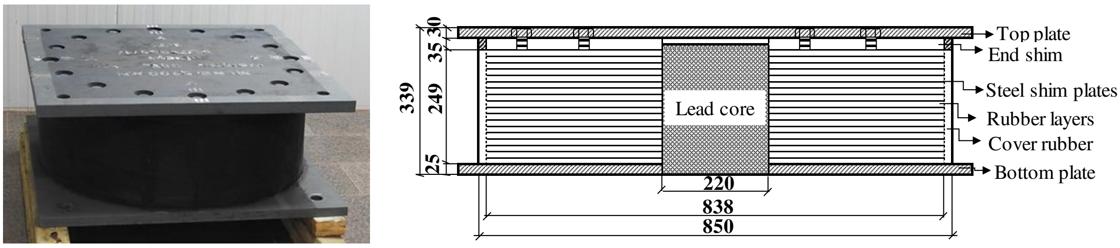

(a) (b)

Figure 2.1. *(a) View, and (b) geometric definition of the tested LRB (units are in mm).*

In Table 2.1, the primary shape factor, S_1, is defined as the ratio of the compressed area to the lateral surface area that is free to bulge. This factor is significant because it influences the capacity of the bearing to withstand compressive forces while accommodating lateral deformations. Seismic isolators with a primary shape factor, S_1, ranging between 5 and 20, are capable of providing effective isolation in both horizontal and vertical directions. In contrast, bearings with a primary shape factor, S_1, exceeding 20 are predominantly effective in providing isolation in the horizontal direction alone (Naeim and Kelly, 1999). On the other hand, the secondary shape factor, S_2, also known as the aspect ratio, is defined as the ratio of the bearing diameter, Φ, to the total thickness of the rubber layers, t_r. This aspect ratio, S_2, is critical for assessing the stability and flexibility of the bearing under shear deformations. Lastly, the shear modulus at 100% shear strain of the rubber used in the tested LRB is 0.6 MPa, while the grade of the steel shims is S235.

Table 2.1. *Geometric properties of the tested lead-rubber bearing.*

Main features of the tested isolator		
Φ (mm)	Isolator diameter	838
Φ_L (mm)	Lead diameter	220
t_s (mm)	Single-steel shim plates thickness	3
t_i (mm)	Single rubber layer thickness	11
t_r (mm)	Total rubber thickness	198
n_r	Number of rubber layer	18
S_1	Primary shape factor (Φ- $\Phi_L/4t_i$)	14.05
S_2	Secondary shape factor ((Φ/t_r)	4.23

2.3. Test Setup

In order to determine the change in hysteretic properties of the LRB introduced in previous section, it was tested under several displacement controlled cyclic motions. Tests were conducted at the ESQUAKE Seismic Isolator Test Laboratory of Eskişehir Technical University. Test set-up is capable of applying force and displacement controlled dynamic motions in both horizontal and vertical directions. Thus, the vertical load level acting on the seismic isolator can be kept constant during the horizontal motion. The maximum loading capacities are 2000 kN and 20000 kN in horizontal and vertical directions, respectively. The maximum loading velocity that can be applied in the horizontal direction is 1000 mm/s with a maximum displacement capacity of ±600 mm. Figures 2.2(a) and (b) present the pictures of test set-up and the accumulator sets used in ESQUAKE. The LRB attached to the test set-up is shown in Figure 2.2(c). Figure 2.2(d) depicts the 3x3x3 m environmental chamber that enables the control of air temperature between -40 and +50°C.

(a) (b) (c) (d)

Figure 2.2. *(a) Lay-out of the thermal chamber and test device (b) accumulator sets (c) seismic isolator test device (d) environmental chamber.*

2.4. Test Program

The LRB under investigation is one of the bearings manufactured to be used in an actual project where the maximum isolator displacement is 266 mm, and the axial load level is 3177 kN. Accordingly, the loading protocol has been established considering these values provided by the manufacturer. Thus, 266 mm, which corresponds to %134 shear strain as defined in Equation 2.1, is the maximum shear strain considered during the cyclic motions. In Equation 2.1, D_{iso} is the isolator displacement, while t_r is the total rubber thickness. Additionally, 50 and 100% shear strains were also considered in the loading protocol in order to assess the effect of shear strain.

$$\gamma = \frac{D_{iso}}{t_r} \tag{2.1}$$

The variation in mechanical properties of the LRB, when exposed to low temperatures, is studied by considering temperatures of -20, -10, and 0°C with an exposure time of 24 hrs. In order to determine the dependency of isolator characteristics to the loading frequency, tests were performed at both 0.1 and 0.5 Hz. These loading frequencies correspond to maximum loading velocities of 167 and 836 mm/s for 266 mm displacement, respectively. It should be noted that (EN-15129, 2018) recommended to consider 0.1, 0.5, and 1.0 Hz loading frequencies at 100% shear strain to determine the dependence of isolator characteristics on the frequency of loading. However, for 134% shear strain (266 mm isolator displacement), which is the maximum shear strain considered in this study, the loading frequency of 1.0 Hz corresponds to 1671 mm/s, which is greater than the capacity (1000 mm/s) of the test setup. This is why 1.0 Hz loading frequency was not considered in the experimental program. Table 2.2 presents the loading protocol followed in the experimental program.

Table 2.2. *Loading protocol followed in the experimental program.*

Test No	Temperature	Exposure Time (hour)	Shear Strain (%)	Frequency (Hz)	Cycle Number
1	20ºC	-	50, 100, 134	0.1, 0.5	3
2	0ºC	24	50, 100, 134	0.1, 0.5	3
3	-10ºC	24	50, 100, 134	0.1, 0.5	3
4	-20ºC	24	50, 100, 134	0.1, 0.5	3

In cold-temperature tests, according to AASHTO (2014), not only the recorded lowest temperature but also the maximum number of consecutive days for which the maximum daily temperature is below 0°C needs to be determined. In order to perform such an analysis, it is assumed that the tested LRB was used in one of the coldest regions with high seismicity in Turkey. Such a scenario leads to the cities of Erzurum, Erzincan, Bingöl, and Muş. For these cities, a database composed of temperature records provided by the Turkish State Meteorological Service (TSMS) is analyzed accordingly. It is to be noted that the temperature measurements are based on thermometers placed in a shelter above the ground and do not account for the effects of wind and humidity. In Figure 2.3, the frequency of a temperature being less than a target temperature is presented. In Figure 2.3, the frequency corresponds to the ratio of a number of temperature readings below a target value (selected to be -20, -15, -10, -5, and 0°C) to the number of all temperature readings. For example, Figure 2.3(d) presents a frequency of 0.5% at Muş for -20°C and 24 consecutive hours, indicating that it is very unlikely to have a temperature reading for a period longer than 24 hours. The corresponding frequencies for Erzurum, Erzincan, and Bingöl are even smaller. Thus, choosing -20°C and 24 hours as minimum temperature and corresponding exposure time, respectively, is appropriate for this study.

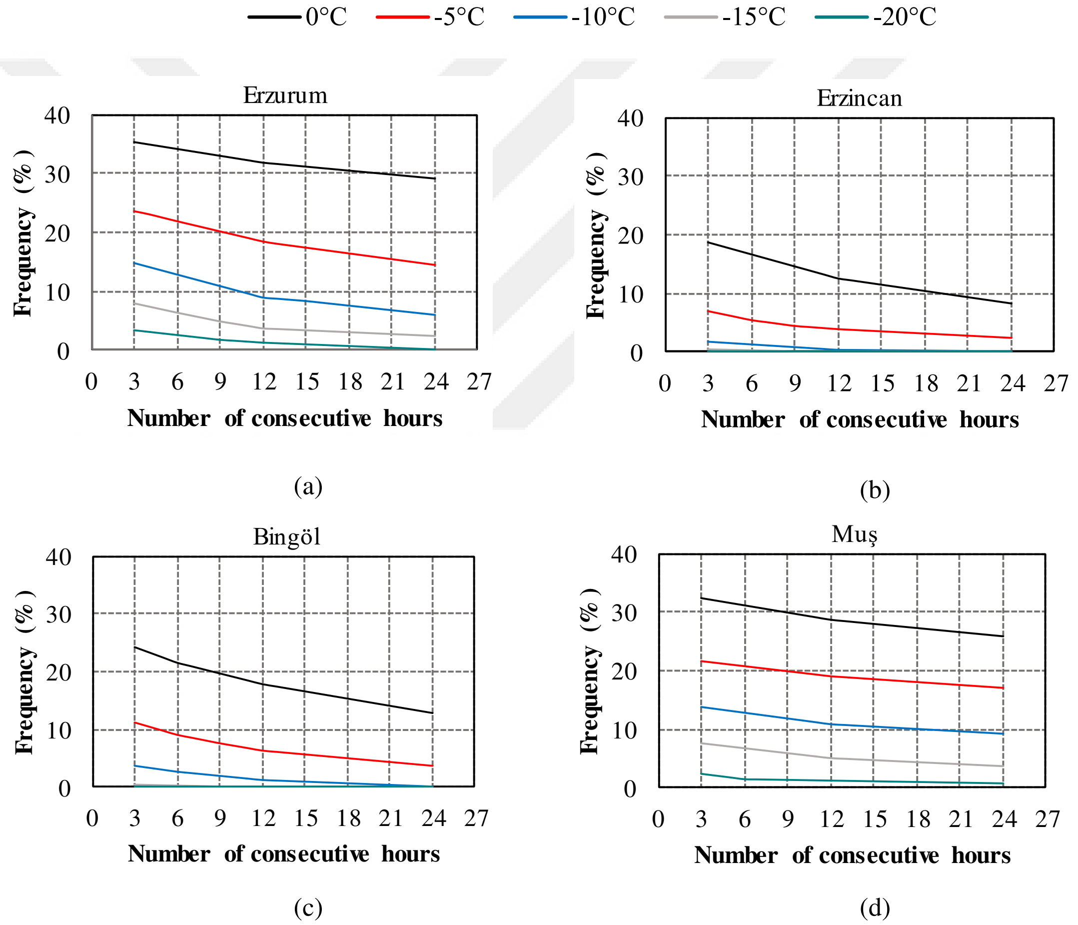

Figure 2.3. *Frequency of having a temperature below a target temperature in terms of consecutive hours for (a) Erzurum (b) Erzincan (c) Bingöl (d) Muş.*

2.5. Test Methodology

During the tests, the LRB under investigation was subjected to displacement-controlled sinusoidal cyclic motions with 3 cycles. In the loading protocols, initial and final half cycles were introduced to prevent results from being influenced by accelerations in the loading table at the beginning and end of the tests. The amplitude of these entrance and exit cycles was set equal to the test amplitude, and the peak velocity was achieved at the point of zero horizontal displacement. Figure 2.4 shows the displacement time history recorded for 0.5 Hz loading frequency and 134% shear strain. In Figure 2.4, the initial and final half cycles of the displacement time history are shown as dashed lines.

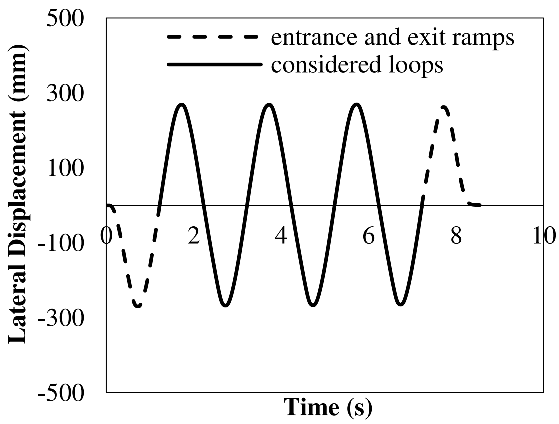

Figure 2.4. *The loading history for 0.5 Hz loading frequency and 134% shear strain.*

In order to investigate the effect of isolator displacement on the behavior of the tested LRB, amplitudes of the motions were set to 99, 198, and 266 mm for 50, 100, and 134% shear strains, respectively. The displacement histories considered in cyclic motions are presented in Figures 2.5(a) and (b) for both loading frequencies of 0.1 and 0.5 Hz. The vertical force applied to the LRB during the cyclic motion was 3177 kN (corresponds to a normal stress of 5.8 MPa). Figure 2.6 presents the force-displacement curve of the LRB obtained from the reference test (20°C), where the amplitude of the motion is 198 mm, and the loading frequency is 0.1 Hz.

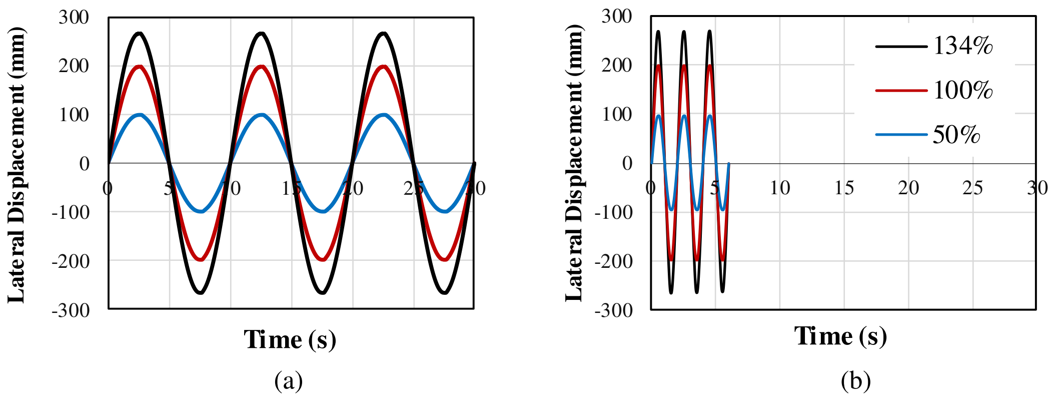

Figure 2.5. *Applied loading history to lead rubber bearing for a frequency of (a) 0.1 Hz (b) 0.5 Hz.*

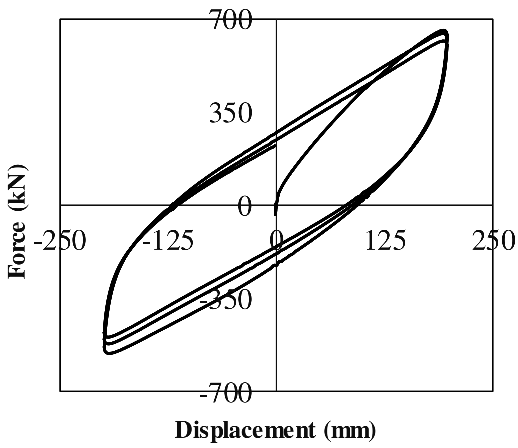

Figure 2.6. *Force-displacement curve of the LRB obtained from reference test when shear strain is 100% and loading frequency is 0.1 Hz.*

Prior to tests, environmental chamber shown in Figure 2.2(d) was set to the desired temperature. Once the chamber reached the desired temperature, the LRB was placed inside and kept in for 24 hours. In order to account for the temperature rise during the installation of the LRB into the test machine, temperature of the environmental chamber was set 2°C lower than the temperatures given in Table 2.2, as indicated by Zhang and Li (2020). Once the LRB was mounted to the test set-up, cyclic motions were conducted in laboratory conditions. The cold-temperature shear test procedure of AASHTO M251-97 (1997) requires completing the bearing test within 30 minutes after the specimen is removed from the cold environment. In accordance with AASHTO M251-97 (1997), it took at most 12 minutes to remove the LRB from the environmental chamber and complete the loading cycles. In Figure 2.7, a scene taken from the cyclic motion is presented together with the corresponding horizontal force-displacement curve and time versus vertical force graph. Figure 2.7(a) clearly shows the ice particles falling apart from the surface of the LRB. Figure 2.7(b) presents the corresponding force-displacement curve of the LRB while Figure 2.7(c) assures that the maximum amount of variation in vertical force during the cyclic motion is in the order of 5%. After each test, the LRB was conditioned at least for 24 hours at the laboratory in order to assure that the response of the LRB is not affected from the previous loading case and also to provide that the temperature of the LRB warms up to its initial value.

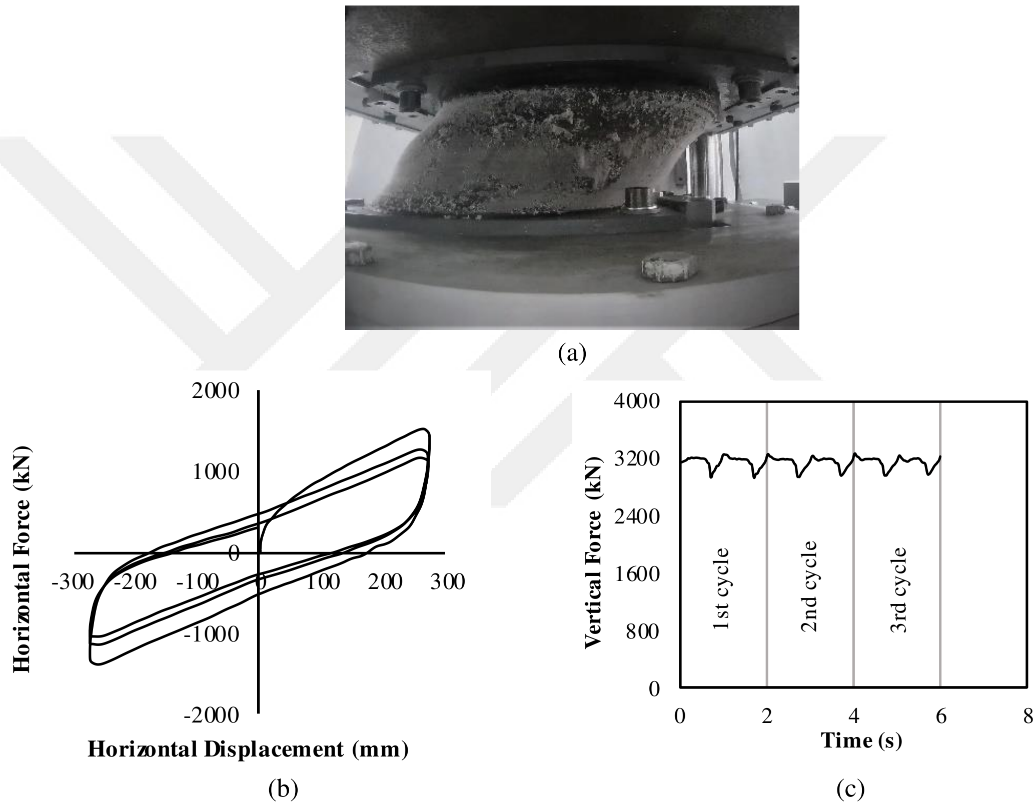

Figure 2.7. *For %134 shear strain, 0.5 Hz frequency and -20°C loading combination (a) view from cyclic motion (b) recorded force-displacement curve (c) variation of vertical force during the horizontal motion.*

2.6. Experimental Results

During the tests, force-displacement curves of the LRB were recorded for each loading combination specified in Table 2.2. The measured values were then processed using the Savitzky-Golay filtering technique to eliminate vibrations (noise) caused by the test equipment. After filtering out the noise from the recorded force values, the frictional force was subtracted. The ultimate force-displacement relationship was then obtained. In this section, variations in force-displacement curves obtained from different loading combinations (defined as functions of shear strain, ambient temperature, and loading frequency) are presented in a comparative manner.

Figure 2.8 depicts the force-displacement curves obtained from the isolator tests. It is evident that as the ambient temperature decreases, both the strength and lateral stiffness of the tested LRB increase. To better observe the change in strength and lateral stiffness of the LRB, Figure 2.9 is presented only for third cycles of force-displacement curves for ambient temperatures of -20 and 20°C. Regardless of the loading frequency, Figure 2.9 clearly shows the amplification in strength and stiffness of the LRB due to a reduction in temperature.

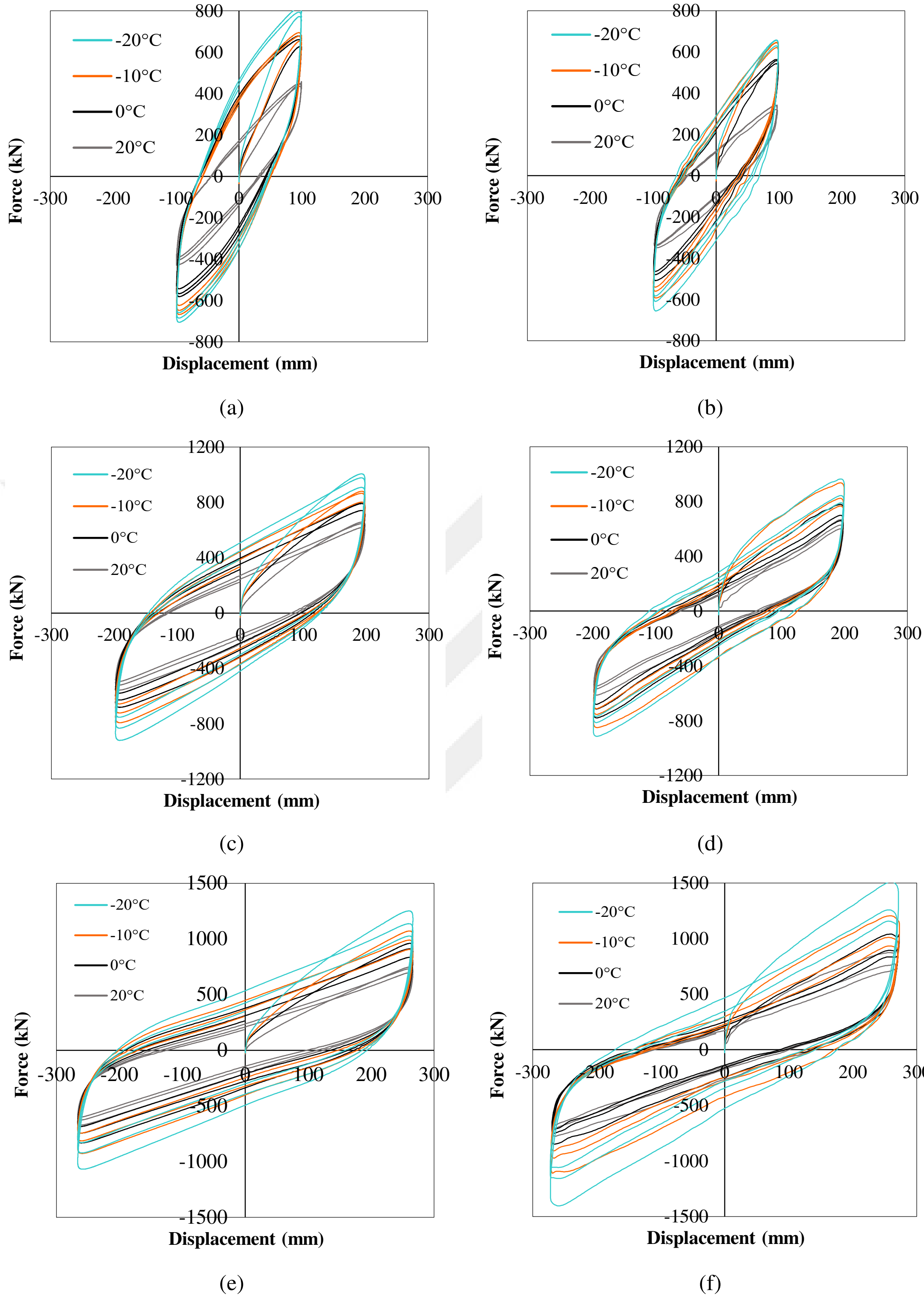

Figure 2.8. *Comparison of force-displacement curves obtained for different shear strains and temperatures (a) 50% shear strain, 0.1 Hz (b) 50% shear strain, 0.5 Hz (c) 100% shear strain, 0.1 Hz (d) 100% shear strain, 0.5 Hz (e) 134% shear strain, 0.1 Hz (f) 134% shear strain, 0.5 Hz.*

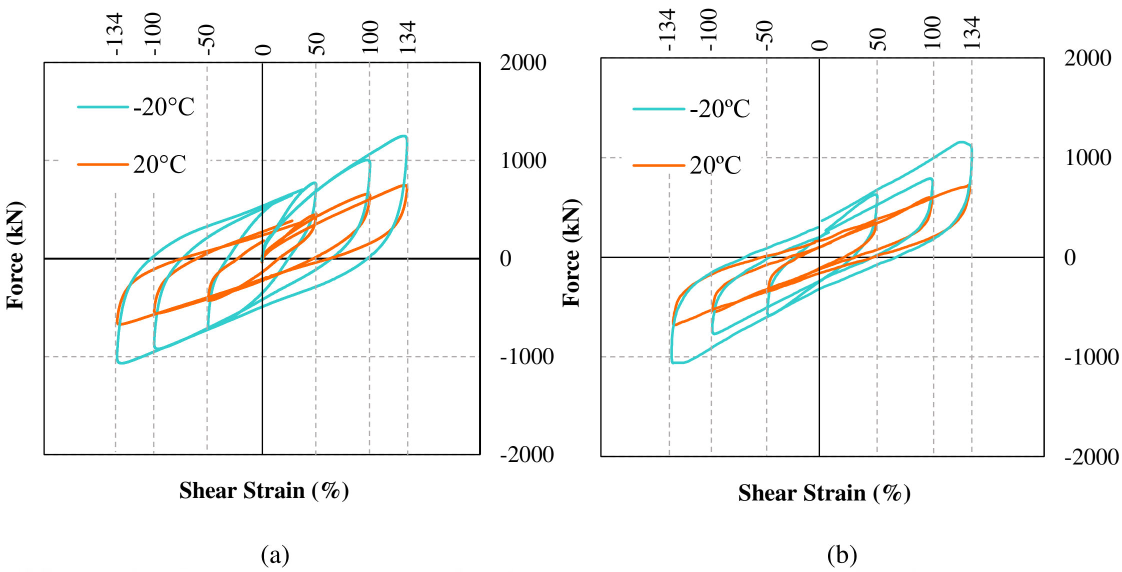

Figure 2.9. *Comparison of third cycles of hysteresis curves recorded for different shear strains (a) 0.1 Hz (b) 0.5 Hz.*

In order to quantify the change in hysteretic properties of LRB due to variation in ambient temperature, post-yield stiffness k_2 and characteristic strength Q (see Figure 1.2 for definitions) are computed for each loading cycle. In accordance with EN-15129 (2018), a best fit straight-line is used to determine isolator characteristics k_2 and Q from the force-displacement curve between ±85% of the peak test displacement, as shown in Figure 2.10. In this study, the Least Square Method (LSM) is used to obtain the best fit by minimizing the sum of the squared differences between the recorded and the fitted value. LSM results in two distinct values for Q (Q_{pos} and Q_{neg}) and k_2 ($k_{2(upper)}$ and $k_{2(lower)}$) for each cycle of motion, as illustrated in Figure 2.10. The representative Q and k_2 values of each cycle are computed by $(Q_{pos}-Q_{neg})/2$ and $(k_{2(upper)}+k_{2(lower)})/2$, respectively.

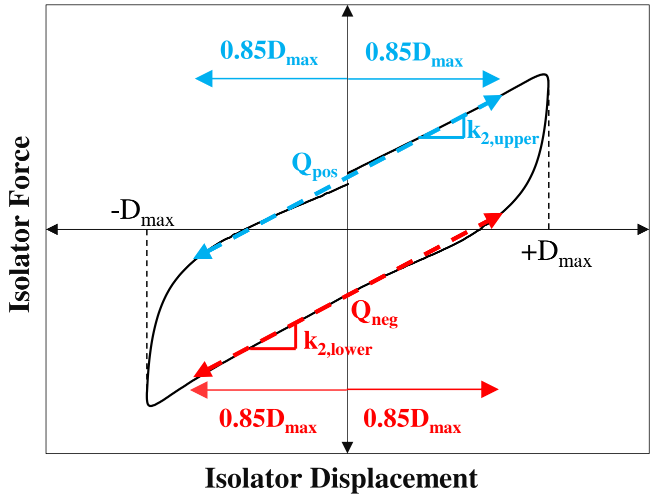

Figure 2.10. *Application of LSM method.*

Tables 2.3 and 2.4 present the properties of LRB computed in accordance with the above definitions for tests conducted at 20°C, 0°C, -10°C and -20°C for frequencies of 0.1 and 0.5 Hz. In these tables, data calculated at 20°C are considered as the reference values for each loading combination and used to normalize the corresponding isolator property obtained for different ambient temperatures. Figures 2.11 and 2.12 show the variation in normalized properties of the LRB for different shear strains, loading frequencies, and ambient temperatures.

Table 2.3. *Mechanical properties of LRB computed at frequency of 0.1 Hz.*

Temp.	Shear Strain	Cycle	Q_{pos} (kN)	Q_{neg} (kN)	Q (kN)	k_{upper} (kN/m)	k_{lower} (kN/m)	k_2 (kN/m)
20ºC	50%	1st	124	-158	141	3766	3523	3645
		2nd	108	-148	128	3557	3403	3480
		3rd	99	-143	121	3422	3323	3372
	100%	1st	185	-259	222	2270	2179	2224
		2nd	156	-236	196	2116	2093	2104
		3rd	137	-220	178	2020	2015	2017
	134%	1st	204	-247	226	1857	1788	1822
		2nd	168	-220	194	1755	1735	1745
		3rd	149	-201	175	1700	1694	1697
0ºC	50%	1st	216	-331	273	5157	4892	5025
		2nd	203	-319	261	5036	4789	4912
		3rd	190	-305	247	4834	4602	4718
	100%	1st	269	-372	321	2609	2427	2518
		2nd	225	-334	280	2468	2328	2398
		3rd	187	-301	244	2311	2257	2284
	134%	1st	320	-383	352	2078	1984	2031
		2nd	251	-319	285	1957	1915	1936
		3rd	204	-275	240	1860	1855	1858
-10ºC	50%	1st	280	-319	300	5458	5183	5320
		2nd	265	-308	286	5302	5101	5202
		3rd	250	-294	272	5112	4936	5024
	100%	1st	331	-414	373	2837	2660	2748
		2nd	274	-363	319	2702	2550	2626
		3rd	225	-320	272	2512	2440	2476
	134%	1st	378	-447	413	2243	2092	2168
		2nd	291	-369	330	2099	2024	2062
		3rd	234	-317	276	1981	1964	1973
-20ºC	50%	1st	279	-397	338	5930	5754	5842
		2nd	263	-382	323	5803	5651	5727
		3rd	245	-364	305	5628	5459	5543
	100%	1st	389	-476	433	3182	2926	3054
		2nd	323	-422	373	3027	2810	2919
		3rd	264	-371	318	2823	2681	2752
	134%	1st	458	-529	493	2540	2360	2450
		2nd	350	-432	391	2327	2212	2270
		3rd	278	-361	320	2168	2147	2158

Table 2.4. *Mechanical properties of LRB computed at frequency of 0.5 Hz.*

Temp.	Shear Strain	Cycle	Q_{pos} (kN)	Q_{neg} (kN)	Q (kN)	k_{upper} (kN/m)	k_{lower} (kN/m)	k_2 (kN/m)
20°C	50%	1st	113	-113	113	3020	2686	2853
		2nd	97	-110	103	2828	2696	2762
		3rd	94	-109	101	2774	2684	2729
	100%	1st	160	-153	156	2037	1963	2000
		2nd	128	-134	131	1881	1849	1865
		3rd	118	-127	122	1834	1782	1808
	134%	1st	236	-238	237	2237	1988	2113
		2nd	178	-201	190	1940	1887	1914
		3rd	159	-186	172	1846	1813	1829
0°C	50%	1st	166	-230	198	4487	4090	4288
		2nd	136	-210	173	4231	3995	4113
		3rd	123	-198	160	4107	3906	4006
	100%	1st	231	-198	215	2902	2488	2695
		2nd	186	-168	177	2596	2396	2496
		3rd	165	-151	158	2437	2327	2382
	134%	1st	231	-281	256	2320	2108	2214
		2nd	171	-242	206	2013	2021	2017
		3rd	152	-224	188	1920	1965	1943
-10°C	50%	1st	206	-270	238	5149	4576	4863
		2nd	165	-238	201	4847	4552	4699
		3rd	145	-221	183	4674	4485	4579
	100%	1st	290	-264	277	3289	2922	3106
		2nd	214	-209	212	2796	2789	2792
		3rd	188	-187	188	2624	2680	2652
	134%	1st	401	-334	368	2905	2480	2693
		2nd	304	-265	284	2460	2315	2388
		3rd	269	-237	253	2264	2196	2230
-20°C	50%	1st	274	-279	277	4806	4431	4619
		2nd	230	-240	235	4477	4483	4480
		3rd	205	-217	211	4377	4416	4397
	100%	1st	318	-295	307	3354	2890	3122
		2nd	255	-251	253	2924	2808	2866
		3rd	229	-231	230	2756	2686	2721
	134%	1st	494	-487	490	3614	2928	3271
		2nd	362	-384	373	2994	2790	2892
		3rd	308	-337	322	2742	2673	2707

Figure 2.11 illustrates the amplifications in characteristic strength of the tested LRB obtained for several loading conditions. Accordingly, the characteristic strength computed for different ambient temperatures is normalized by the reference one and presented as $Q/Q_{20°C}$ for temperatures of -20°C, -10°C, and 0°C. Corresponding values for both Q_{pos} and Q_{neg} are given in Figure 2.11 for all three loading cycles. The first impression of Figure 2.11 is that the amplifications in isolator strength are more significant for 50% shear strain (the maximum loading velocities are 62.2 and 311 mm/s for 0.1 and 0.5 Hz, respectively). This is especially evident in the loading frequency of

0.1 Hz. The reason for such observation is that the temperature rise in the lead core is smaller in the case of 50% shear strain compared with those for 100% and 134% shear strains. Thus, the strength of the isolator experiences only a minor reduction and stays almost constant at each loading cycle. This is parallel to the findings of Ozdemir et al. (2008), where authors stated that the strength reduction in LRB due to cyclic motion gets more prominent as both the amplitude and velocity of the motion increase. Figure 2.8(a) also supports such inference by having almost nondeteriorating force-displacement curves for all ambient temperatures.

Amplifications in characteristic strength, Q of Tables 2.3 and 2.4 vary roughly between 2.5 and 1.0. For instance, for 134% shear strain and 0.5 Hz loading frequency, the amplifications are 2.07, 1.97, and 1.87 for the first, second, and third cycles of motion at -20°C indicating that the amount of amplification decreases with the increasing number of cycles as shown in Fig. 2.12. Although the general trend in $Q/Q_{(20°C)}$ is to decrease with the increasing number of loading cycles, the experimental outputs for 50% shear strain at 0.1 Hz loading frequency show an opposite tendency. This may be due to a low temperature rise in the lead core compared with other cyclic motions. Ozdemir et al. (2018) showed that the temperature rise in the lead core is a function of both the amplitude and the loading frequency of the motion applied to the LRB. Since the amplitude and frequency of the motion considered in 50% shear strain and 0.1 Hz are the smallest among the other values considered in this study, the corresponding temperature rises will also be the smallest. Accordingly, for that loading case, the reduction in initial strength of the LRB due to temperature rise in the lead core will also be smaller than the others. In addition, much of the reduction in strength of LRB may not be greater than the amplification in strength due to low temperature. Thus, $Q/Q_{(20°C)}$ ratio does not decrease with increasing number of cycles.

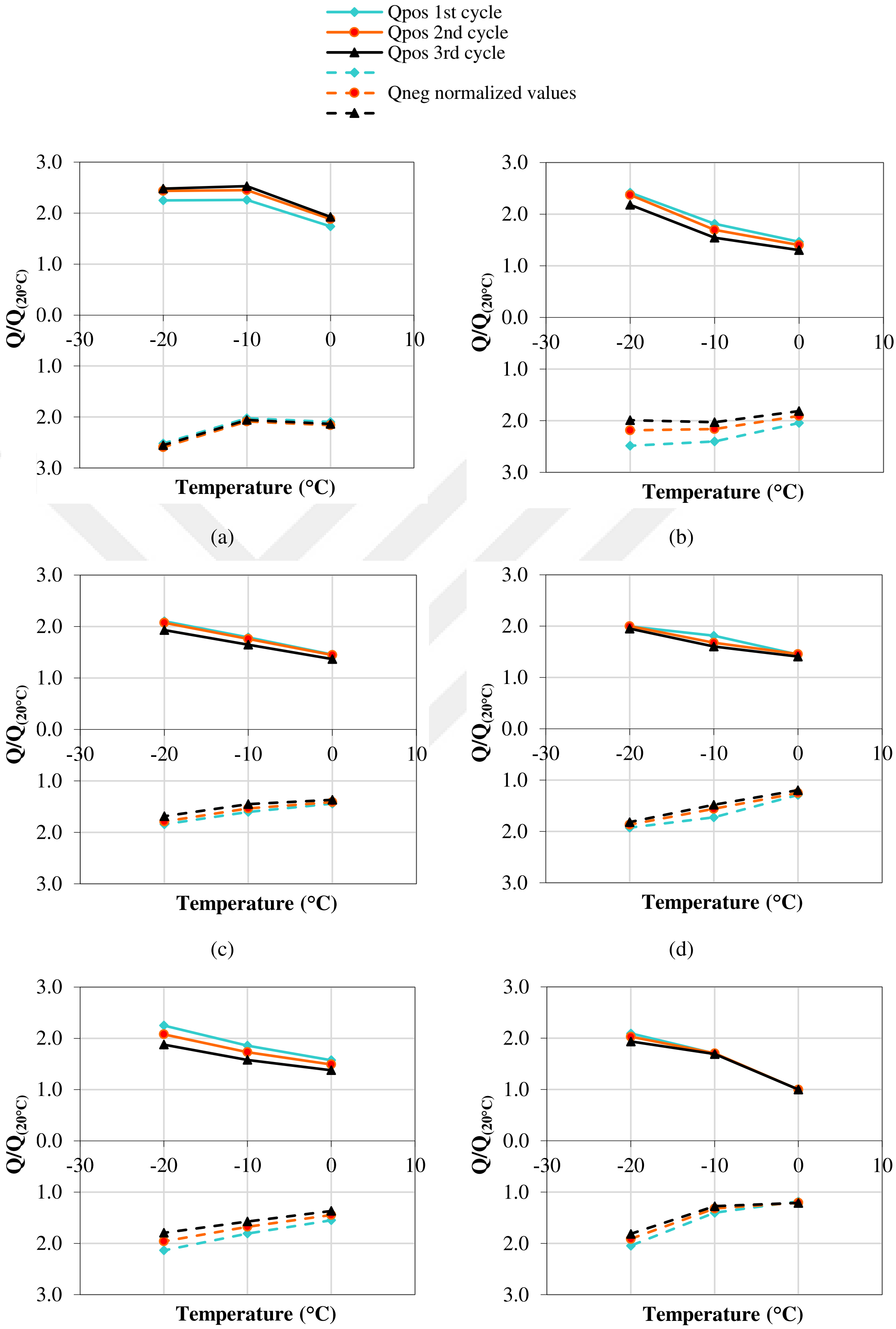

(a)

(b)

(c)

(d)

(e)

(f)

Figure 2.11. *Comparison of normalized positive and negative characteristic strengths (a) 50% shear strain, 0.1 Hz (b) 50% shear strain, 0.5 Hz (c) 100% shear strain, 0.1 Hz (d) 100% shear strain, 0.5 Hz (e) 134% shear strain, 0.1 Hz (f) 134% shear strain, 0.5 Hz.*

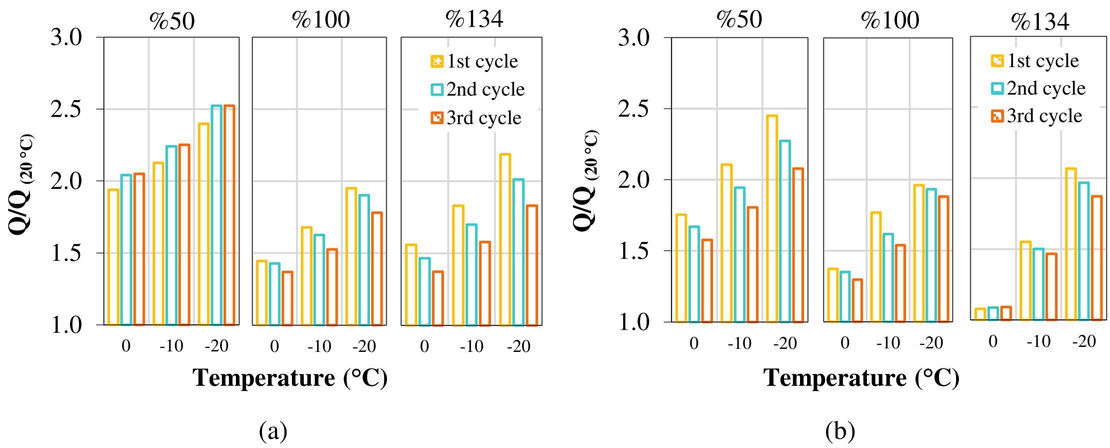

Figure 2.12. *Comparison of normalized characteristic strengths for (a) 0.1 Hz; and (b) 0.5 Hz loading frequency.*

Figures. 2.13 and 2.14 present the amplification in post-yield stiffness of the LRB, introduced in Figure 2.1, due to a change in ambient temperature. In Figures 2.13 and 2.14, the post-yield stiffnesses calculated using LSM for different ambient temperatures are normalized by the reference one and presented as $k_2/k_{2(20°C)}$. Figure 2.13 graphically shows the variation in $k_2/k_{2(20°C)}$ values for $k_{2(upper)}$ and $k_{2(lower)}$ (see Figure 2.10 for definitions) individually at each loading cycle, whereas Figure 2.14 depicts their average, which is representative of the corresponding loading cycle. As seen from Figure 2.14, similar to $Q/Q_{(20°C)}$, $k_2/k_{2(20°C)}$ values obtained for 50% shear strain in the case of 0.1 Hz loading velocity correspond to the most extensive amplifications. Moreover, for that loading combination, the $k_2/k_{2(20°C)}$ ratio tends to increase as the number of loading cycles increases. This indicates that the variation in post-yield stiffness from cycle to cycle of the reference test is less than the ones obtained for the considered ambient temperatures. The trend in the $k_2/k_{2(20°C)}$ ratio is to decrease with increasing shear strain and temperature. The maximum amount of variation in the $k_2/k_{2(20°C)}$ ratio from cycle to cycle is 3.7%. Since cycle-to-cycle variation of the $k_2/k_{2(20°C)}$ ratio is very limited, the $k_2/k_{2(20°C)}$ ratio computed for the second cycle of loading can also be used for the first and third cycles. Figure 2.15 shows the accuracy of using the $k_2/k_{2(20°C)}$ ratio of the second loading cycle for the remaining cycles.

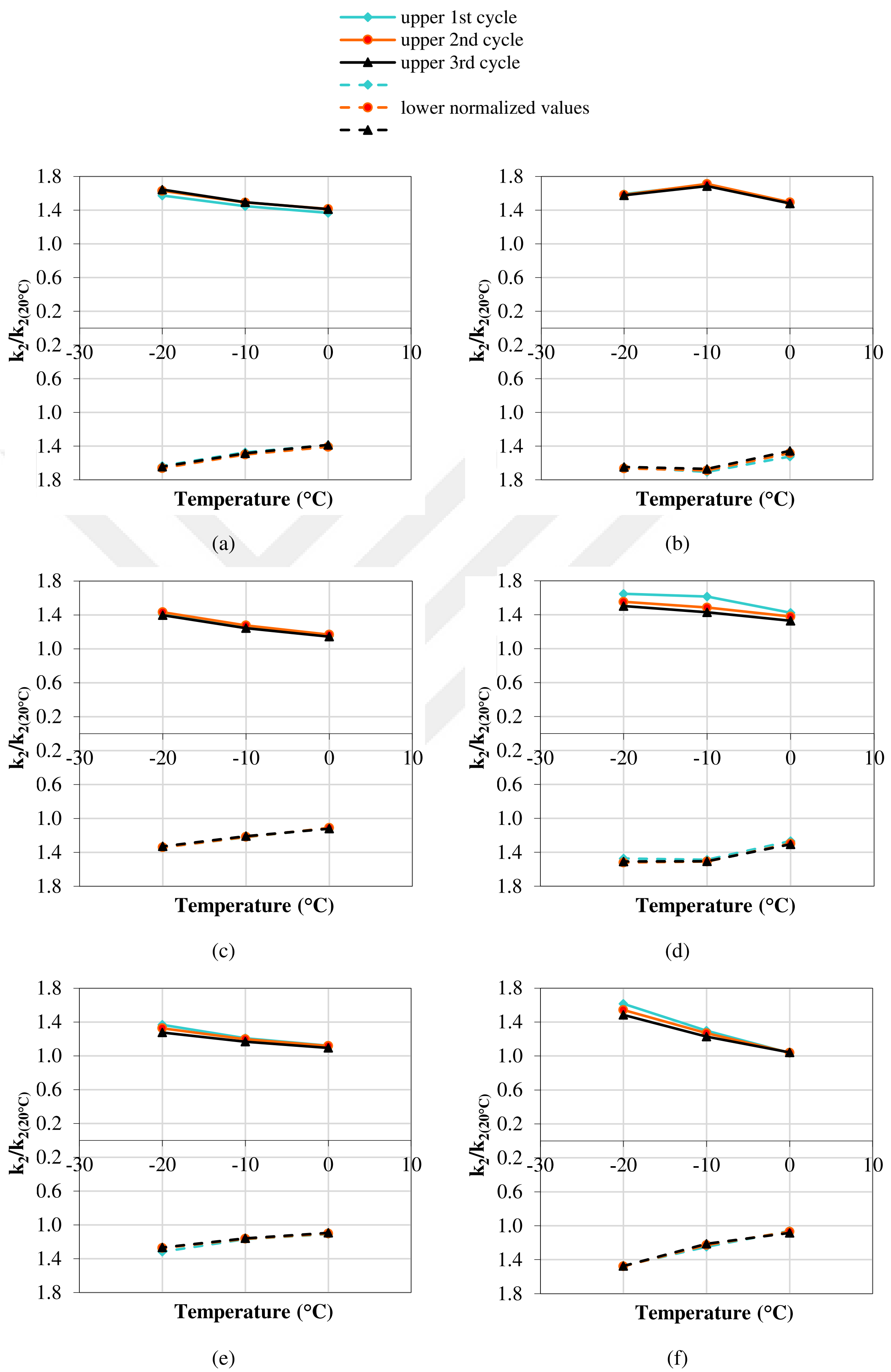

Figure 2.13. *Comparison of normalized upper and lower post-yield stiffnesses (a) 50% shear strain, 0.1 Hz (b) 50% shear strain, 0.5 Hz (c) 100% shear strain, 0.1 Hz (d) 100% shear strain, 0.5 Hz (e) 134% shear strain, 0.1 Hz (f) 134% shear strain, 0.5 Hz.*

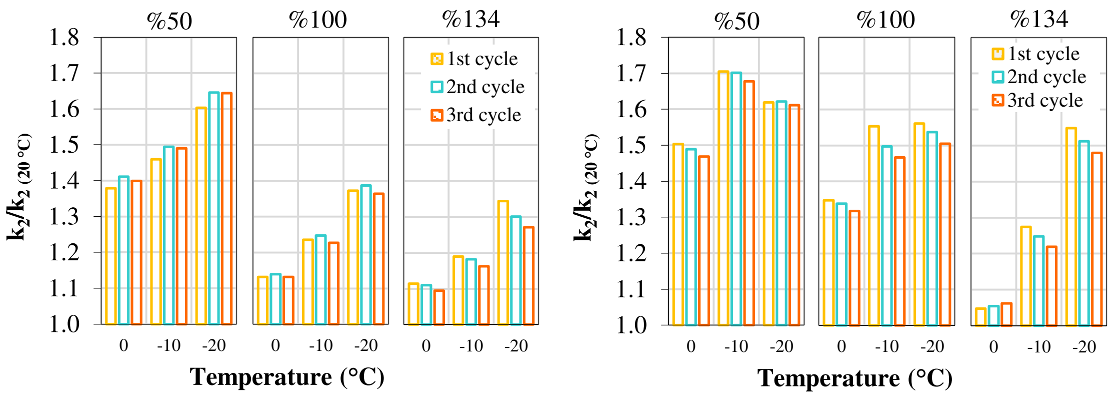

(a) (b)

Figure 2.14. *Comparison of normalized post-yield stiffnesses for (a) 0.1 Hz; and (b) 0.5 Hz loading frequency.*

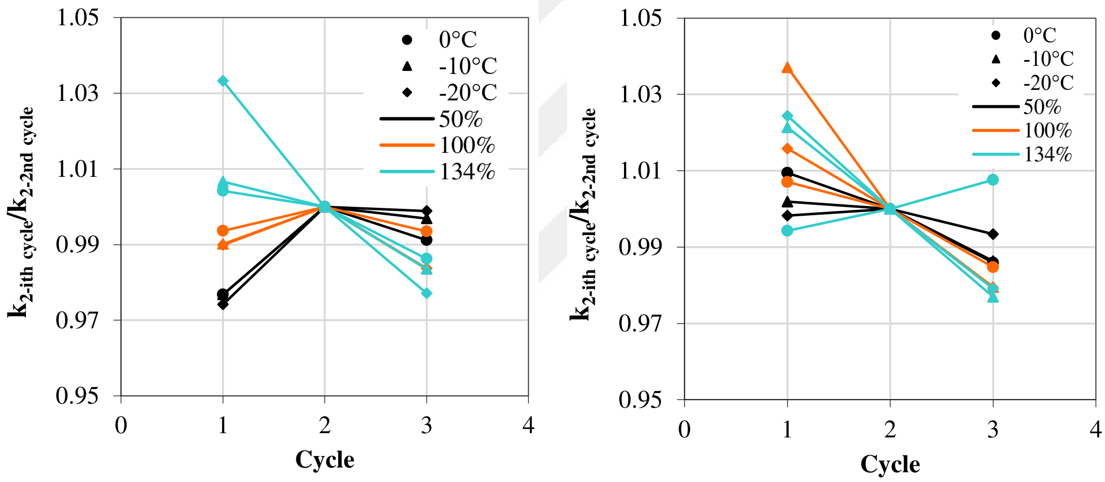

(a) (b)

Figure 2.15. *Ratio of amplification in post-yield stiffness of each cycle to that of second cycle: (a) 0.1 Hz; and (b) 0.5 Hz.*

In an attempt to investigate the variation in characteristics of the tested LRB from cycle to cycle, Figures 2.16 and 2.17 are presented for Q_i/Q_{ave} and k_i/k_{ave} ratios, respectively. Figure 2.16 shows that the range of Q_i/Q_{ave} ratios becomes more expansive as the shear strain increases for both loading frequencies. For instance, when the loading frequency is 0.1 Hz, Q_i/Q_{ave} ratios are between 0.93 and 1.10 for 50% shear strain while ranging from 0.80 to 1.24 for 134%. This indicates that the reduction in characteristic strength of the LRB from cycle-to-cycle increases with increasing shear strain. Figure 2.16 also indicates that the effect of low temperature on Q_i/Q_{ave} ratios can be neglected.

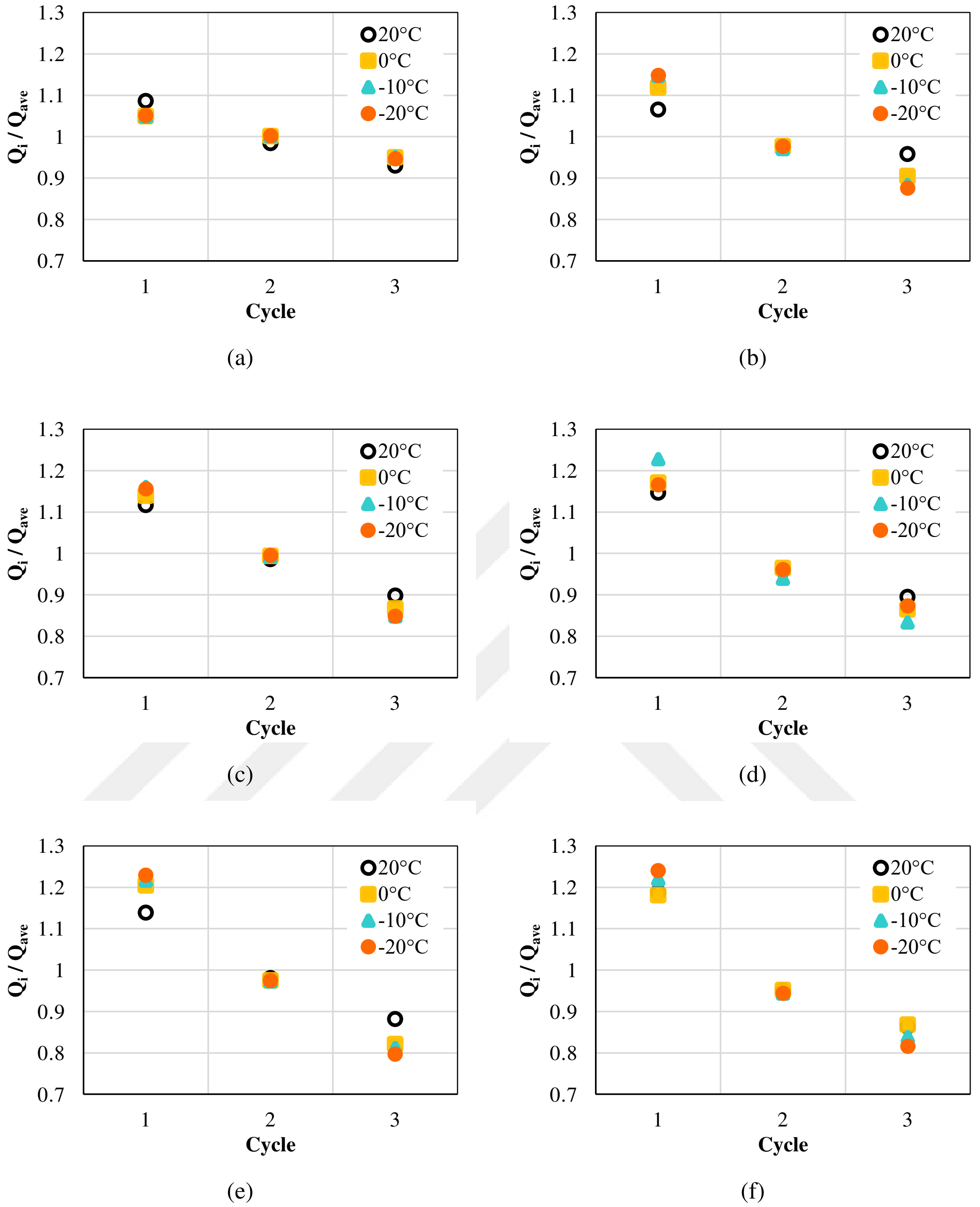

Figure 2.16. *Ratio of characteristic strength computed for each cycle to the average of three cycles (a) 50% shear strain, 0.1 Hz (b) 50% shear strain, 0.5 Hz (c) 100% shear strain, 0.1 Hz (d) 100% shear strain, 0.5 Hz (e) 134% shear strain, 0.1 Hz (f) 134% shear strain, 0.5 Hz.*

Similar to the observations for Figure 2.16, Figure 2.17 shows that the range of k_i/k_{ave} ratios becomes more expansive as the shear strain increases for both loading frequencies. For a loading frequency of 0.1 Hz, k_i/k_{ave} ratios for 50% and 134% shear strains are between 0.96-1.03 and 0.92-1.08. Although the reduction in post-yield stiffness from cycle-to-cycle also increases with increasing shear strain, they are in a minimal range compared to those computed for characteristic strength. In Figure 2.17, k_i/k_{ave} ratios calculated for different temperatures are almost indifferent to each other, indicating that the effect of low temperature can be neglected.

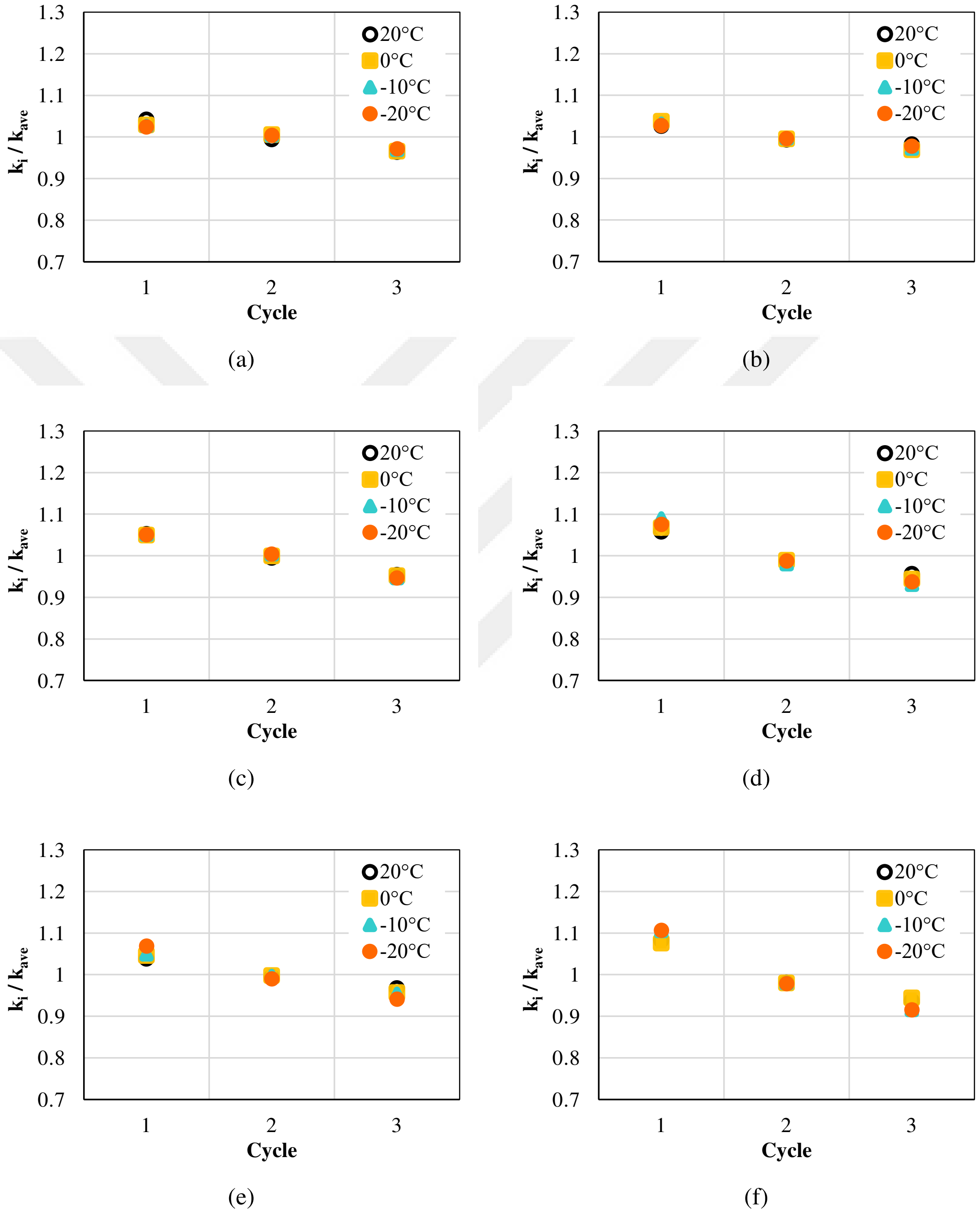

Figure 2.17. *Ratio of post-yield stiffness computed for each cycle to the average of three cycles (a) 50% shear strain, 0.1 Hz (b) 50% shear strain, 0.5 Hz (c) 100% shear strain, 0.1 Hz (d) 100% shear strain, 0.5 Hz (e) 134% shear strain, 0.1 Hz (f) 134% shear strain, 0.5 Hz.*

3. ASSESSMENT OF MECHANICAL PROPERTIES OF A LEAD RUBBER BEARING IN CASE OF DIFFERENT EXPOSURE TIMES TO LOW TEMPERATURE

3.1. Introduction

In this chapter, the effect of exposure time to low temperatures is discussed. For this purpose, the LRB, defined in the previous chapter (see Figure 2.1), was tested at temperatures of -20, -10, 0, and 20°C for 3- and 6-hours exposure times. Experiments were conducted for two levels of shear strains (100% and 134%) and loading frequencies (0.1 Hz and 0.5 Hz). The hysteretic properties obtained at -20, -10, 0, and 20°C for 3 and 6 hours were then compared with the ones calculated for a 24-hour exposure time in the previous chapter. Besides, the accuracy of existing equations to estimate the amount of amplifications in mechanical properties was evaluated through the experimental results. Finally, new equations were proposed to predict the post-yield stiffness and characteristic strength of LRB at low temperatures considering also the effect of exposure time.

Section 3.2 presents the test program followed in this chapter, whereas Section 3.3 presents the comparative experimental results. Section 3.4 evaluated the accuracy of the existing modification factors to estimate the amplifications in isolator characteristics. Ultimately, new formulations to predict the change in mechanical properties, namely, post-yield stiffness and characteristic strength of lead rubber bearings (LRBs) at low ambient temperatures, are proposed in Section 3.5.

3.2. Test Program

The LRB under investigation has a diameter of 850 mm with a lead core of 220 mm in diameter, as described in Section 2.2. The loading protocol followed in this section is developed based on the information provided in Section 2.4. However, a shear strain of 50% was not considered in the loading protocol, as we observed that the isolator behavior remains within elastic limits under this displacement limit. The applied test protocol is given in Table 3.1.

Table 3.1. *Loading protocol followed in the experimental program to investigate the effect of the exposure time.*

Test No	Temperature	Exposure Time (hour)	Shear Strain (%)	Frequency (Hz)	Cycle Number
1	20ºC	-	100, 134	0.1, 0.5	3
2	0ºC	3, 6	100, 134	0.1, 0.5	3
3	-10ºC	3, 6	100, 134	0.1, 0.5	3
4	-20ºC	3, 6	100, 134	0.1, 0.5	3

During the tests, three cycles of sinusoidal motion were applied to the LRB as shown in Figure 3.1(a) and (b) for loading frequencies of 0.1 and 0.5 Hz, respectively. The vertical force acting on the LRB during the cyclic motion was 3177 kN, corresponding to a normal stress of 5.8 MPa.

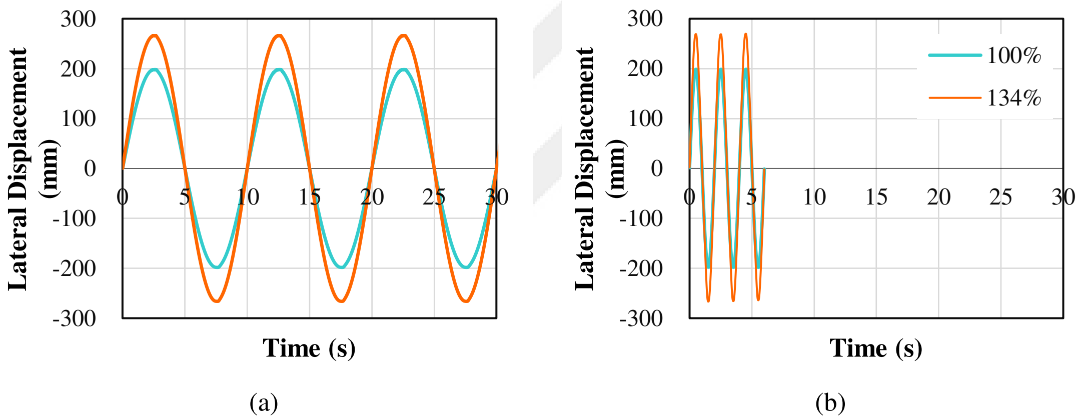

Figure 3.1. *Applied loading history to lead rubber bearing for a frequency of (a) 0.1 Hz (b) 0.5 Hz.*

3.3. Experimental Results

In this section, recorded hysteretic curves will be presented for comparative analysis. However, before proceeding, it is essential to confirm that the LRB has not experienced any permanent deformation after all the loading sequences outlined in Tables 2.2 and 3.1. To verify this, photographs of the LRB taken both before the initial loading and after the final loading cases are shown in Figure 3.2. Besides, as shown in Figure 3.3, having almost identical reference force-displacement curves reveals that the cyclic response of the LRB remains almost the same after the testing campaign was completed. Thus, testing the same LRB at all loading cases defined in Table 2.2 and 3.1 did not introduce any bias.

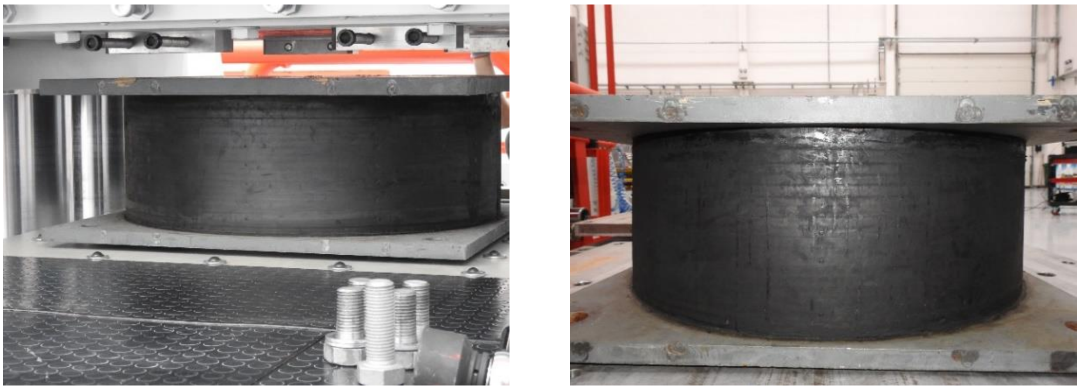

(a) (b)

Figure 3.2. *Physical condition of the LRB (a) before the initial loading and (b) after the final loading cases.*

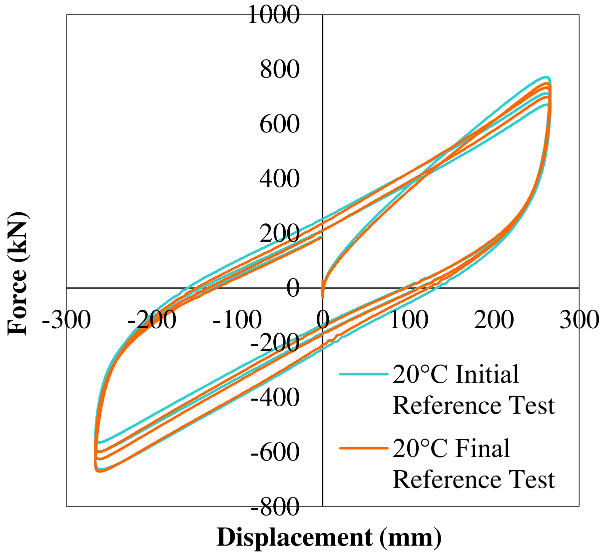

Figure 3.3. *Comparison of reference force-displacement curves of the LRB.*

Figures 3.4 and 3.5 depict the force-displacement curves recorded under different shear strains and ambient temperatures for exposure times of 3, 6, and 24 hours. The curves presented for the 24-hour exposure were obtained in the previous chapter. To reveal the effect of exposure time to low temperatures, those results are compared with the results recorded for the 3- and 6-hour exposure times in this chapter. It is evident that both the strength and lateral stiffness of the LRB tend to increase, regardless of the loading frequency, when the ambient temperature decreases. Another observation is that the hysteretic behavior of the LRB is sensitive to exposure time at low temperatures.

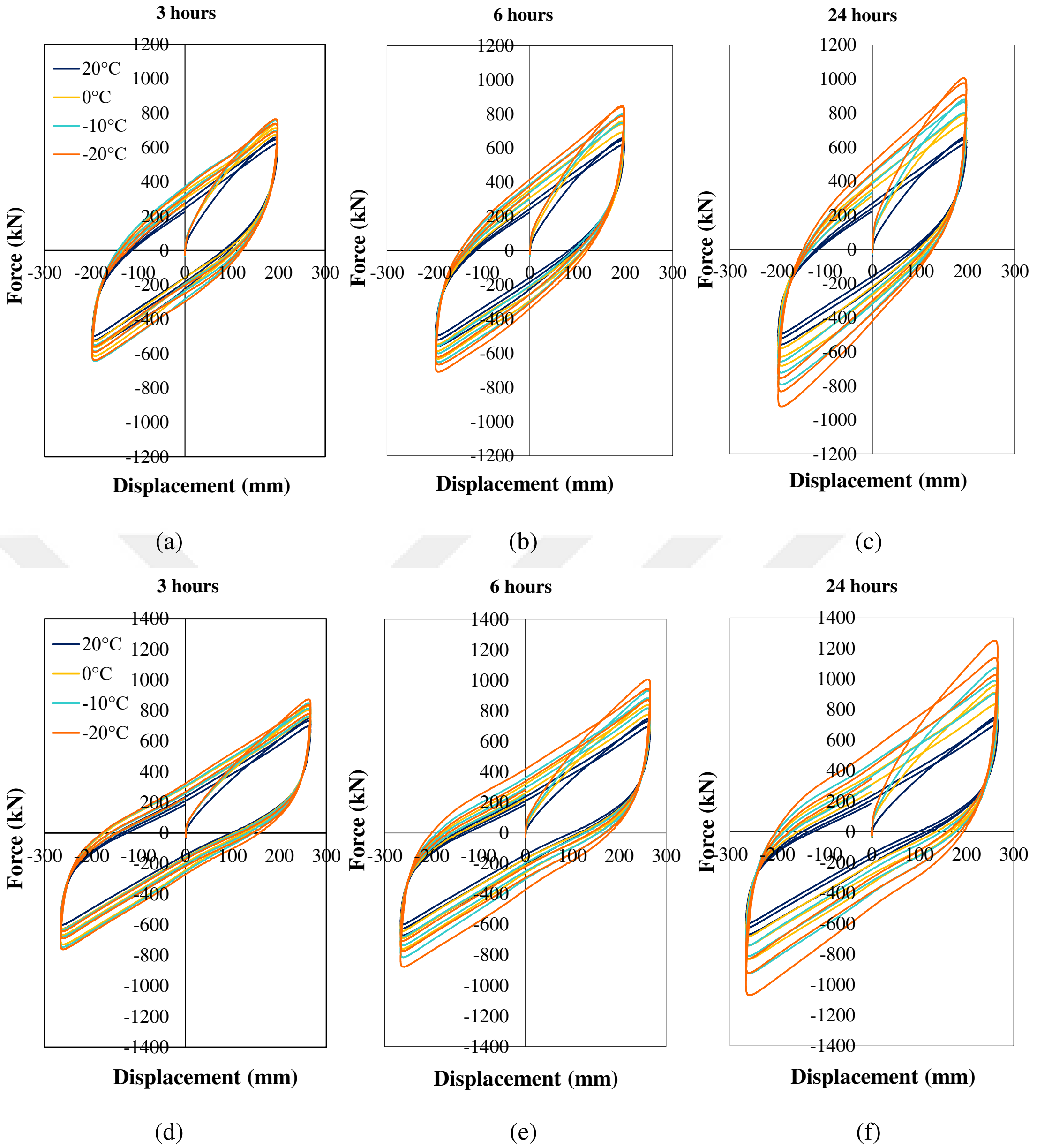

Figure 3.4. *Comparison of force-displacement curves obtained for different shear strains, temperatures and exposure times at loading frequency of 0.1 Hz for (a), (b) and (c) 100% shear strains (d), (e) and (f) 134% shear strains.*

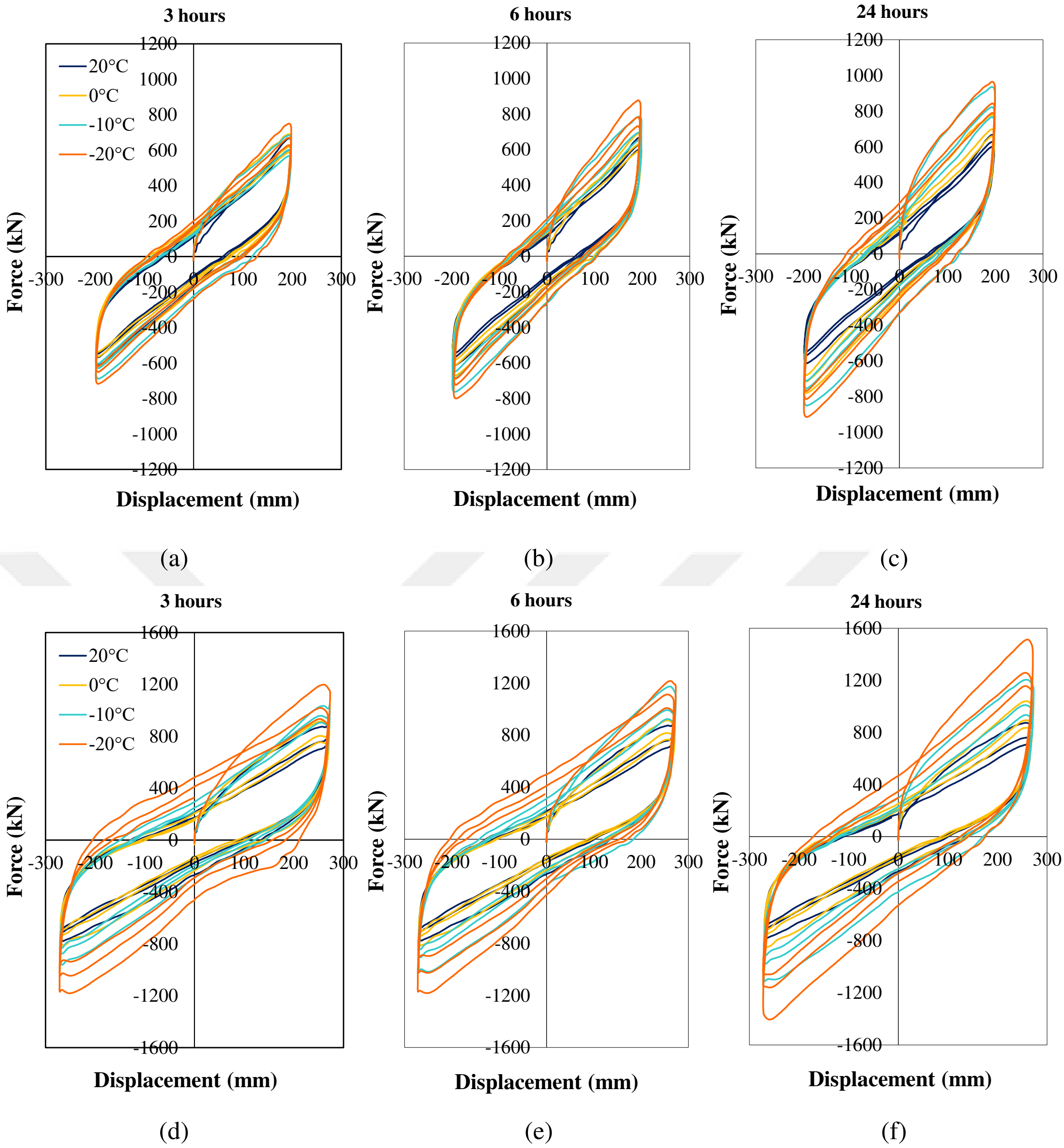

Figure 3.5. *Comparison of force-displacement curves obtained for different shear strains, temperatures and exposure times at loading frequency of 0.5 Hz for (a), (b) and (c) 100% shear strains (d), (e) and (f) 134% shear strains.*

In order to better reveal the trend of change in isolator mechanical properties, characteristic strength, Q and post-elastic stiffness, k_2 (see Figure 1.2 for definitions) of the LRB were obtained using recorded force-displacement curves. Q and k_2 are calculated by the straight-line fit method suggested by EN-15129 (2018). In this study, the Least Square Method (LSM) is used to find the best fit for data by minimizing the sum of the squared errors as defined in Figure 2.10. Tables 3.2 and 3.3 present the corresponding isolator characteristics calculated for different loading cases.

Table 3.2. *Mechanical properties of LRB computed at the frequency of 0.1 Hz.*

	Temperature (°C)	-20			-10			0			20
	Exposure Time (hour)	3	6	24	3	6	24	3	6	24	-
100% Shear Strain	k2 (1st cycle), kN/m	2286	2564	3054	2288	2442	2748	2234	2312	2518	2224
	k2 (2nd cycle), kN/m	2196	2525	2919	2177	2368	2626	2127	2236	2398	2104
	k2 (3rd cycle), kN/m	2124	2404	2752	2101	2262	2476	2046	2143	2284	2017
	Q (1st cycle), kN	296	344	433	298	310	373	269	291	321	222
	Q (2nd cycle), kN	253	305	373	255	267	319	232	250	280	196
	Q (3rd cycle), kN	224	268	318	224	230	272	206	219	244	178
134% Shear Strain	k2 (1st cycle), kN/m	1941	2080	2450	1914	1987	2168	1908	1934	2031	1822
	k2 (2nd cycle), kN/m	1848	1984	2270	1829	1916	2062	1815	1848	1936	1745
	k2 (3rd cycle), kN/m	1781	1904	2158	1768	1841	1973	1757	1784	1858	1697
	Q (1st cycle), kN	297	385	493	282	331	413	272	294	352	226
	Q (2nd cycle), kN	244	306	391	234	272	330	229	240	285	194
	Q (3rd cycle), kN	209	254	320	204	231	276	201	206	240	175

Table 3.3. *Mechanical properties of LRB computed at the frequency of 0.5 Hz.*

	Temperature (°C)	-20			-10			0			20
	Exposure Time (hour)	3	6	24	3	6	24	3	6	24	-
100% Shear Strain	k2 (1st cycle), kN/m	2431	2928	3122	2303	2694	3106	2254	2373	2695	2000
	k2 (2nd cycle), kN/m	2251	2687	2866	2155	2452	2792	2113	2221	2496	1865
	k2 (3rd cycle), kN/m	2158	2568	2721	2070	2331	2652	2033	2122	2382	1808
	Q (1st cycle), kN	223	241	307	198	223	277	183	191	215	156
	Q (2nd cycle), kN	185	194	253	166	181	212	156	162	177	131
	Q (3rd cycle), kN	170	174	230	153	165	188	143	147	158	122
134% Shear Strain	k2 (1st cycle), kN/m	2529	2700	3271	2456	2620	2693	2153	2163	2214	2113
	k2 (2nd cycle), kN/m	2415	2506	2892	2319	2337	2388	1965	1990	2017	1914
	k2 (3rd cycle), kN/m	2275	2333	2707	2227	2197	2230	1897	1915	1943	1829
	Q (1st cycle), kN	477	472	490	315	350	368	243	239	256	237
	Q (2nd cycle), kN	389	393	373	260	277	284	191	193	206	190
	Q (3rd cycle), kN	330	333	322	237	246	253	171	178	188	172

In Tables 3.2 and 3.3, the results obtained for 20°C are considered reference values. In order to have clear observations in terms of amplification in mechanical properties of the tested LRB at low temperatures (-20°C, -10°C, and 0°C), experimental data was normalized with the ones obtained from the reference tests. Accordingly, Figures 3.6 and 3.7 illustrate the normalized characteristic strength $Q/Q_{(20°C)}$ at ambient temperatures of -20, -10, and 0°C for 0.1 and 0.5 Hz loading frequencies, respectively. Figures 3.6 and 3.7 clearly show that the characteristic strength, Q, of the LRB increases with decreasing temperature. The increase becomes more pronounced with longer exposure times at all temperatures. It is apparent that the time of exposure to low temperatures has a significant impact on the amplification of the LRB strength.

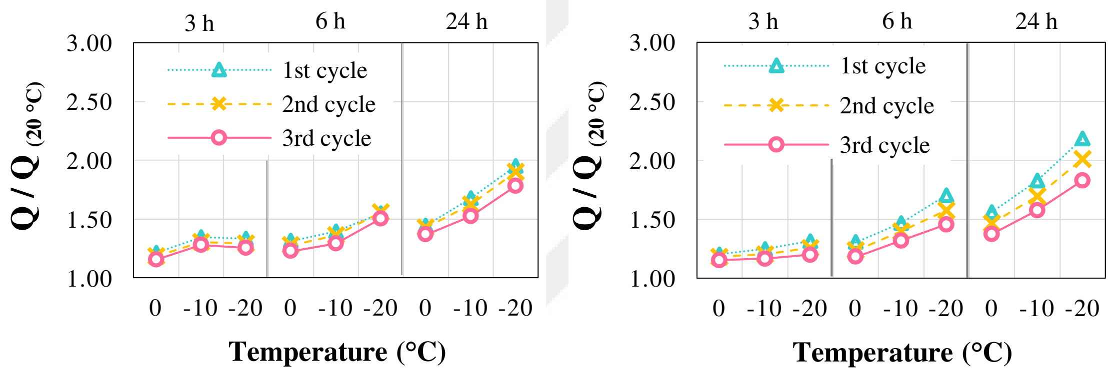

(a) (b)

Figure 3.6. *Comparison of normalized characteristic strengths for 0.1 Hz loading frequency at (a) 100% and (b) 134% shear strains.*

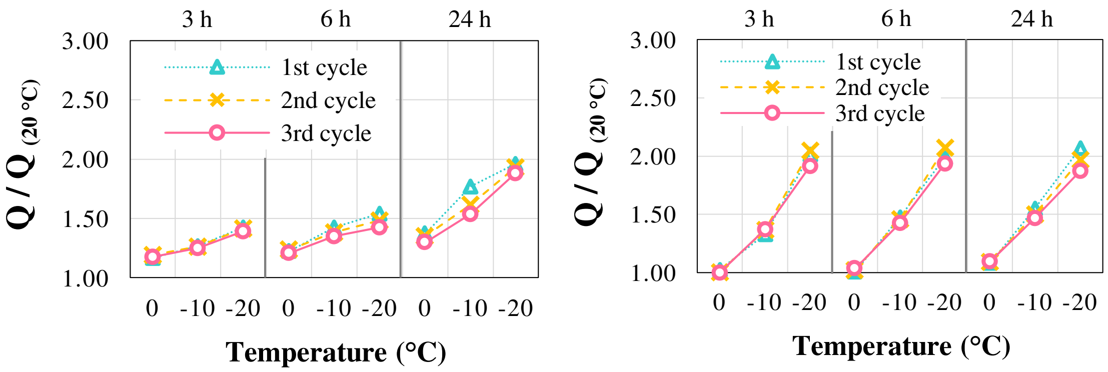

(a) (b)

Figure 3.7. *Comparison of normalized characteristic strengths for 0.5 Hz loading frequency at (a) 100% and (b) 134% shear strains.*

In Figure 3.6, it is also observed that the amplification in LRB strength tends to decrease with the increasing number of loading cycles. Such observation can be ascribed to the temperature rises at the lead core of LRB during cyclic motion. Kalpakidis et al. (2008) revealed that the strength of an LRB deteriorates during cyclic motion as a function of the lead core heating. The rise in temperature at the lead core will result in a thermal transient, and the corresponding temperature of the lead core at each loading cycle will increase gradually. For instance, for the loading case where the temperature is -20°C and the exposure time is 24 hours, the lead core temperature will be close to -20°C at the first cycle. However, because of the rise in temperature at the lead core, it will be greater than -20°C in the second and third cycles. Accordingly, the amplifications in the strength of LRB with respect to the reference case will decrease with the increasing number of cycles. Apart from Figure 3.6, in Figure 3.7, the change in $Q/Q_{(20°C)}$ ratios from cycle-to-cycle is minimal, especially for 134% shear strain. For the data presented in Figure 3.7, the loading velocity is five times larger than the one in Figure 3.6. In the 0.5 Hz loading frequency case, the maximum loading velocities were 622 and 835 mm/s for 100 and 134% shear strains, respectively. Moreover, the temperature rise in the lead core will be much higher compared to loading cases with a 0.1 Hz frequency. As a result, the gradual deterioration in the strength of LRB will be higher at each cycle and has a very close trend with the deterioration in the reference test (see Figure 3.8). Thus, the corresponding amplifications in the strength of LRB (or $Q/Q_{(20°C)}$ ratios) at each loading cycle get almost identical values, as presented in Figure 3.7.

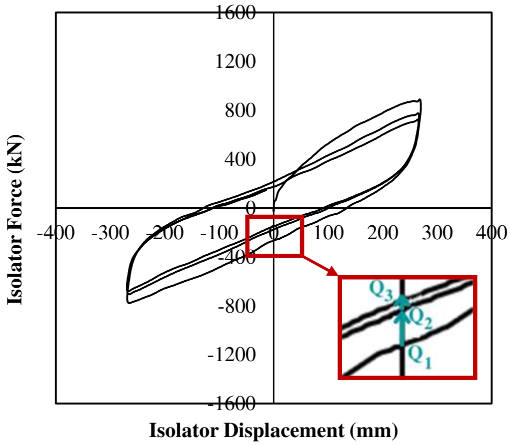

(a)

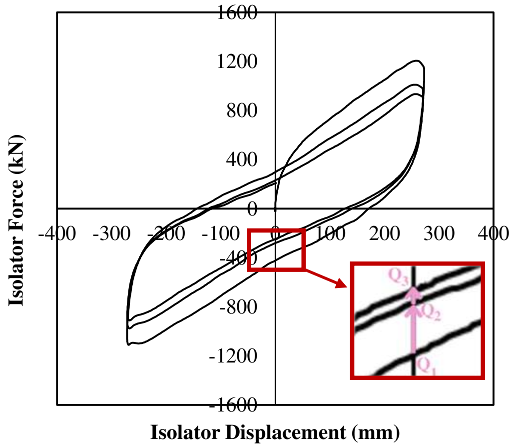

(b)

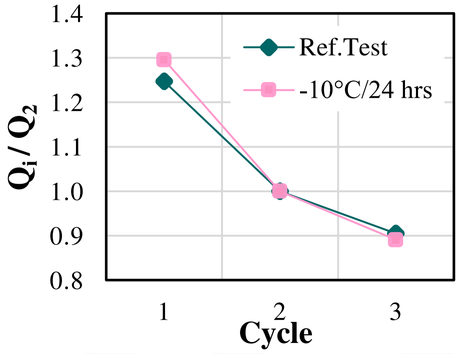

(c)

Figure 3.8. *Force-displacement curves of the LRB for 134% shear strain and 0.5 Hz loading frequency (a) reference test (b) 24 hrs exposure time at -10°C, (c) ratio of characteristic strength each cycle to that of the second cycle.*

Figures 3.9 and 3.10 show the amplifications in post-yield stiffness of the LRB for different temperatures and exposure times. Post-yield stiffnesses computed for each temperature and exposure time are normalized with the ones calculated for 20°C, $k_2/k_{2(20°C)}$. Similarly, Figures 3.9 and 3.10 indicate that $k_2/k_{2(20°C)}$ ratios increase with decreasing temperature and increasing exposure time. However, the amplifications in post-yield stiffness are less than those computed for characteristic strength. Furthermore, $k_2/k_{2(20°C)}$ ratios are almost not sensitive to changes in lead core temperature during the cyclic motion and remain the same at all cycles. This is because the thermal conductivity of rubber (0.16 W/mK) is very low compared to lead (35.3 W/mK). Hence, the rise in the temperature of the lead core does not change the temperature of the rubber layers during the test. Such observation is also parallel to the findings of Kalpakidis et al. (2008). It is also noted that amplifications in post-yield stiffness due to low-temperature exposure are higher for loadings with 0.5 Hz frequency compared to those with 0.1 Hz frequency.

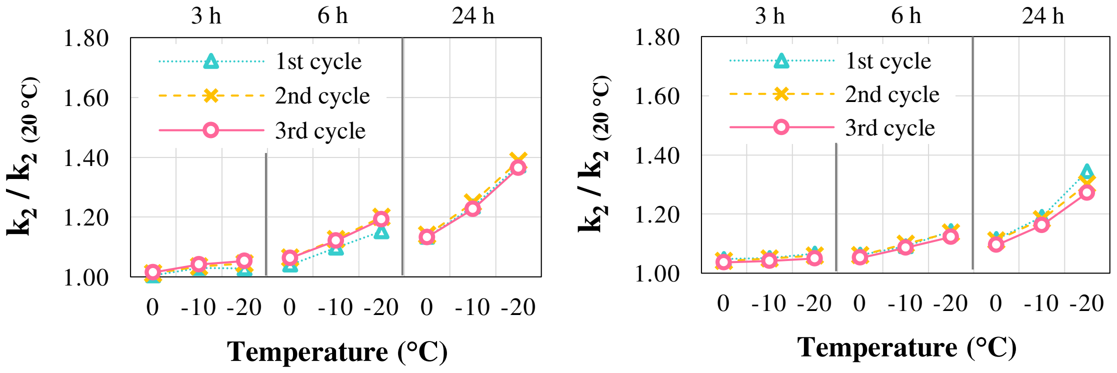

(a) (b)

Figure 3.9. *Comparison of normalized post-yield stiffness for 0.1 Hz loading frequency at (a) 100% and (b) 134% shear strains.*

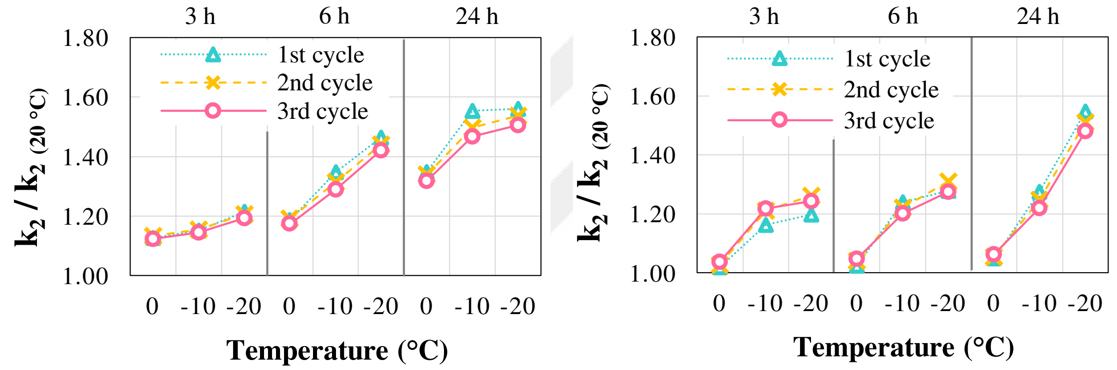

(a) (b)

Figure 3.10. *Comparison of normalized post-yield stiffness for 0.5 Hz loading frequency at (a) 100% and (b) 134% shear strains.*

3.4. Accuracy of the Existing Modification Factors to Estimate the Amplifications in Isolator Characteristics

In the literature, there are studies that proposed modification factors to estimate the variation in mechanical properties of LRBs exposed to low temperatures. In this section, three of those studies (see Table 3.4) are cited to evaluate their accuracy in estimating the amplifications in both characteristic strength and post-yield stiffness. The reason for considering the proposals of Constantinou et al. (2007), Li et al. (2009) and Park et al. (2012) is that they were conducted with large-size LRBs having similar dimensions to the LRB tested in this research. Table 3.4 presents the amplification factors suggested for both characteristic strength and post-yield stiffness. Figures 3.11-3.14 compare the experimentally calculated amplifications of the current study with the proposals of the studies cited above. Figures 3.11 and 3.12 compare characteristic strength, Q, for loading frequencies of 0.1 and 0.5 Hz, respectively. In these figures, for 100% shear strain, it is clear that regardless of the loading frequency, the proposals given in Table 3.4 are consistent with the test results for all considered temperatures when the exposure time is 3 and 6 hrs. However, for an exposure time of 24 hours, proposed amplification factors underestimate the computed ones. Moreover, the amount of underestimation increases with decreasing temperature. When the shear strain is 134%, the loading frequency seems to affect the accuracy of the proposed factors. For 0.1 Hz frequency, they provide close estimations for 3 and 6 hours of exposure times. However, their estimations lack representing the actual behavior when the exposure time is 24 hours for all considered temperatures. For 0.5 Hz frequency, cited proposals lead to close or overestimated amplifications for -10 and 0°C while they underestimate the amplification in Q for all of the exposure times at -20°C.

Table 3.4. *Amplification factors suggested in literature for different temperatures.*

	Parameters	**Temperature**		
		0°C	**-10°C**	**-20°C**
Constantinou et al. (2007)	Q	1.20	1.40	-
	k_2	1.10	1.10	-
Li et al. (2009)	Q	1.22	1.32	1.45
	k_2	1.04	1.10	1.14
Park et al. (2012)	Q	1.19	1.30	1.42
	k_2	1.06	1.08	1.11

‘‘-’’ means there is no available amplification factor

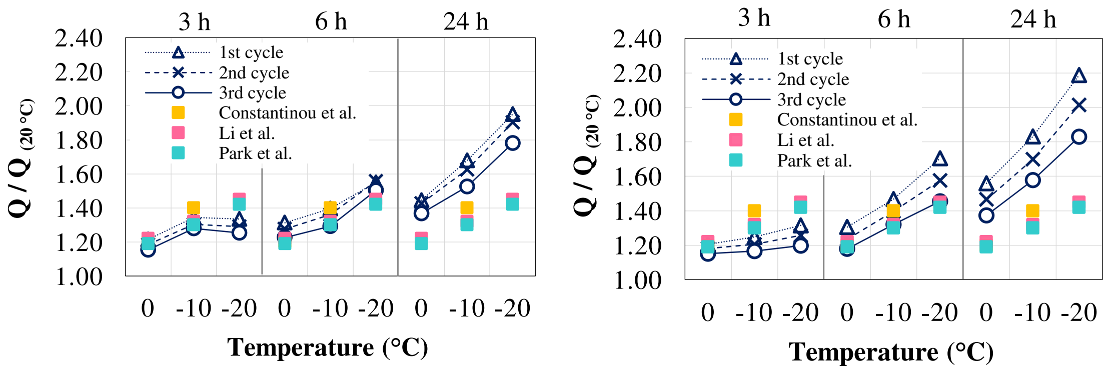

(a) (b)

Figure 3.11. *Comparison of amplifications in Q with the available amplification factors in literature for a loading frequency of 0.1 Hz, at (a) 100% and (b) 134% shear strains.*

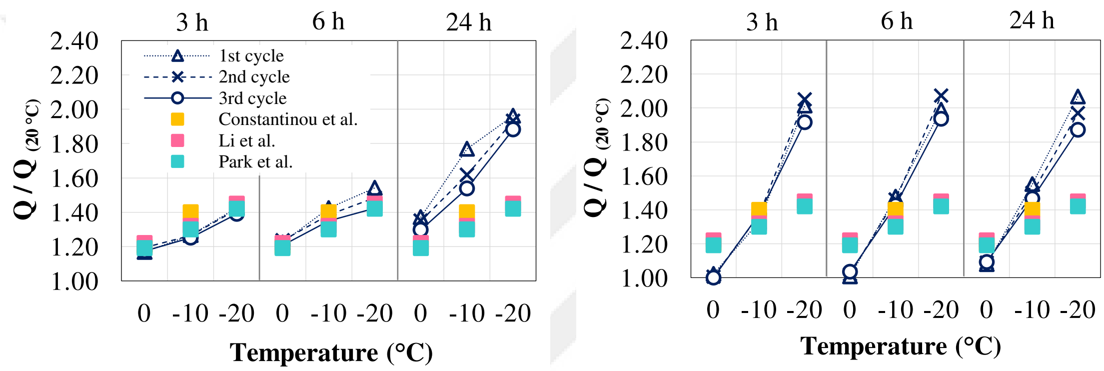

(a) (b)

Figure 3.12. *Comparison of amplifications in Q with the available amplification factors in literature for a loading frequency of 0.5 Hz, at (a) 100% and (b) 134% shear strains.*

Figures 3.13 and 3.14 compare the estimations of amplification factors given in Table 3.4 with the experimental data in terms of post-yield stiffness, k_2. Figure 3.13 presents results that are very similar to those for characteristic strength. The amplification factors in Table 3.4 give very close estimations for all temperatures when the exposure time is 3 and 6 hours. On the other hand, they underestimate the experimental data for 24 hours of exposure time. In Figure 3.14, where the loading frequency is 0.5 Hz, the amplifications in post-yield stiffness are underestimated for almost all of the temperatures and exposure times. Furthermore, the amount of underestimation tends to increase with decreasing temperature and increasing exposure time.

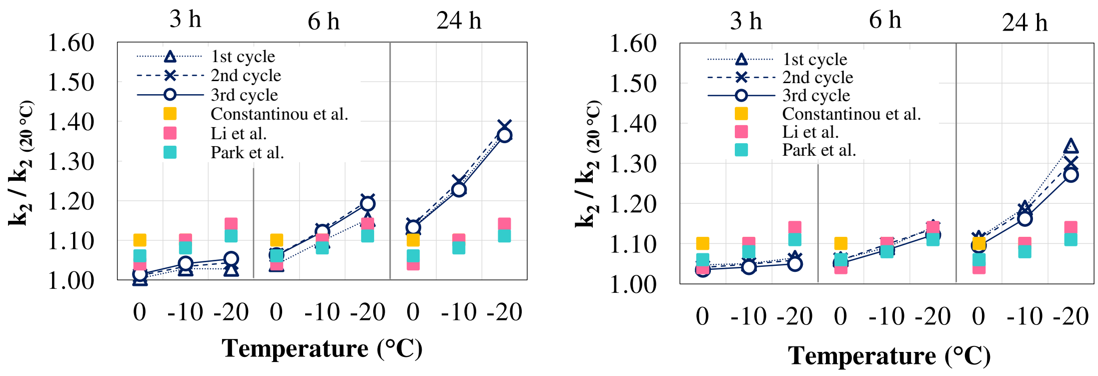

(a) (b)

Figure 3.13. *Comparison of amplifications in k_2 with the estimations of amplification factors in literature for a loading frequency of 0.1 Hz, at (a) 100% and (b) 134% shear strains.*

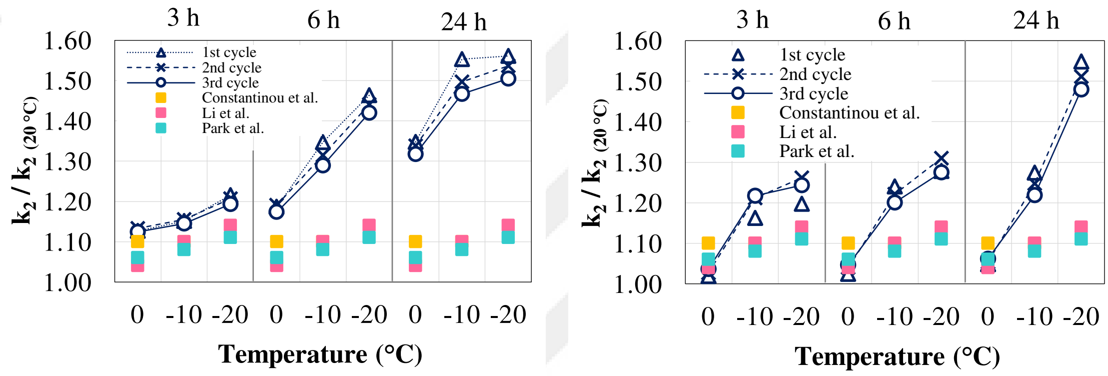

(a) (b)

Figure 3.14. *Comparison of amplifications in k_2 with the estimations of amplification factors in literature for loading frequency of 0.5 Hz, at (a) 100% and (b) 134% shear strains.*

The American Association of State Highway and Transportation Officials (AASHTO, 2014) and the Turkish Seismic Isolated Bridge Design Specifications (SIBDS, 2020) have proposed amplification factors to account for the influence of low temperatures on the hysteretic behavior of LRBs. In this section, these amplification factors, as presented in Table 3.5, are also examined.

Table 3.5. *Amplification factors recommended in the specifications for various temperatures.*

	Parameters	**Temperature**		
		0°C	**-10°C**	**-20°C**
AASHTO (2014)	Q	1.30	1.40	1.45
	k_2	1.10	1.10	1.20
SIBDS (2020)	Q	1.00	1.00	1.00
	k_2	1.10	1.10	1.20

Figures 3.15 and 3.16 compare the characteristic strength, Q, for loading frequencies of 0.1 and 0.5 Hz, respectively. These figures illustrate that, according to the Turkish Seismic Isolated Bridge Design Specifications (SIBDS, 2020), the characteristic strength of the LRB remains unaffected by exposure to low temperatures. On the other hand, the recommendations from the American Association of State Highway and Transportation Officials (AASHTO, 2014) are generally consistent with the experimental results obtained for a loading frequency of 0.1 Hz when the exposure time is 3 and 6 hours. For the loading frequency of 0.5 Hz, the same observation is valid for the shear strain of 100%. However, at a shear strain of 134%, the trends of the obtained and recommended values diverge, except at a temperature of -10°C.

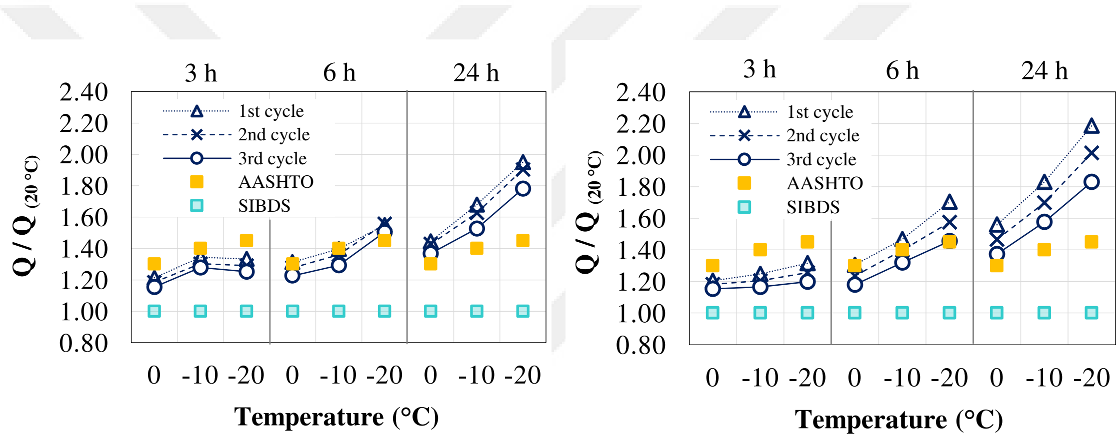

(a) (b)

Figure 3.15. *Comparison of the amplification factors in Q with those recommended in the specifications for a loading frequency of 0.1 Hz, at (a) 100% and (b) 134% shear strains.*

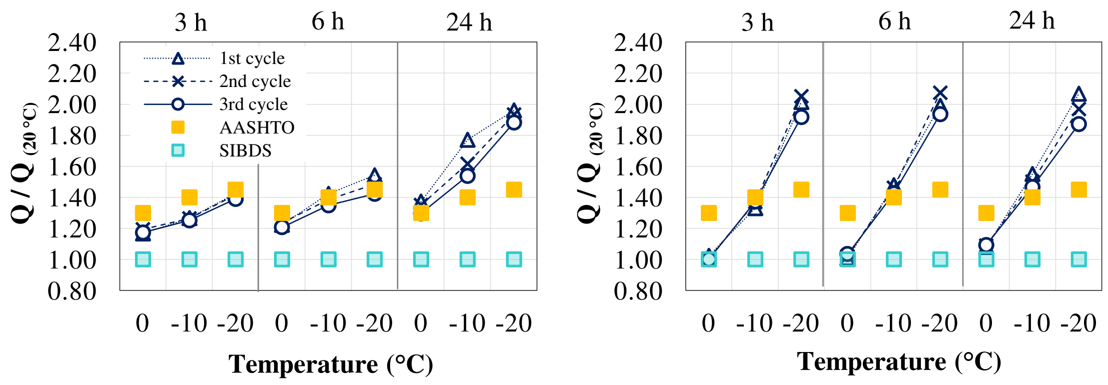

(a) (b)

Figure 3.16. *Comparison of the amplification factors in Q with those recommended in the specifications for a loading frequency of 0.5 Hz, at (a) 100% and (b) 134% shear strains.*

Figures 3.17 and 3.18 compare the amplification factors recommended by the specifications listed in Table 3.5 with experimental data in terms of post-yield stiffness, k_2. According to Figure 3.17, the amplification factors in Table 3.5 tend to overestimate the experimental data at all temperatures for an exposure time of 3 hours, while providing estimates that are very close to the experimental data for an exposure time of 6 hours. Conversely, for an exposure time of 24 hours, the amplification factors underestimate the experimental data at temperatures of -10°C and -20°C, regardless of the shear strain. The experimental values become higher as the loading frequency increases to 0.5 Hz, as seen in Figure 3.18. For a shear strain of 100%, the amplifications in post-yield stiffness are underestimated at almost all temperatures for exposure times of 6 and 24 hours, while a good estimation is observed for an exposure time of 3 hours. In Figure 3.18(b), when the shear strain is 134%, the recommended values overestimate the experimental data at 0°C for all exposure times, while they underestimate the experimental data at -10°C and -20°C.

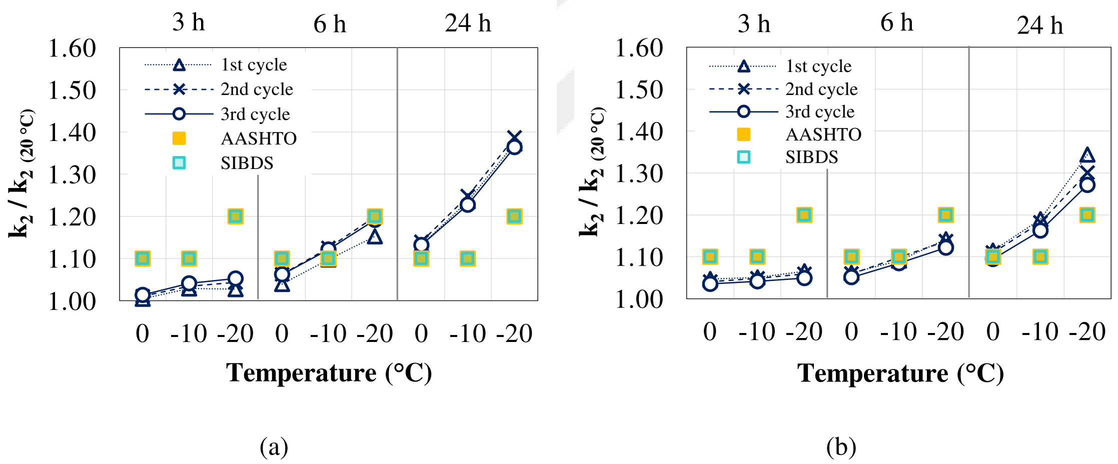

Figure 3.17. *Comparison of the amplification factors in k_2 with those recommended in the specifications for a loading frequency of 0.1 Hz, at (a) 100% and (b) 134% shear strains.*

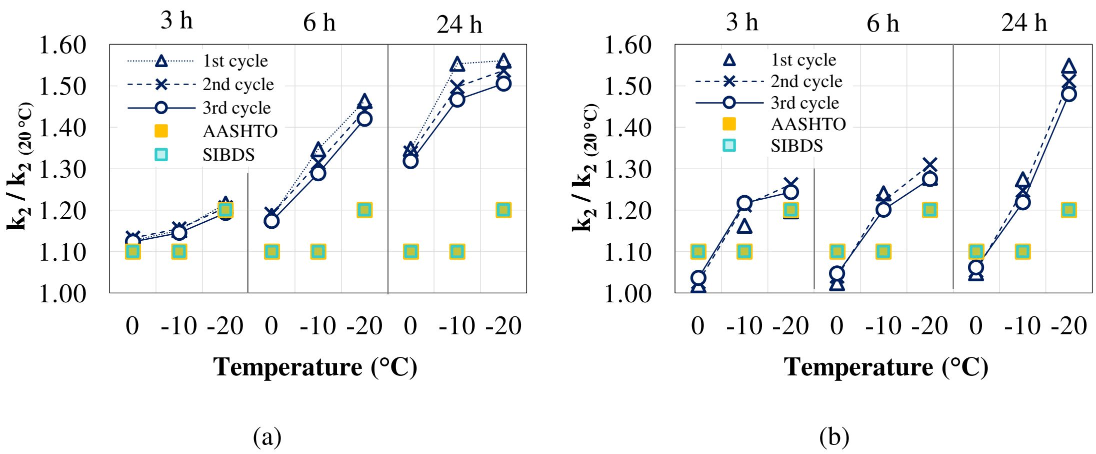

Figure 3.18. *Comparison of the amplification factors in k_2 with those recommended in the specifications for a loading frequency of 0.5 Hz, at (a) 100% and (b) 134% shear strains.*

Figures 3.11–3.18 reveal that the existing proposals in the literature and specifications for estimating the amplification of characteristic strength in LRBs exposed to low temperatures need improvement to account for the effects of exposure time. Similarly, observations clearly indicate that the cited proposals for estimating amplification in post-yield stiffness of LRBs do not address the effects of exposure time and loading frequency. It should be noted that these findings are limited to the isolators tested in this study and the loading protocol considered.

3.5. Proposed Formulations to Consider Also the Effects of Exposure Time and Loading Frequency

This section proposes empirical relations to predict the amplifications in both characteristic strength and post-yield stiffness of LRBs due to low-temperature exposure. The proposed formulations were derived by extending the equations provided in the Turkish Seismic Isolated Bridge Design Specifications (SIBDS, 2020) for various temperature intervals. The equations from the Turkish Seismic Isolated Bridge Design Specifications are presented in Table 3.6. This section aims to improve the existing formulations by incorporating exposure time as an additional parameter.

Table 3.6. *The formulations proposed by the Turkish Seismic Isolated Bridge Design Specifications (SIBDS, 2020).*

	Temperature interval	Q	k_2
λ_{sc}	-30°C ≤ T_{min} < -10°C	1.0	1.0+0.01|T_{min}|
	-10°C ≤ T_{min} < 0°C	1.0	1.1
	0°C ≤ T_{min} < 20°C	1.0	1.1-0.005|T_{min}|

In this study, a multiple linear regression model was developed using the experimental data. This model was used to estimate the ratios $Q/Q_{(20°C)}$ and $k_2/k_{2(20°C)}$ for LRBs exposed to low temperatures. To achieve this, the dependent and independent variables were first defined for the model. The loading parameters from the experiments, specifically temperature (T) and exposure time (t), serve as the independent variables. The corresponding amplification values for each loading combination (see Figures 3.6–3.7 and 3.9–3.10) constitute the dependent variables. For characteristic strength, the derived equations are identical for both loading frequencies due to the relatively similar amplification effects observed. In contrast, loading frequency has an impact on the amplification of post-yield stiffness. Consequently, two separate empirical relations have been proposed to account for this effect. The derived equations are given in Table 3.7 and 3.8 for characteristic strength and post-yield stiffness, respectively. The R^2 values, which serve as a statistical measure of the goodness-of-fit for the regression line to the observed data at the point of termination of each regression analysis, are presented in Table 3.9. The accuracy of the proposed formulations to estimate the amplifications in characteristic strength and post-yield stiffness of the tested LRB is discussed by means of Figures 3.19-3.22.

Table 3.7. *The proposed empirical expressions for LRB's characteristic strength at low ambient temperatures.*

Loading Frequency	Temperature Interval	Characteristic Strength, $Q/Q_{(20°C)}$
0.1 and 0.5 Hz	-30°C ≤ T < -10°C	1.0+0.02|T|+0.02t
	-10°C ≤ T < 0°C	1.3+0.015t
	0°C ≤ T < 20°C	1.2-0.005|T|+0.005t

*T: temperature (°C), t: exposure time (hour)

Table 3.8. *The proposed empirical expressions for LRB's post-yield stiffness at low ambient temperatures.*

Loading Frequency	Temperature Interval	Post-Yield Stiffness, $k_2/k_{2(20°C)}$
0.1 Hz	-30°C ≤ T < -10°C	1.0+0.01|T|+0.005t
	-10°C ≤ T < 0°C	1.1+0.005t
	0°C ≤ T < 20°C	1.1-0.005|T|
0.5 Hz	-30°C ≤ T< -10°C	1.0+0.01|T|+0.015t
	-10°C ≤ T < 0°C	1.15+0.01t
	0°C ≤ T< 20°C	1.1-0.005|T|+0.005t

*T: temperature (°C), t: exposure time (hour)

Table 3.9. *R^2 values of the regression analyses.*

Mechanical Property	Loading Frequency	R^2
Q	0.1 Hz and 0.5 Hz	0.83
k_2	0.1 Hz	0.89
	0.5 Hz	0.87

Figures 3.19 and 3.20 compare the experimental results and computed estimations using formulations in terms of characteristic strength. Accordingly, experimental and estimated values generally do not differ by more than 10%. However, for loading combination at a loading frequency of 0.5 Hz and 134% shear strain, there are differences on the order of 25%. In this loading combination, the corresponding amplifications in the strength of the LRB (or $Q/Q_{(20°C)}$ ratios) at each exposure time result in nearly identical values, as shown in Figure 3.20(b). This can be attributed to the heating of the lead core, which is more significant compared to the other loading combinations (Figure 3.19 and Figure 3.20.a). Consequently, for this combination, the effect of lead core heating is more dominant than the effect of low temperatures in the experimental results. Regarding post-yield stiffness, there is generally good consistency, with differences typically less than 10%, as illustrated in Figures 3.21 and 3.22. Only three comparisons exceed this 10% threshold. Consequently, it can be concluded that the proposed formulations are largely effective in predicting the mechanical properties of the LRB tested in this study under various low

ambient temperatures and exposure times. These conclusions are based on the specific loading protocols used in this study.

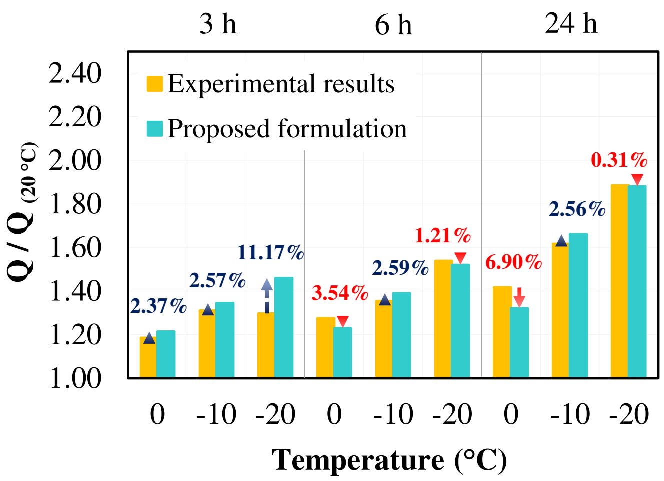

(a)

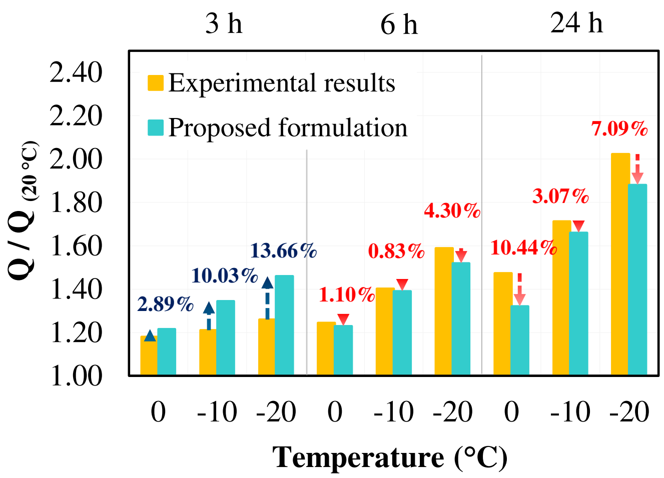

(b)

Figure 3.19. *Comparison of experimental amplifications in Q with the proposed formulation estimations for 0.1 Hz loading frequency at (a) 100% and (b) 134% shear strains.*

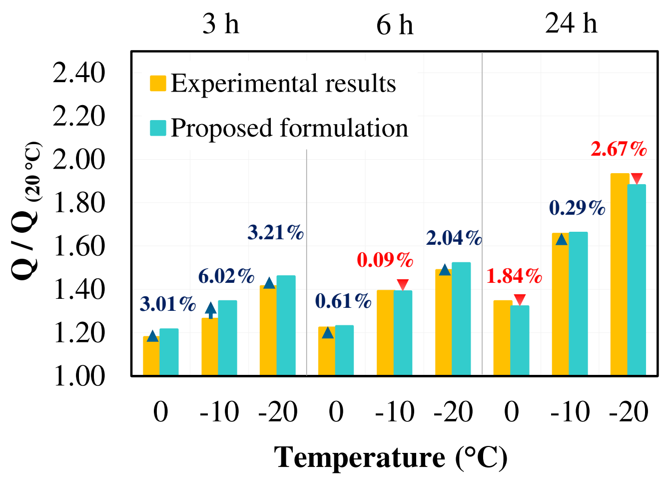

(a)

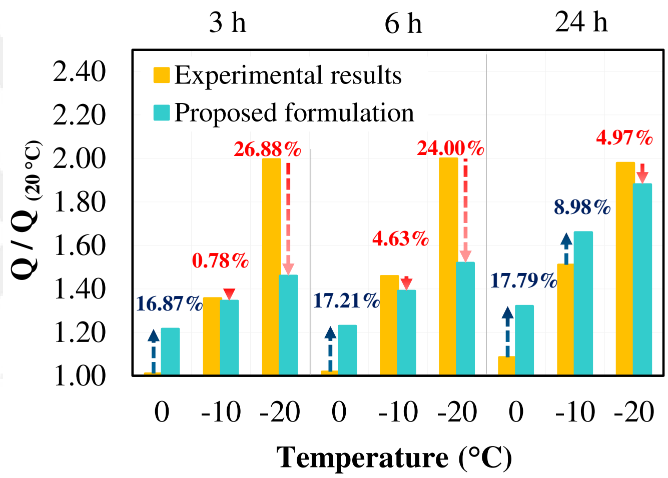

(b)

Figure 3.20. *Comparison of experimental amplifications in Q with the proposed formulation estimations for 0.5 Hz loading frequency at (a) 100% and (b) 134% shear strains.*

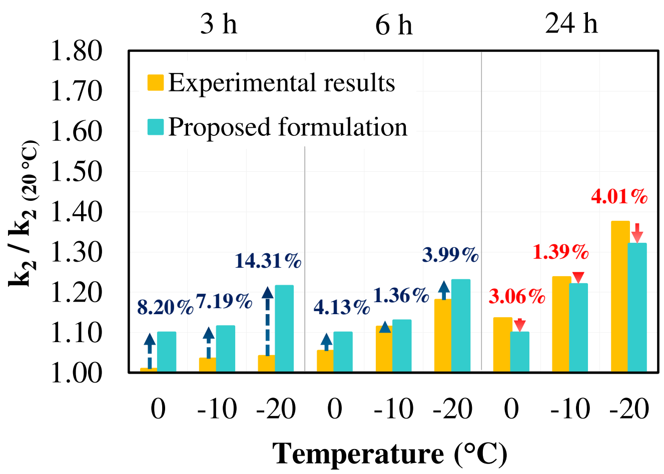

(a)

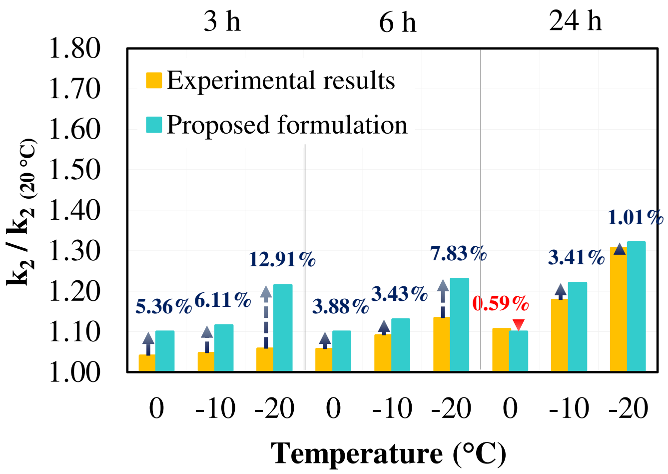

(b)

Figure 3.21. *Comparison of experimental amplifications in k_2 with the proposed formulation estimations for 0.1 Hz loading frequency at (a) 100% and (b) 134% shear strains.*

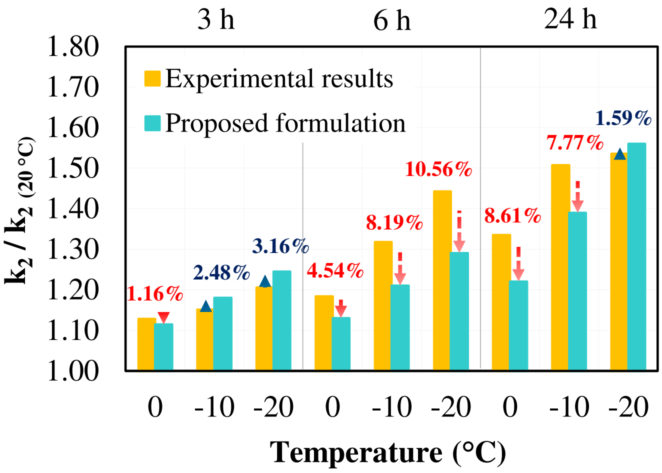

(a)

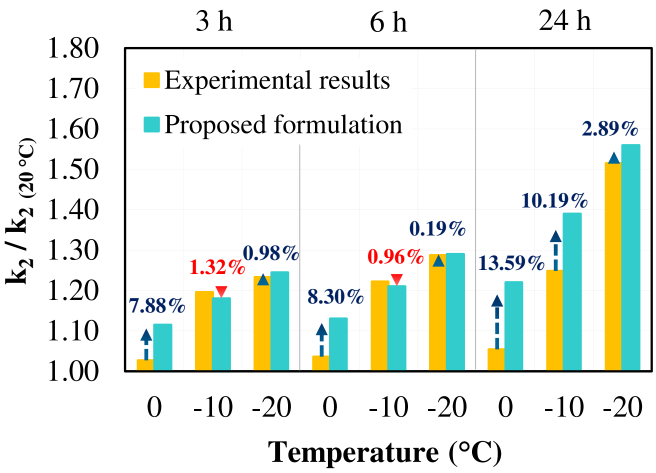

(b)

Figure 3.22. *Comparison of experimental amplifications in k_2 with the proposed formulation estimations for 0.5 Hz loading frequency at (a) 100% and (b) 134% shear strains.*

4. MODIFICATIONS IN BOTH LEAD AND RUBBER PROPERTIES OF LRBS AT LOW TEMPERATURES CONSIDERING THE SIZE EFFECT

4.1. Introduction

In this chapter, test results for both large- and small-size LRBs are presented. For each size, tests were conducted on two geometrically identical bearings: one with a lead core and the other with a hole in place of the lead core. It is important to note that a different set of isolators was used than the isolator tested in Chapters 2 and 3. The primary objective of the test program carried out in this chapter is to quantify the contribution of rubber and lead core to both energy dissipation capacity and post-yield stiffness of LRBs at low temperatures.

Section 4.2 details the geometric and material characteristics of the tested LRBs. Section 4.3 outlines the loading protocol utilized in this chapter. Section 4.4 describes the test methodology implemented across all loading conditions. Finally, Section 4.5 presents the hysteretic behaviors observed for each bearing.

4.2. Test Specimen

In order to observe the size effect on the results, LRBs of two different sizes were considered in the experimental program. One represents a large-size bearing, while the other stands for a small-size bearing. Two identical bearings (with and without a lead core) were tested for each size, resulting in a total of four isolators tested. The large-size bearings are 940 mm in diameter. They consist of 27 layers of rubber plates with an individual thickness of 10 mm. The number of steel plate layers is 26, each of which is 4 mm in thickness. The overall height of the large-size bearings is 474 mm, including the top and bottom plates and the end shims on the top and bottom. The lead core diameter of the large-size bearing is 240 mm. On the other hand, the small-size bearings have a diameter of 350 mm. The diameter of the lead core inserted in the small-size bearing is 70 mm. The total height of the small-size bearings is 138 mm. There are 5 layers of rubber and 4 layers of steel plates with 12 mm and 3 mm thicknesses, respectively. The shear modulus of low damping natural rubber at 100% shear strain is the same for both bearing sizes and equal to 0.67 MPa. Table 4.1 and Figure 4.1 illustrate the mechanical and geometrical features of bearings, respectively.

Table 4.1. *Test specimen characteristics.*

Main features		Large-size bearings		Small-size bearings	
		With lead	Without lead	With lead	Without lead
Φ (mm)	Isolator diameter	896	896	335	335
Φ_L(mm)	Lead diameter	240	-	70	-
t_s (mm)	Single-steel shim plates thickness	4	4	3	3
t_i (mm)	Single rubber layer thickness	10	10	12	12
t_r (mm)	Total rubber thickness	270	270	60	60
n_r	Number of rubber layer	27	27	5	5
S_1	Primary shape factor (Φ- $\Phi_L/4t_i$)	16.40	22.40	5.52	6.98
S_2	Secondary shape factor ((Φ/t_r)	3.32	3.32	5.58	5.58

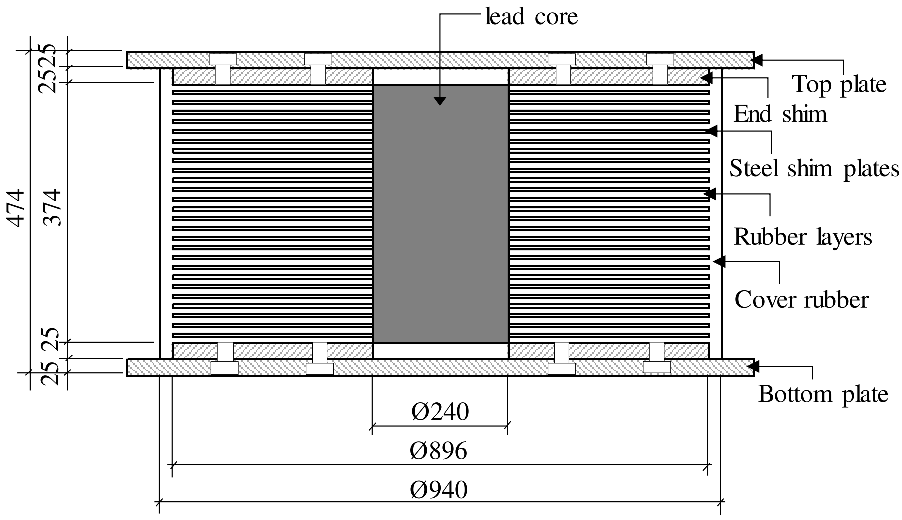

(a)

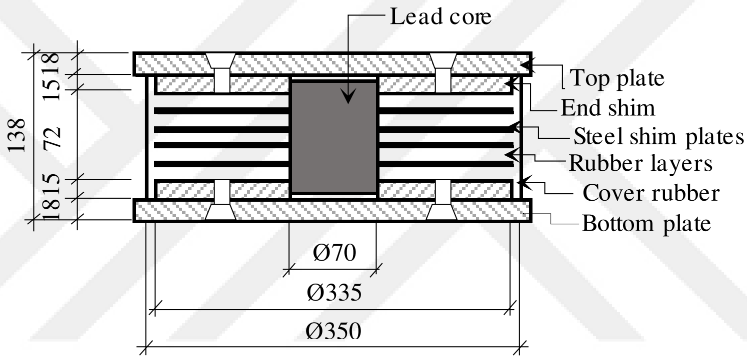

(b)

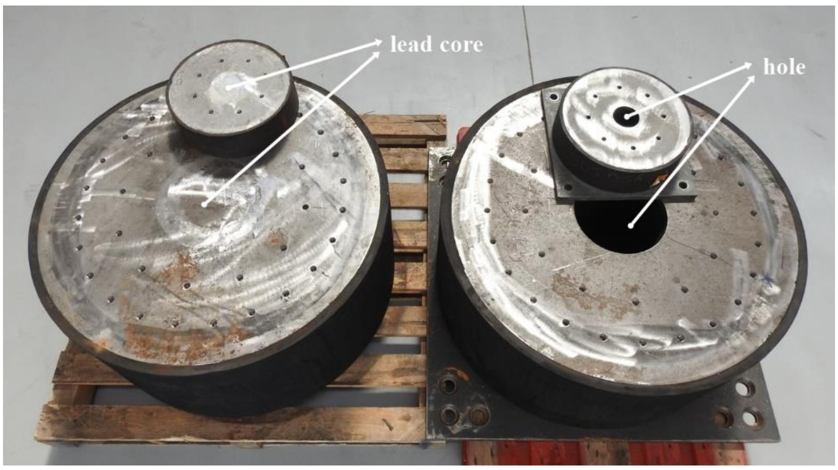

(c)

Figure 4.1. *Geometric definitions of (a) large-size and (b) small-size bearings with lead core (c) view of the tested bearings (all units are in mm).*

4.3. Test Program

The loading protocol followed in this research was established in accordance with Section 8.2.1.2.4 of EN-15129 (2018) and given in Table 4.2. Section 8.2.1.2.4 of EN-15129 (2018) is devoted to determining the dependence of isolator characteristics to temperature and assures that the horizontal characteristics of the isolators shall be measured at a rubber shear strain of 100%. It is also stated in EN-15129 (2018) that the loading frequency shall not be less than 0.01 Hz. In accordance with these criteria, the amplitudes of the cyclic motions applied to the bearings correspond to 100% rubber shear strain. The displacement-controlled cyclic motions were conducted at amplitudes of 270 and 60 mm for large- and small-size bearings, respectively. All tests were performed with a loading frequency of 0.1 Hz and the corresponding maximum loading velocities for large- and small-size bearings are 170 and 38 mm/s, respectively. Low temperatures given in Table 4.2 were determined according to a statistical investigation on recorded temperatures at the coldest regions that possess high seismicity in Türkiye as explained in Section 2.4. According to this investigation, it is revealed that the possibility of having -20°C for a period longer than 24 hours is almost zero for the selected regions. Thus, the low temperatures, for an exposure time of 24 hours, were selected as -20, -10 and 0°C. As shown in Table 4.2, both large- and small-size bearings were tested under displacement-controlled motions as per code provisions where the characterization tests of seismic isolators are defined to be performed mostly for 3 cycles of motions (ASCE, 2017; EN-15129, 2018; TBEC, 2018). All tests were performed at a normal stress of 6 MPa which correspond to vertical forces of 3780 kN and 480 kN for large- and small-size bearings, respectively.

Table 4.2. *Loading protocol applied to the bearings.*

Test No	Temperature	Exposure Time (hour)	Shear Strain (%)	Frequency (Hz)	Cycle Number
1	20ºC	-	100	0.1	3
2	0ºC	24	100	0.1	3
3	-10ºC	24	100	0.1	3
4	-20ºC	24	100	0.1	3

4.4. Test Methodology

For each bearing, the testing campaign started with the reference tests (test no 1 in Table 4.2), which are used to determine the mechanical properties of bearings at 20±1°C, which is the room temperature of the test laboratory. Then, low temperature tests were performed in a decreasing order. Prior to low temperature tests, the thermal chamber shown in Figure 2.2(d) was adjusted to the selected temperature. Once the chamber reached the desired temperature, the bearing was conditioned inside it for 24 hours. After this conditioning period, the bearing was removed from the chamber, connected to the test device (see Figure 2.2(a)), and tested dynamically at room temperature. The tests were completed in a maximum of 12 minutes once the bearing was removed from the environmental chamber. It is important to note that, according to the AASHTO M251-97 (1997), the total time between removing the bearing from the conditioning environment and completing the low temperature test should not exceed 30 minutes. After each low temperature test, the bearings were conditioned at room temperature for 24 hours (20ºC) so that they could revert to their initial temperature. Also, such a dwell period provides a way to refrain from the effects of previous loadings on the response of bearings. Figure 4.2 compares large- and small-size bearings with a lead core obtained from cyclic tests performed at -20°C. Figures 4.2(a) and 4.2(b) define the sinusoidal displacement-time histories applied to the tested bearings. Scenes from the corresponding loadings are given in Figures 4.2(c) and 4.2(d), at which ice particles at the surface of the bearings can be seen. Figures 4.2(e) and 4.2(f) illustrate the recorded force-displacement loops from these loadings. On the other hand, Figures 4.2(g) and 4.2(h) are given to show that the vertical forces acting on the bearings during the cyclic motion remain almost the same.

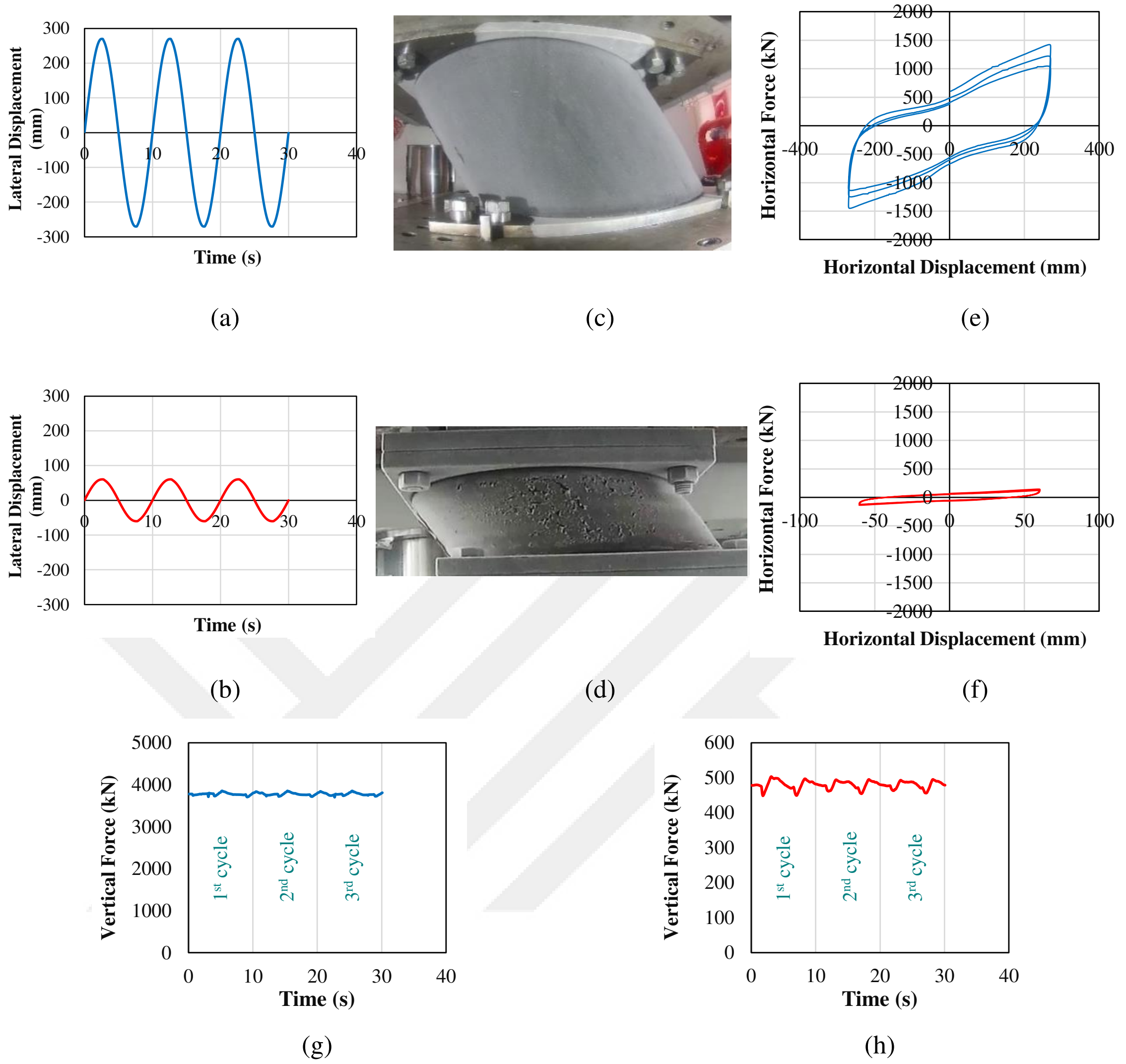

Figure 4.2. *Applied loading history to the (a) large- and (b) small-size bearing with a lead core, (c) and (d) scenes from tests performed at -20°C, (e) and (f) corresponding force-displacement loops (g) and (h) corresponding vertical force-time graphs.*

4.5. Experimental Results

In this section, force-displacement loops obtained for both large- and small-size bearings are presented comparatively under varying temperature conditions. Figure 4.3 illustrates the force-displacement loops recorded for large-size bearings, both with and without lead cores, during testing. Similarly, Figure 4.4 provides the corresponding comparison for small-size bearings. Analysis of Figures 4.3 and 4.4 reveals that as temperature decreases, there is an increase in lateral stiffness. This trend is consistent for bearings with and without a lead core. Another important observation is the occurrence of pinching in the force-displacement curve of the large-size bearing with a lead core (see Figure 4.3.a). This pinching effect, observed around zero displacement in the hysteresis loop, is expected when the lead plug is small relative to the bonded diameter of the bearing or small on an absolute scale (Coria, 2015). According to Coria (2015), the pinching effect would be significantly reduced or eliminated in bearings where the lead plug is designed with a diameter that is at least 1/6 of the bonded diameter of the bearing. For the present study, the bonded diameter of the large-size lead rubber bearing tested in this chapter is 896 mm, while the diameter of the lead plug is 240 mm, as seen in Figure 4.1(a). This design results in a ratio of approximately 1/4, which exceeds the minimum dimension recommended by Coria (2015). Based on the findings in this chapter, it is possible to observe the pinching effect even when the lead core diameter is 1/4 of the bonded diameter. However, although the dimension of the isolator tested in Chapters 2 and 3 is very close to that of the large-size lead rubber bearing used in this chapter, the lack of observed pinching in that case may be attributed to differences in the manufacturing processes of the isolator sourced from different producers.

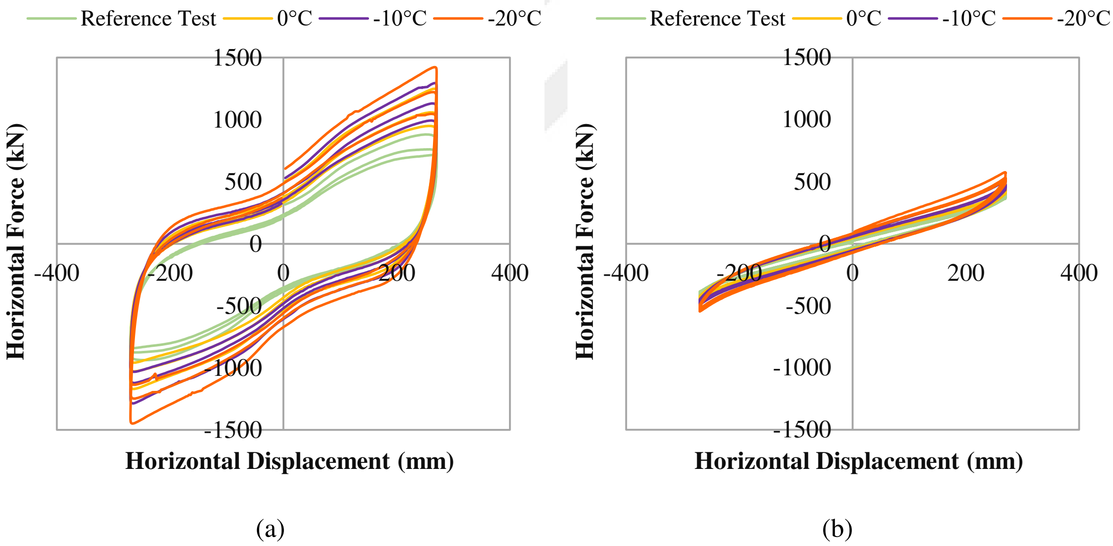

Figure 4.3. *Comparison of force-displacement loops obtained from testing of large-size bearings for different temperatures (a) with a lead core (b) without a lead core.*

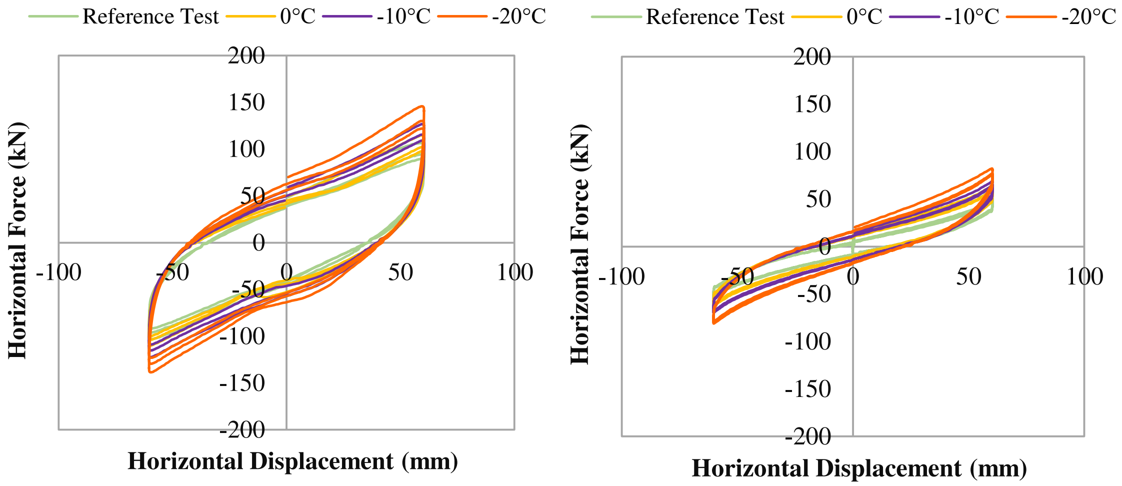

(a) (b)

Figure 4.4. *Comparison of force-displacement loops obtained from testing of* *small-size bearings* *for different temperatures (a) with a lead core (b) without a lead core.*

Force-displacement loops (Figures 4.3 and 4.4) recorded during the tests were used to compute the hysteretic properties of bearings with and without a lead core. The hysteretic properties under investigation are post-yield stiffness (k_2), dissipated energy, and equivalent damping ratio (ξ_{eq}).

4.5.1. Post-yield stiffness

The post-yield stiffness (k_2) was computed by the Least Square Method (LSM), as described in Figure 2.10 and presented in Table 4.3 and 4.4 for large and small-size bearings, respectively. It should be noted that even though bearings without a lead core do not exhibit yielding, the term k_2 is also used to represent the elastic stiffness of these bearings for the sake of completeness. Figure 4.5 presents the post-yield stiffness values obtained for large-size isolators, comparing those with and without a lead core. In order to evaluate the effect of low temperature, this comparison includes both the room temperature test (reference test) and the low temperature test (-20°C, 24 hours), each represented by a single cycle. Figure 4.6 gives the same comparison for the small-size isolators. According to the assumption that only the rubber is responsible for the stiffness in lead rubber bearings, identical stiffness values would be expected for isolators with and without a lead core. However, as can be seen from the graphs, identical results were not calculated for the isolators with and without a lead core for both reference and low temperature tests.

Table 4.3. *Calculated post-yield stiffnesses of the large-size bearings.*

	Mechanical Properties	Cycle	Temperature			
			20°C	**0°C**	**-10°C**	**-20°C**
With lead core	**k_2 (kN/m)**	**1st**	2304	2592	2659	2841
		2nd	2117	2402	2476	2644
		3rd	2013	2255	2319	2468
Without lead core	**k_2 (kN/m)**	**1st**	1257	1359	1455	1594
		2nd	1228	1299	1369	1485
		3rd	1217	1282	1346	1455

Table 4.4. *Calculated post-yield stiffnesses of the small-size bearings.*

	Mechanical Properties	Cycle	Temperature			
			20°C	**0°C**	**-10°C**	**-20°C**
With lead core	**k_2 (kN/m)**	**1st**	1176	1322	1382	1587
		2nd	1042	1244	1256	1440
		3rd	976	1156	1204	1353
Without lead core	**k_2 (kN/m)**	**1st**	618	748	801	942
		2nd	595	695	753	873
		3rd	588	681	741	856

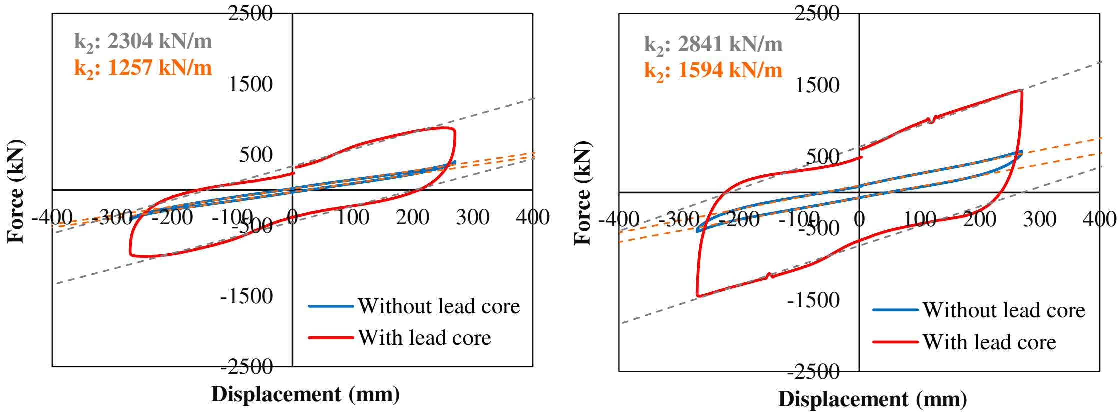

(a) (b)

Figure 4.5. *Comparison of post-yield stiffnesses (k_2) <u>for large-size isolators</u> with and without a lead core: (a) reference test (b) -20°C, 24-hour exposure.*

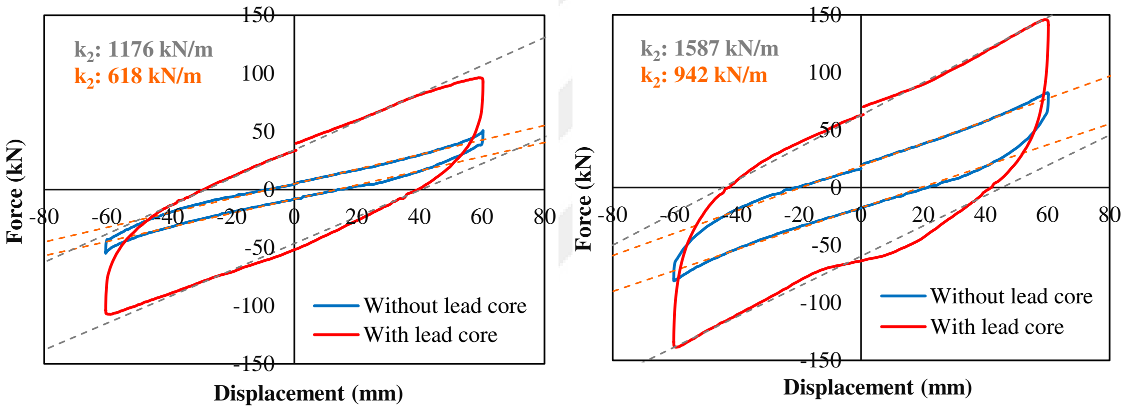

(a) (b)

Figure 4.6. *Comparison of post-yield stiffnesses (k_2) <u>for small-size isolators</u> with and without a lead core: (a) reference test (b) -20°C, 24-hour exposure.*

Figure 4.7(a) depicts the computed post-yield stiffnesses obtained for each loading cycle of the large-size bearings at temperatures of 20, 0, -10, and -20°C, comparing cases with and without a lead core. In this graph, data computed at 20°C are considered as reference values and used to normalize the corresponding k_2 values acquired at 0, -10 and -20°C. The normalized k_2 values, $k_2/k_{2(20°C)}$, are illustrated in Figure 4.7(b). In Figure 4.8, a similar comparison is presented for small-size isolators. Accordingly, post yield stiffness of the bearings tends to increase as the temperature decreases, regardless of whether there is a lead core or not. For large-size bearings, in Figure 4.7(b), the maximum amounts of $k_2/k_{2(20°C)}$ ratios, which represents the normalization of post-yield stiffness computed for low temperatures by the one calculated for 20°C, correspond to -20°C and are around 1.23 for the bearing with a lead core. The amplifications in post yield stiffness of large-size bearings for cases with and without a lead core are relatively close to each other when compared to those of small-size bearings. Figure 4.8(b) indicates that the $k_2/k_{2(20°C)}$ ratios of small-size bearings without a lead core are larger than the ones computed for the bearing with a lead core. For instance, at -20 °C, $k_2/k_{2(20°C)}$ ratios calculated for the 1st cycle of motion for small-size bearings with and without a lead core are 1.35 and 1.52, respectively.

A further observation in Figures 4.7(a) and 4.8(a) is the cycle-to-cycle reduction in post-yield stiffness, k_2, of the bearings with a lead core. And the inter-cycle variation in k_2 is getting larger as the temperature decrease. At -20°C, the reduction from cycle-to-cycle is 7% for the large-size bearing. For the small-size bearing, it is 10% (between 1st and 2nd cycle) and 6% (between 2nd and 3rd cycle) at the same temperature.

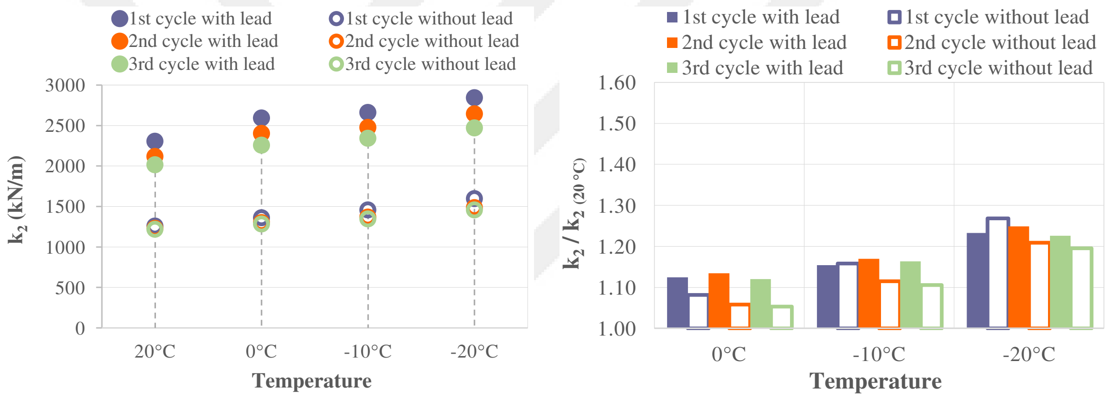

(a) (b)

Figure 4.7. *<u>For large-size bearings</u>, comparison of (a) post-yield stiffness values (b) normalized post-yield stiffnesses.*

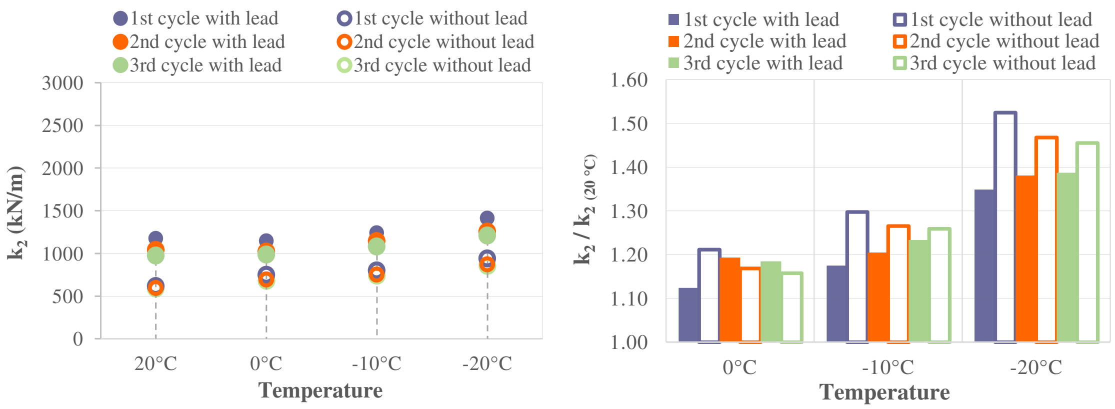

(a) (b)

Figure 4.8. *<u>For small-size bearings</u>, comparison of (a) post-yield stiffness values (b) normalized post-yield stiffnesses.*

4.5.2. Dissipated energy and equivalent damping ratio

The Energy Dissipated per Cycle (EDC) was determined by calculating the area enclosed by the hysteresis loop for each cycle using integration, as described in Figure 4.9. The equivalent damping ratio (ξ_{eq}) is a key parameter used to quantify the energy dissipation capacity of a system. The relationship between EDC and ξ_{eq} is defined by Equation 4.1. In Equation 4.1, F_{max} and F_{min} are the absolute maximum and minimum isolator forces corresponding to positive and negative isolator displacements D_{max} and D_{min}, respectively.

$$\xi_{eq} = \frac{EDC}{\pi\,(F_{max}D_{max} + F_{min}D_{min})} \tag{4.1}$$

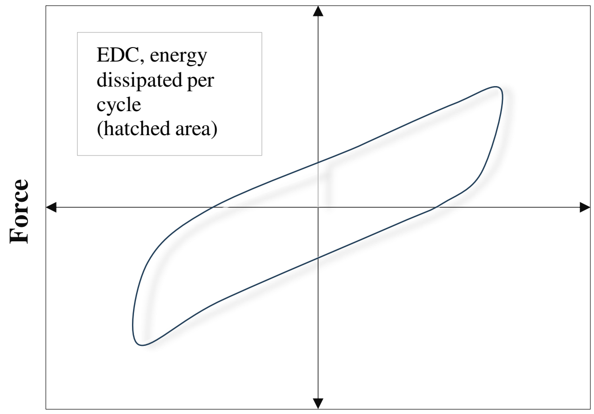

Figure 4.9. *Definition of the EDC.*

4.5.2.1. Results for the bearings with a lead core

Tables 4.5 present the mechanical properties, namely EDC and ξ_{eq}, calculated for large- and small-size bearings with a lead core at different temperatures, while Figures 4.10 and 4.11 illustrate the EDC and normalized EDC values for these bearings, respectively. The results presented in Figures 4.10 and 4.11 revealed that EDC increases when the temperature decreases. For instance, for the large-size bearings, the maximum $EDC/EDC_{(20°C)}$ ratios at -20°C are approximately 1.8, while for the small-size bearings, the maximum amplification reaches roughly 1.5. These results indicate that, in terms of EDC, as the bearing size increases, the effect of low temperature becomes more significant. It can also be seen in Figures 4.10(a) and 4.11(a) that EDC decreases with the increasing number of loading cycles regardless of the bearing size. The reduction in EDC from cycle to cycle is found to be temperature dependent, and the trend increases with decreasing temperature. Furthermore, the cyclic reduction of EDC is more pronounced for large-size bearings than small ones. For instance, based on the test results of large-size bearing conditioned at -20°C, the reduction in EDC from the 1^{st} cycle to the 2^{nd} cycle is 15%, whereas it is 11% from the 2^{nd} to the 3^{rd} cycle. The same comparison for small-size bearing results in an 11% reduction in EDC between the 1^{st} and 2^{nd} cycles and 7% between the 2^{nd} and 3^{rd} cycles. The reason for such variation in EDC is the gradual reduction in characteristic strength, Q (force intercept at zero displacement, see Figure 1.2) of the bearings with a lead core. Kalpakidis (2008) revealed a temperature rise at the lead core of an LRB during cyclic motion. That rise in temperature reduces the amplification in EDC as the number of loading cycles increases.

Table 4.5. *Calculated hysteretic properties of the bearings with a lead core.*

	Mechanical Properties	**Cycle**	**Temperature**			
			20°C	**0°C**	**-10°C**	**-20°C**
Large-size	**EDC (kNm)**	**1^{st}**	406	582	632	715
		2^{nd}	366	494	538	607
		3^{rd}	343	448	482	539
	ξ_{eq} (%)	**1^{st}**	26.3	28.3	28.8	29.3
		2^{nd}	26.4	27.9	28.1	29.0
		3^{rd}	26.0	27.6	28.0	29.1
Small-size	**EDC (kNm)**	**1^{st}**	9.3	10.7	12.5	14.2
		2^{nd}	8.3	9.5	11.4	12.6
		3^{rd}	8.0	9.1	10.4	11.7
	ξ_{eq} (%)	**1^{st}**	24.1	25.1	26.4	26.3
		2^{nd}	23.7	24.4	26.0	25.7
		3^{rd}	23.7	24.1	25.0	25.3

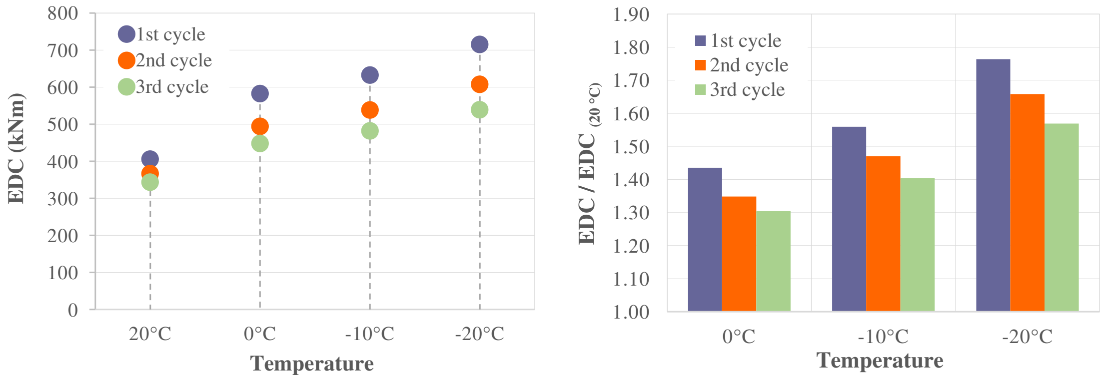

(a) (b)

Figure 4.10. *<u>For large-size bearings with a lead core</u>, comparison of (a) energy dissipated per cycle (b) normalized energy dissipated per cycle.*

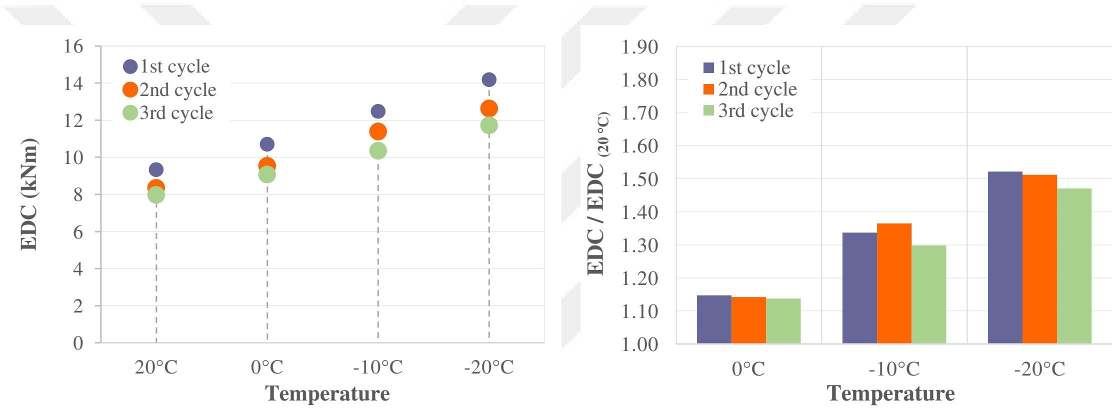

(a) (b)

Figure 4.11. *<u>For small-size bearings with a lead core</u>, comparison of (a) energy dissipated per cycle (b) normalized energy dissipated per cycle.*

The equivalent damping ratios (ξ_{eq}) computed using Equation 4.1, along with the corresponding $\xi_{eq}/\xi_{eq(20°C)}$ ratios, are presented in Figures 4.12 and 4.13 for large- and small-size LRBs, respectively. Notably, as shown in Figures 4.12(a) and 4.13(a), regardless of bearing size, the computed ξ_{eq} values remain nearly constant across all low temperatures. As depicted in Figures 4.12(b) and 4.13(b), the maximum amplification in ξ_{eq} values for both large- and small-size bearings due to low-temperature exposure is approximately 10%. The minimal variation in ξ_{eq} values under low-temperature conditions, despite significant changes in EDC, can be attributed to the form of Equation 4.1 as specified by relevant codes (ASCE, 2017; EN-15129, 2018; TBDY, 2018). In this equation, EDC is divided by the sum of the absolute values of isolator forces at maximum and minimum displacements. Consequently, if the variations in EDC and isolator forces are comparable, ξ_{eq} will exhibit only marginal changes. This behavior is particularly evident in bearings with a lead core.

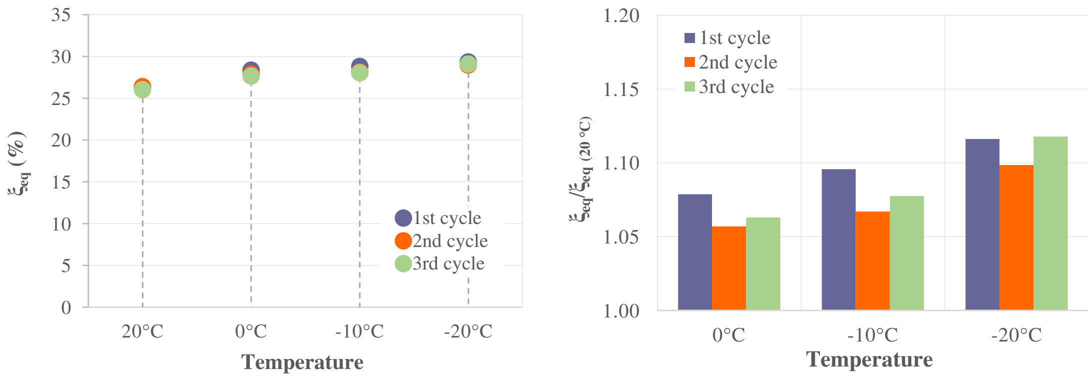

(a) (b)

Figure 4.12. *<u>For large-size bearings with a lead core</u>, comparison of (a) equivalent damping ratios (b) normalized equivalent damping ratios.*

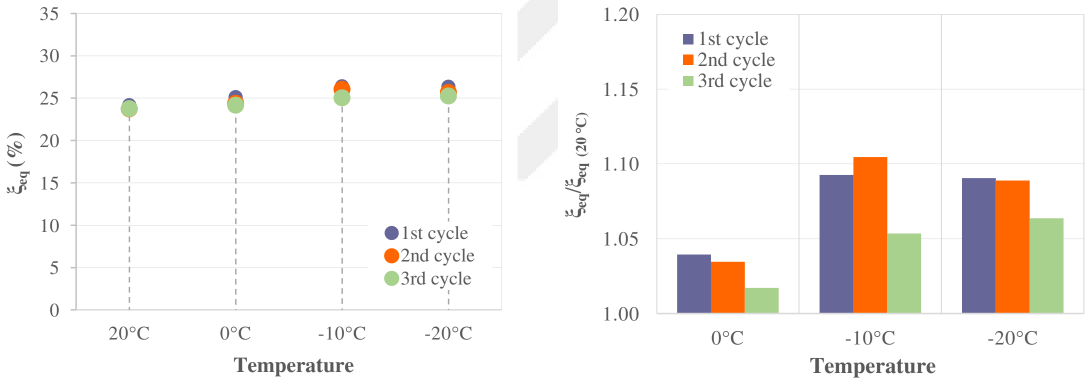

(a) (b)

Figure 4.13. *<u>For small-size bearings with a lead core</u>, comparison of (a) equivalent damping ratios (b) normalized equivalent damping ratios.*

4.5.2.2. Results for the bearings without a lead core

In lead rubber bearings, the lead core enhances the energy dissipation capacity of the bearing. As seen in Table 4.6, the amount of dissipated energy per cycle (EDC) and the equivalent damping ratio (ξ_{eq}) are significantly lower compared to bearings with a lead core. Moreover, the increase in EDC is significantly larger for bearings without a lead core as seen in Figures 4.14 and 4.15. For instance, in the case of large-size bearings, the maximum EDC/EDC$_{(20°C)}$ ratios at -20°C are approximately 1.8 for bearings with a lead core, whereas this value increases to 3.6 for bearings without a lead core.

Table 4.6. *Calculated hysteretic properties of the bearings without a lead core.*

	Mechanical Properties	Cycle	Temperature			
			20°C	0°C	-10°C	-20°C
Large-size	EDC (kNm)	1st	24	47	62	87
		2nd	22	42	54	76
		3rd	21	40	52	73
	ξ_{eq} (%)	1st	3.4	6.0	7.3	9.2
		2nd	3.2	5.5	6.7	8.4
		3rd	3.1	5.4	6.6	8.3
Small-size	EDC (kNm)	1st	1.5	2.5	3.1	4.2
		2nd	1.5	2.3	2.8	3.8
		3rd	1.4	2.2	2.7	3.7
	ξ_{eq} (%)	1st	7.8	10.5	11.6	13.6
		2nd	7.5	9.9	11.0	12.8
		3rd	3.1	5.4	6.6	8.3

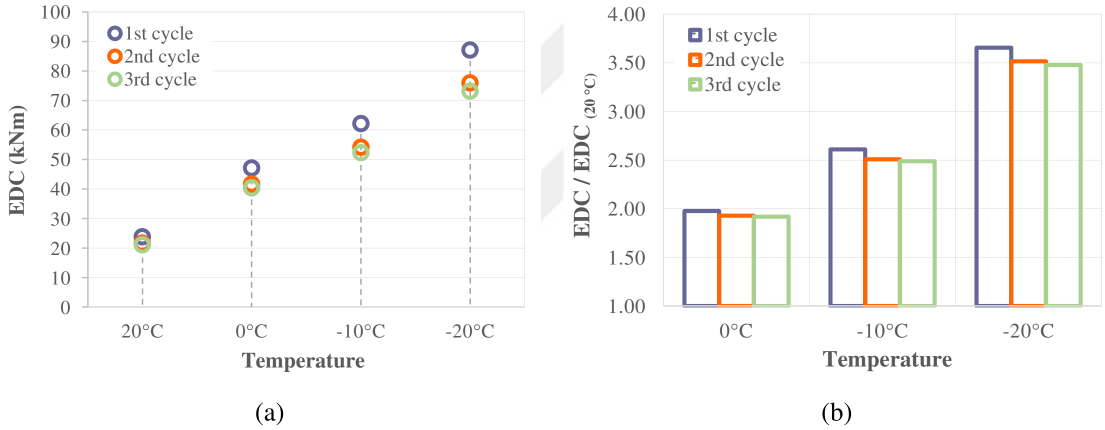

Figure 4.14. *For large-size bearings without a lead core, comparison of (a) equivalent damping ratios (b) normalized equivalent damping ratios.*

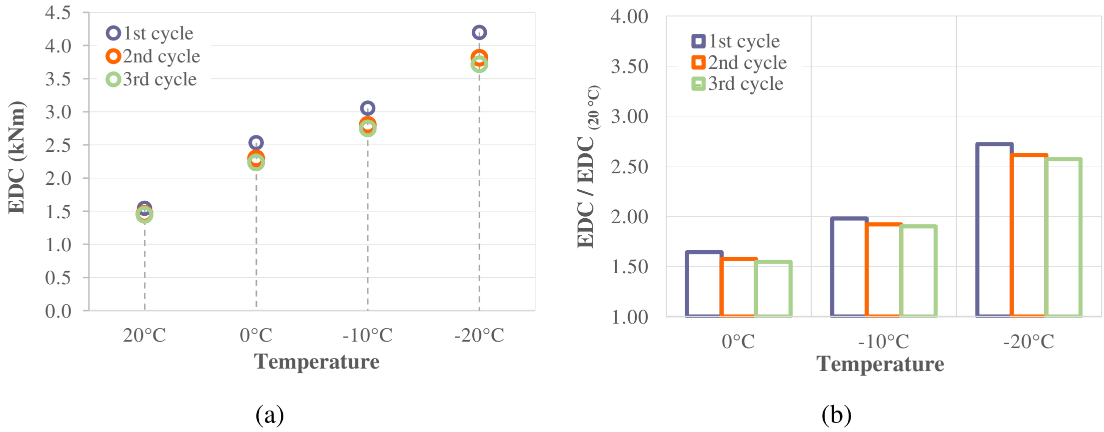

Figure 4.15. *For small-size bearings without a lead core, comparison of (a) equivalent damping ratios (b) normalized equivalent damping ratios.*

Figures 4.16 and 4.17 illustrate the regarding ξ_{eq} values for the large- and small-size bearings. Accordingly, for bearings without a lead core, ξ_{eq} values increase as the temperature decreases, whereas they remain constant for bearings with a lead core. This is basically due to the fact that the amounts of amplifications in EDC and isolator forces at maximum and minimum isolator displacements are not similar to each other. The experimental data for both large- and small-size bearings without a lead core indicate that amplifications in EDCs are more significant than those of isolator forces at low temperatures. Thus, for bearings without a lead core, $\xi_{eq}/\xi_{eq(20°C)}$ ratios increase with decreasing temperature.

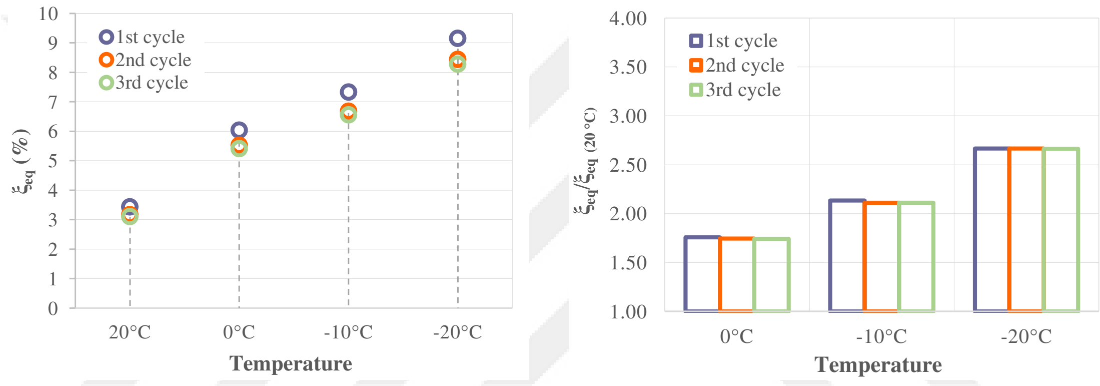

(a) (b)

Figure 4.16. *For large-size bearings without a lead core, comparison of (a) equivalent damping ratios (b) normalized equivalent damping ratios.*

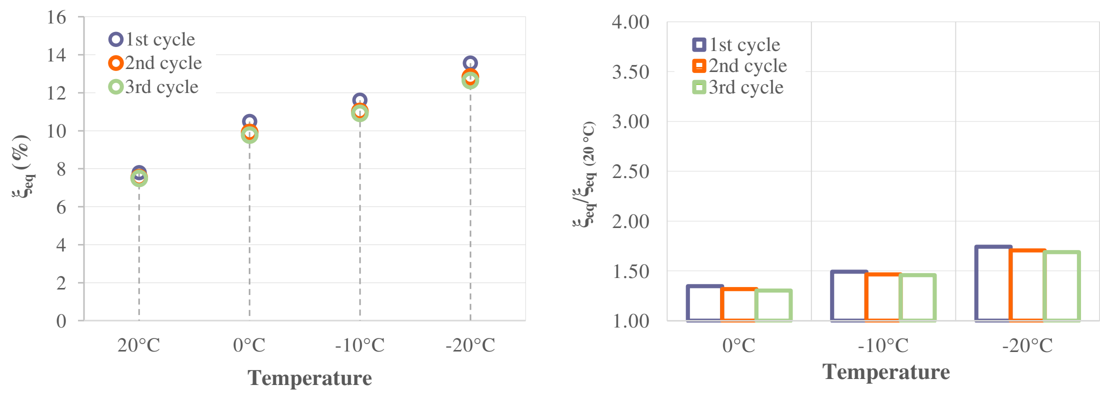

(a) (b)

Figure 4.17. *For small-size bearings without a lead core, comparison of (a) equivalent damping ratios (b) normalized equivalent damping ratios.*

4.6. Contribution of Lead Core to the Post-Yield Stiffness of LRB

The post-yield stiffness of an LRB is influenced by both the rubber and the lead core. However, despite more complex representations existing in the literature for simulating force-displacement loops of LRBs (Vaiana & Rosati, 2023; Vaiana et al., 2023), for simplicity, analytical models often assume that the post-yield stiffness is related solely to rubber properties. As a result, a bilinear force-displacement curve (see Figure 4.18(a)) of an LRB can be decomposed as shown in Figure 4.18(b). This approach assumes that the lead core does not contribute to the post-yield stiffness of the LRB. While this assumption is acceptable to a degree in normal conditions, further research is needed to verify it under low temperature conditions (Constantinou et al., 2007; Kalpakidis, 2008). This section investigates the contribution of the lead core to the post-yield stiffness of both large- and small-size bearings at different temperatures.

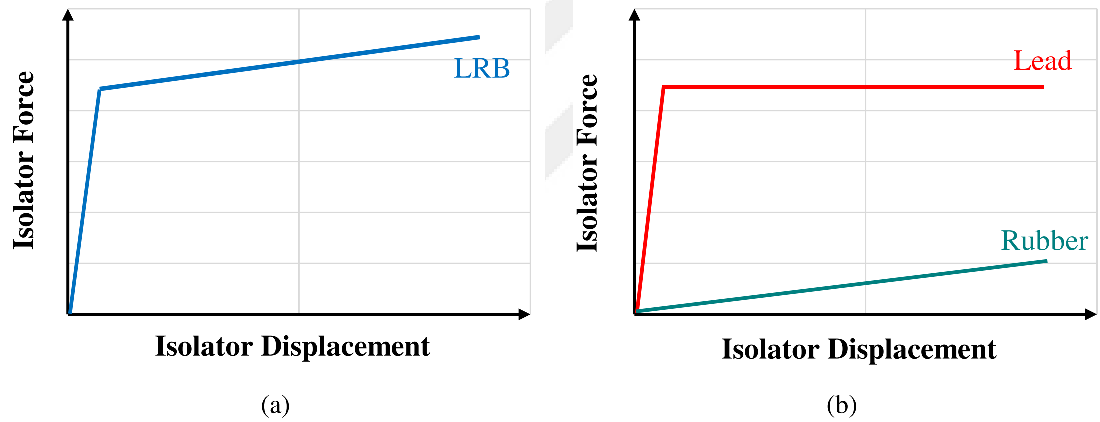

Figure 4.18. *(a) Representative bilinear force displacement curve of a LRB and (b) contributions of rubber and lead core.*

In order to reveal the contribution of LRB components to the post-yield stiffness for isolators of different sizes at low temperature, test results discussed in the Section 4.5.1 are presented accordingly. The post-yield stiffnesses of both large- and small-size bearings without a lead core serve as the reference values and the corresponding shear modulus (G_r) values are calculated based on these stiffness values. The computed G_r values are given in Table 4.7. Subsequently, for the identical loading cases, the corresponding f_L values are calculated by means of Equation 1.2. The computed f_L values for different temperatures are provided in Table 4.8. Furthermore, Figures 4.19(a) and 4.15(b) illustrate the variation in f_L with temperature for large- and small-sized bearings.

Table 4.7. *Calculated G_r values correspond to the bearings without a lead core.*

		Cycle	Temperature			
			20°C	**0°C**	**-10°C**	**-20°C**
Large-size bearing without a lead core	**G_r (MPa)**	**1st**	0.58	0.63	0.67	0.74
		2nd	0.57	0.60	0.63	0.68
		3rd	0.56	0.59	0.62	0.67
Small-size bearing without a lead core	**G_r (MPa)**	**1st**	0.44	0.53	0.57	0.67
		2nd	0.42	0.49	0.54	0.62
		3rd	0.42	0.48	0.53	0.61

Table 4.8. *Calculated f_L coefficients of the LRBs.*

		Cycle	Temperature			
			20°C	**0°C**	**-10°C**	**-20°C**
Large-size LRB	**f_L coefficient**	**1st**	1.83	1.91	1.83	1.78
		2nd	1.72	1.85	1.81	1.78
		3rd	1.65	1.76	1.72	1.70
Small-size LRB	**f_L coefficient**	**1st**	1.90	1.77	1.72	1.69
		2nd	1.75	1.79	1.67	1.65
		3rd	1.66	1.70	1.62	1.58

In Figures 4.19(a) and 4.19(b), it is seen that f_L values calculated at room temperature for both large- and small-size bearings are almost identical (f_L values vary in a range between 1.90 and 1.65 during the loading cycles). However, as the temperature decreases the corresponding f_L values get different values and the size effect becomes more evident. The f_L value calculated for large-size bearing slightly increases when the temperature decreases from room temperature to 0°C. But, it tends to decrease with further decrease in temperature. However, f_L values computed for large-size bearing at room temperature is found to provide close estimations for f_L values that corresponds to selected low temperatures. On the other hand, for small-size bearing, the f_L value computed at room temperature decreases gradually as the temperature decreases. Furthermore, the f_L value calculated at room temperature is suitable to estimate f_L values at 0°C while overestimates the computed ones at -10 and -20°C. Another observation from Figures 4.19(a) and 4.19(b) is that the f_L value decreases as the number of loading cycle increases. And, the amount of reduction is temperature dependent, especially for large-size bearing. As the temperature decreases the range of reduction gets smaller.

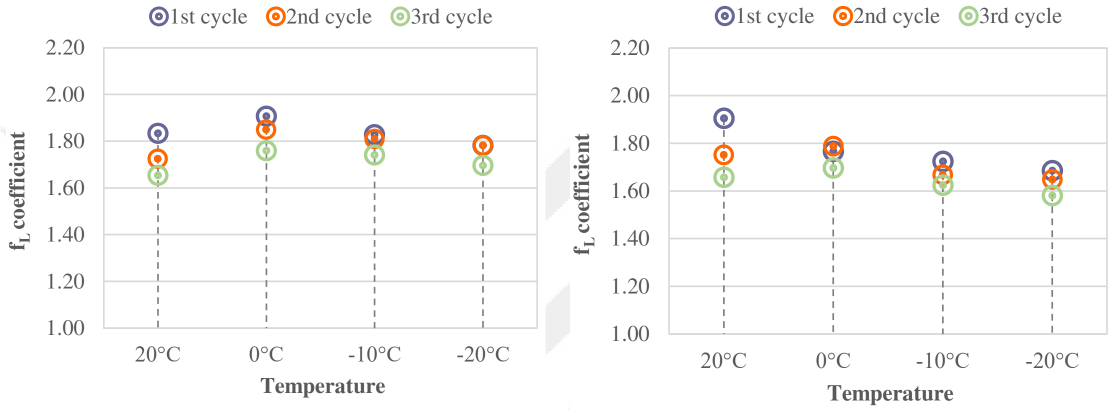

(a) (b)

Figure 4.19. *Comparison of f_L coefficients for (a) large-size LRB (b) small-size LRB.*

As mentioned before, Constantinou et al. (2007) addressed the lead contribution to the post-yield stiffness of LRBs. In that study, the authors conducted tests on bearings with a diameter of 185 mm and a lead core diameter of 38 mm. For the bearing they tested, the f_L values can reach up to a maximum of 1.2. Results of the present study show that the upper bound value of f_L can be up to 2.0 for a full-scale LRB. This difference can be attributed to the ratio of the lead core diameter to the bonded diameter of the isolator, which affects the confinement effect, as well as the shear modulus of the rubber used in the isolator. In the study conducted by Constantinou et al. (2007), the shear modulus of the rubber is reported to be 0.36 MPa under 114% shear strain. In contrast, the low-damping rubber used in the present study has a shear modulus of 0.67 MPa under 100% shear strain. As the hardness of the rubber increases, the degree of confinement of the lead becomes more pronounced. Consequently, the contribution of the lead to the stiffness of the isolator increases.

5. SUMMARY AND CONCLUSIONS

This study investigated the changes in the mechanical properties of Lead Rubber Bearings (LRBs) exposed to low temperatures and the contributions of the LRB components (rubber and lead core) to these changes. The questions addressed in this dissertation regarding the low-temperature behavior of Lead Rubber Bearings (LRBs) are:

1. What modifications are observed in the properties of full-scale LRBs when subjected to various levels of low ambient temperatures, and to what extent are these modifications sensitive to loading frequency and shear strain? This question was investigated in Chapter 2.

2. How are the hysteretic properties of LRBs affected by the duration of exposure to low temperatures? How successful are the amplification factors proposed in the literature and recommended in the regulations in predicting the characteristics of isolators exposed to low temperatures for various durations? This question was investigated in Chapter 3.

3. What is the contribution of the lead core and rubber to the amplification in post-yield stiffness of Lead Rubber Bearings (LRBs) of different sizes when subjected to low temperatures? Chapter 4 investigated this question.

A comprehensive experimental program was conducted to answer the above questions. The same large-size isolator was used in Chapters 2 and 3, whereas a different set consisting of four isolators was used in Chapter 4. Each question was answered in three different chapters, and the findings are as follows:

<u>Findings from Chapter 2:</u>

In Chapter 2, an experimental program was conducted considering several temperatures (−20°C, −10°C, 0°C, and 20°C), shear strains (50%, 100%, and 134%), and loading frequencies (0.1 and 0.5 Hz). The exposure time to low temperatures was 24 hours. In the tests, an 850 mm diameter LRB was subjected to cyclic motions for numerous loading combinations. Amplification in mechanical properties of LRB, namely, characteristic strength and post-yield stiffness, was investigated. The results of this chapter reveal that:

- It is observed an increase in both characteristic strength and post-yield stiffness of the LRB as the temperature decreases. For instance, for 134% shear strain and 0.5 Hz loading frequency, the amplifications in characteristic strength are 2.07, 1.97, and 1.87 for the first, second, and third cycles of motion at -20°C. In the same loading condition, the amplifications in post-yield stiffness are 1.55, 1.51, and 1.48, respectively. Accordingly, it is possible to say that the amplification in characteristic strength is more pronounced compared with that of post-yield stiffness.
- The amplification in characteristic strength due to low-temperature exposure generally decreases with increasing loading cycles. However, an exception was observed in the experimental results for 50% shear strain at a 0.1 Hz loading frequency, where an opposite trend was noted. This may be due to a smaller temperature rise in the lead core compared to other cyclic motions. Since the amplitude and frequency at 50% shear strain and 0.1 Hz are the smallest among the values studied, the temperature rise is minimal. Consequently, the reduction in the initial strength of the LRB for this loading case is also smaller. On the other hand, the change in the amplification of post-yield stiffness from cycle to cycle is very limited compared with the characteristic strength. The maximum variation in the $k_2/k_{2(20°C)}$ ratio from cycle to cycle is 3.7%. Given this limited variation, the $k_2/k_{2(20°C)}$ ratio computed for the second loading cycle can also be applied to the first and third cycles.
- Amplifications in characteristic strength are roughly the same for loading frequencies of 0.1 and 0.5 Hz. However, in terms of post-yield stiffness, the loading frequency does affect the amplification. The $k_2/k_{2(20°C)}$ ratios are greater at a loading frequency of 0.5 Hz.
- Increasing the shear strain leads to reduced amplifications in post-yield stiffness, particularly under the loading combination of 134% shear strain and temperatures of 0°C and -10°C. The most pronounced increases in post-yield stiffness were observed for the 50% shear strain at both loading frequencies, as the isolator remains within its elastic limits under this condition. A similar observation applies to characteristic strength with respect to the degree of shear strain.

Findings from Chapter 3:

In this chapter, the same LRB used in Chapter 2 was exposed to low temperatures (0, -10, and -20°C) for various durations (3 and 6 hours) and tested under dynamic conditions. Displacement-controlled cyclic motions were applied with different shear strains (100% and 134%) and loading frequencies (0.1 Hz and 0.5 Hz). The obtained results were compared with those from a 24-hour exposure period in Chapter 2. Based on these test results, amplifications in characteristic strength and post-yield stiffness of the tested LRB were investigated. Additionally, the accuracy of existing equations in the literature and specifications was evaluated, and the new equations that account for the exposure time were proposed to estimate the amplification in the mechanical properties of LRBs. The following conclusions are drawn from the results:

- Amplifications in both characteristic strength and post-yield stiffness are highly sensitive to the duration of exposure to low temperatures. Longer exposure times resulted in larger amplifications in both properties of the LRB. For example, for a 0.1 Hz loading frequency and 100% shear strain, the $Q/Q_{(20°C)}$ ratios are 1.18, 1.31, and 1.29 for 3 hours of exposure at 0°C, -10°C, and -20°C, respectively. The ratios for 24 hours of exposure are 1.41, 1.61, and 1.88. However, for the loading combination of 0.5 Hz loading frequency and 134% shear strain, the effect of exposure time becomes negligible because this combination has the highest loading velocity among the considered scenarios. As a result, the gradual deterioration in the strength of the LRB will be higher with each cycle and closely resembles the deterioration observed in the reference test. In terms of post-yield stiffness, the amplifications are less than those computed for characteristic strength. For the loading combination of 0.1 Hz loading frequency and 100% shear strain, the $k_2/k_{2(20°C)}$ ratios are 1.01, 1.03, and 1.04 for 3 hours of exposure at 0°C, -10°C, and -20°C, respectively. These ratios increase to 1.13, 1.24, and 1.37 for 24 hours of exposure.
- The existing equations proposed to predict the amplifications in the characteristic strength and post-yield stiffness of LRBs at low temperatures do not consider the effects of exposure time and the loading frequency. The proposals generally align with the test results when the exposure time is 3 and 6 hours. However, for an exposure time of 24 hours, the proposed amplification factors underestimate the actual values, with the degree of underestimation increasing as the temperature decreases. The empirical equations proposed in this study consider the effects of loading velocity and

exposure time, and their estimations are in agreement with the experimental data. For characteristic strength, the agreement between the proposed equations and test results generally remains within 10% at a loading frequency of 0.1 Hz. At a loading frequency of 0.5 Hz, particularly for a shear strain of 134%, the heating of the lead core becomes more pronounced, leading to a reduced alignment between the proposed equations and the experimental results. In terms of post-yield stiffness, there is a strong agreement for all loading combinations, with differences being less than 10% for both loading frequencies of 0.1 Hz and 0.5 Hz.

Findings from Chapter 4:

This chapter investigated the contribution of the LRB components (rubber and lead core) to isolator mechanical properties, especially post-yield stiffness, at various low temperatures with an emphasis on the size effect. For this purpose, two small-size and two large-size bearings were subjected to dynamic motions where the amplitudes of the motions correspond to 100% rubber shear strain. Tests were conducted at a horizontal loading frequency of 0.1 Hz. Prior to tests, LRBs were exposed to temperatures of 0°C, -10°C and -20°C for 24 hours. All LRBs considered in the experimental research were identical in terms of material properties, but one of the specimens of the same size was manufactured with a lead core, while the other one had a hole instead of lead core. Based on the test results, amplification in Energy Dissipated per Cycle (EDC) and post-yield stiffness (k_2) of the tested bearings were investigated. According to the results of this study, the following conclusions can be revealed:

- The energy dissipation capacity (EDC) of the tested bearings increases as the temperature decreases. The rate of increase in EDC is greater than that of post-yield stiffness for both small and large-size bearings. The amplification in EDC of the large-size bearings due to low-temperature exposure is 1.7 and 3.6 at -20°C for bearings with and without a lead core, respectively. In both small and large-size bearings, the increase in EDC for bearings without a lead core is more pronounced compared to their counterparts with a lead core. Considering post-yield stiffness, for large-size bearings, the maximum $k_2/k_{2(20°C)}$ ratio is around 1.23 at -20°C for bearings with a lead core. The $k_2/k_{2(20°C)}$ ratios for large-size bearings with and without a lead core are relatively similar. In contrast, small-size bearings without a lead core have higher $k_2/k_{2(20°C)}$ ratios than those with a lead core. For instance, at -20°C, the $k_2/k_{2(20°C)}$ ratios for the 1st cycle of motion for small-size bearings with and without a lead core are 1.35 and 1.52, respectively.

- The equivalent damping ratios of large- and small-size bearings with a lead core are not affected by the temperature change because the amounts of amplifications in EDC and isolator forces at low temperatures are almost the same. On the other hand, regardless of the bearing size, the equivalent damping ratios of bearings without a lead core increase with decreasing temperature.
- The force-displacement loops of both large- and small-size bearings deteriorate due to temperature rise at the lead core during cyclic motion. The amount of deterioration from cycle-to-cycle gets larger as the temperature decreases. Moreover, a larger amount of deterioration is recorded for the large-size bearing compared to the small-size bearing. Furthermore, the pinching effect was observed in the force-displacement curve of the large-size bearing with a lead core. This pinching effect occurs around zero displacement in the hysteresis loop when the lead core diameter is less than 1/6 of the bonded diameter of the bearing. In the present study, pinching was still observed even though the ratio for the large-size LRB tested in this chapter was approximately 1/4. Despite the similarity in dimensions between the isolators tested in Chapters 2 and 3 and the large-size LRB used in Chapter 4, the lack of pinching observed in the tests from Chapters 2 and 3 may be attributed to variations in the manufacturing processes of isolators from different producers.
- The f_L coefficient, which represents the contribution of the lead core to the post-yield stiffness of an LRB, can be up to 2 for the LRBs tested in this chapter. The f_L coefficient computed for test results obtained at room temperature provides reasonable estimates even for low temperature conditions of large-size bearing. However, for the small-size bearing, the f_L coefficient computed for room temperature overestimates the f_L coefficients for low temperature. It should also be noted that, for both sizes of bearings, the f_L coefficient decreases with an increasing number of loading cycles. Additionally, the larger f_L coefficients obtained in this study compared to those proposed in the literature can be attributed to the ratio of the lead core diameter to the bonded diameter of the isolator, as well as the shear modulus of the rubber used in the isolator. Both of these factors affect the confinement effect of an LRB.

As a result, it is important to note that the findings are limited to the tested isolators and the specific low-temperature conditions considered in this study. Future research could improve upon this study by exploring different loading combinations.

REFERENCES

AASHTO. (2014). *Guide Specification for Seismic Isolation.* American Association of State Highway and Transportation Officials (AASHTO).

AASHTO/M251-97. (1997). *Standard Specification for Plain and Laminated Elastomeric Bridge Bearings.* Washington: American Association of State Highway and Transportation Officials (AASHTO).

ASCE. (2017). *Minimum design loads and associated criteria for buildings and other structures.* American Society of Civil Engineers, ASCE/SEI 7-17.

ASTM Standard D4014. (1998). *American Society for Testing and Materials.*

Buckle, I. G., Constantinou, M., Dicleli, M., & Ghasemi, H. (2006). *Seismic Isolation of Highway Bridges.* Research Rep. No. 06-SP07. Buffalo, NY: Multidisciplinary Center.

Cardone, D., & Gesualdi, G. (2012). Experimental evaluation of the mechanical behavior of elastomeric materials for seismic applications at different air temperatures. *International Journal of Mechanical Sciences*, 127-143.

Cavdar, E., Ozdemir, G., & Karuk, V. (2022). Modification in Response of a Bridge Seismically Isolated with Lead Rubber Bearings Exposed to Low Temperature. *IMO Technical Journal*, 1-24.

Chen, Y. Y., Tan, P., Liu, B. C., Ning, X. L., Shen, C. Y., Ma, Y. H., . . . Zhou, F. L. (2015). An experimental study on the temperature dependency for horizontal shear performance of 300 × 300 square lead–rubber bridge bearing. *Materials Research Innovations*, 953-958.

Cho, C. B., Khawk, I. J., & Kim, Y. J. (2008). An experimental study for the shear property and the temperature dependency of seismic isolation bearings. *Journal of the Earthquake Enginerring Society of Korea* , 67-77.

Constantinou, M. C., Whittaker, A. S., Kalpakidis, Y., Fenz, D. M., & Warn, G. P. (2007). *Performance of Seismic Isolation Hardware under Service and Seismic Loading.* Technical Report, MCEER-07-0012, Multidisciplinary Center for Earthquake Engineering Research. Buffalo, New York: State University of New York.

Coria, C. B. (2015). *Response of Lead Rubber Bearings in a Hybrid Isolation System During a Large Scale Shaking Experiment of an Isolated Building.* Reno: University of Nevada.

Dilsiz, A., Gunay, S., Mosalam, K., Miranda, E., Arteta, C., Sezen, H., . . . S. Andrus, J. A. (2023). *Mw 7.8 Kahramanmaras, Türkiye Earthquake Sequence Preliminary Virtual Reconnaissance Report (PVRR).* in StEER- February 6, 2023, Kahramanmaras, Türkiye, Mw 7.8 Earthquake. DesignSafe-CI.

EN 1337-3. (2005). *Structural bearings-Part 3: Elastomeric bearings.* SUTN.

EN-15129. (2018). *Anti-seismic devices.* European Committee for Standardization.

Eyre, R., & Stevenson, A. (1991). Performance of Elastomeric Bridge Bearings at Low Temperatures. *Third World Congress on Joint Sealing and Bearing Systems for Concrete Structures,*, (pp. 27–31).

Fuller, K. N., Gough, J., & Thomas, A. G. (2004). The effect of low-temperature crystallization on the mechanical behavior of rubber. *Journal of Polymer Science Part B-Polymer Physics*, 2181-2190.

Guruswamy, S. (2000). *Engineering Properties and Applications of Lead Alloys.* New York: Marcel Dekker, Inc.

Hasegawa, O., Shimoda, I., & Ikenaga, M. (1997). Characteristic of Lead Rubber Bearing by Temperature. *Structural Dynamics Nuclear Power Plants, B-2. Summaries of Technical Papers of Annual Meeting Architectural Institute of Japan*, 511-512.

Hayır, A., Yıldırım, H., & Orakdöğen, E. (2023). *Istanbul Technical University (ITU) Final Report of Kahramanmaras Earthquakes in Turkiye on February 6.* İTÜ.

Hofmann, W. (1970). *Lead and Lead Alloys: Properties and Technology.* Verlag, Berlin: Springer.

Jangid, R. S. (2007). Optimum lead–rubber isolation bearings for near-fault motions. *Engineering Structures*, 2503-2513.

Jangid, S. R., & Datta, T. K. (1995). Seismic Behaviour of Base-Isolated Buildings: A State-of-the Art Review. *Structures and Buildings*, 186–203.

Kalpakidis, I. V. (2008). *Effects of Heating and Load History on the Behavior of Lead-Rubber Bearings.* New York: State University of New York at Buffalo.

Kelly, J. M. (1986). A seismic base isolation: review and bibliography. *Soil Dynamics and Earthquake Engineering*, 202-216.

Li, J., Ye, K., & Jiang, Y. C. (2009). Thermal effect on the mechanical behavior of lead-rubber bearing. *Journal of Huazhong University of Science and Technology*, 867-876.

Mark, J. E., Erman, B., & Roland, C. M. (2013). *The Science and Technology of Rubber.* Cambridge: Academic Press.

Mendez-Galindo, C., Moor, G., & Rassy, S. (2017). Lead rubber bearings for seismic isolation of structures in cold climates - new development. *IABSE Symposium: Engineering the Future*, (pp. 54-63). Vancouver, Canada.

Miyazaki, M. (2008). The Next Generation of Seismic Isolation Going Beyond Seismic Design Dominated by Earthquakes. *Journal of Disaster Research*, 479–502.

Murray, R. M., & Detenber, J. D. (1961). First and Second Order Transitions in Neoprene. *Rubber Chemistry and Technology*, 668–685.

Naeim, F., & Kelly, J. M. (1999). *Design of seismic isolated structures: From theory to practice.* New York: Wiley.

Nakano, O. N. (1993). Temperature-dependence of base-isolation bearings. *In Proceedings of the 2nd US-Japan Workshop on Earthquake Protective Systems for Bridges.* Tsukuba Science City, Japan: Public Works Research Institute.

Ozdemir, G., Bayhan, B., & Gulkan, P. (2008). Variations in the hysteretic behavior of LRBs as a function of applied loading. *Structural Engineering and Mechanics*, 69-78.

Ozkula, G., Numanoglu, O., Ilhan, O., Uludag, T., & Baser, T. (2023). *Turkiye Earthquake Sequence on February 6, 2023: Preliminary Earthquake*

Reconnaissance Report. in Turkiye & Syria Earthquake on February 6, 2023. DesignSafe-CI.

Park, J. Y., Jang, K.-S., Lee, H.-P., Hak Lee, Y., & Kim, H. (2012). Experimental Study on the Temperature Dependency of Full Scale. *Journal of the Computational Structural Engineering Institute of Korea*, 533-540.

Pinarbasi, S., Akyuz, U., & Ozdemir, G. (2007). An experimental study on low temperature behavior of elastomeric bridge bearing. . *In: Proceedings of the 10th World Conference on Seismic Isolation, Energy Dissipation and Active Vibrations Control of Structures.* İstanbul.

Qayyum, B. (2016). *Low Temperature Performance Of Elastomeric Bearings In A Full Size Field Experimental Bridge.* University at Buffalo, State University of New York.

Ritchie, D. F. (1989). Neoprene Bridge Bearing Pads, Gaskets and Seals, Rubber World. *Lippincott and Petto Inc*, 27–31.

Robinson, W. H. (1982). Lead-rubber hysteretic bearings suitable for protecting structures during earthquakes. *Earthquake Engineering and Structural Dynamic*, 593-604.

Roeder, C. W., Stanton, J. F., & Feller, T. (1990). Low-temperature performance of elastomeric bearings. *Journal of Cold Regions Engineering*, 113-132.

Semedi, P., & Prasetya, A. (2014). Oil Palm versus Rubber:GIS Empirical Check for Land Grabbing in West Kalimantan. *Journal of Asian Network for GIS-based Historical Studies*, 43-50.

Skinner, R. I. (1992). *An introduction to seismic isolation.* New York: Wiley.

Sorrentino, P., Guidi, L. G., Brandonisio, G., & Antonello, D. L. (2023). Design spectra to be used in Base Isolation Design in light of recent strong motion records. *Procedia Structural Integrity*, 1300-1307.

Stevenson, A. (1983). The influence of low-temperature crystallization on the tensile elastic modulus of natural rubber. *Journal of Polymer Science: Polymer Physics Edition*, 553-572.

TBEC. (2018). *Turkish Building Earthquake Code, Specifications for building design under earthquake effects.* Ankara, Türkiye: Disaster and Emergency Management Presidency.

Turkish Seismic Isolated Brigde Design Specification. (2020). Ankara: Ministry of Transport and Infrastructure.

Turkish State Meteorological Service (TSMS). (2024).

Tyler, R. H., & Robinson, W. H. (1984). High-strain tests on lead-rubber bearings for earthquake loadings. *Bulletin of the New Zealand Society for Earthquake Engineering*, 90-105.

Vaiana, N., & Rosati, L. (2023). Analytical and differential reformulations of the Vaiana–Rosati model for complex rate-independent mechanical hysteresis phenomena. *Mechanical Systems and Signal Processing*, 1-20.

Vaiana, N., Capuano, R., & Rosati, L. (2023). Evaluation of path-dependent work and internal energy change for hysteretic mechanical systems. *Mechanical Systems and Signal Processing*, 1-20.

Yakut, A., & Yura, J. A. (2002a). Parameters influencing performance of elastomeric bearings at low temperatures. *Journal of Structural Engineering* , 986-994.

Yakut, A., & Yura, J. A. (2002b). Evaluation of low-temperature test methods for elastomeric bridge bearings. *Jornal of Bridge Engineering* , 50-56.

Zhang, R.-j., & Li, A.-q. (2020). Experimental study on temperature dependence of mechanical properties of scaled high-performance rubber bearings. *Composites Part B: Engineering*.

CURRICULUM VITAE

ORCID ID: 0000-0002-1810-6669

Name Surname : **Cansu YAŞAR**

Foreign Language : **English**

Education Background:

- 09/2016-07/2019, Eskişehir Technical University, Institute of Graduate programs/Engineering Faculty, Civil Engineering Department
- 09/2010-06/2015, Anadolu University, Engineering Faculty, Civil Engineering Department
- 09/2006-06/2010, Kırklareli Anadolu High School

Professional Background:

- 07/2023- present, R&D Engineer, TİS Teknolojik İzolatör Sistemleri, Ankara
- 09/2016-09/2019, Structural Engineer, Dumlupınar Kentsel Dönüşüm, Eskişehir
- 06/2015-08/2016, Site Engineer, Kırçıllar Yapı, Eskişehir

Publications and/or Scientific/Artistic Activities:

- Yaşar, C., Karuk, V., Cavdar, E., & Ozdemir, G. (2024). "Modifications in both lead and rubber properties of LRBs at low temperatures considering the size effect." Engineering Structures, 307, 1–12. https://doi.org/10.1016/j.engstruct.2024.117902
- Ozdemir, G., Yaşar, C., Karuk, V., & Cavdar, E. (2024). "Contribution of Lead to Stiffness of an LRB at Low Temperatures with an Emphasis to Size Effect." 18th World Conference on Earthquake Engineering, Milan. 1-9.
- Yasar, C., Karuk, V., Kaplan, O., Cavdar, E., & Ozdemir, G. (2023). "Amplification in Mechanical Properties of a Lead Rubber Bearing for Various Exposure Times to Low Temperature." Buildings, 13(2), 1–18. https://doi.org/10.3390/buildings13020478

- Yaşar, C., Karuk, V., Cavdar, E., & Ozdemir, G. (2023). “Variation in Mechanical Properties of a Lead–Rubber Bearing Exposed to Low Temperature.”” Journal of Cold Regions Engineering, 37(3), 1–13. https://doi.org/10.1061/jcrgei.creng-698
- Karuk, V., Yaşar, C., Cavdar, E., & Ozdemir, G. (2023). Check for updates Performance Assessment of a Bridge Seismically Isolated with Lead Rubber Bearings at Low Temperature. Seismic Isolation, Energy Dissipation and Active Vibration Control of Structures: 17th World Conference on Seismic Isolation (17WCSI). 426-437.
- Yasar, C., Çavdar, E., Karuk, V., Ertaş, M. C., Şorman, A. A., & Özdemir, G. (2021). “Farklı Dış Ortam Sıcaklıkları Ve Maruz Kalma Süreleri İçin Kurşun Çekirdekli Kauçuk İzolatör Mekanik Özelliklerinin İncelenmesi.” 6. Uluslararası Deprem Mühendisliği ve Sismoloji Konferansı, Gebze, 1-10.
- Yasar, C., Çavdar, E., Karuk, V., Ertaş, M. C., Şorman, A. A., & Özdemir, G. (2021). “Assessment of Existing Definitions to Estimate Properties of Lead Rubber Bearings Exposed to Low Temperature.” 14. International Congress on Advances in Civil Engineering, İstanbul, 1–8.